

Gap Junctions and Connexin Expression in the Mouse Inner Ear

JILL CAROLE EDWARDS

A Thesis Submitted for the Degree of Doctor of
Philosophy at the University of London
2004

Institute of Laryngology and Otology,
University College London

UMI Number: U602825

All rights reserved

INFORMATION TO ALL USERS

The quality of this reproduction is dependent upon the quality of the copy submitted.

In the unlikely event that the author did not send a complete manuscript and there are missing pages, these will be noted. Also, if material had to be removed, a note will indicate the deletion.



UMI U602825

Published by ProQuest LLC 2014. Copyright in the Dissertation held by the Author.
Microform Edition © ProQuest LLC.

All rights reserved. This work is protected against
unauthorized copying under Title 17, United States Code.



ProQuest LLC
789 East Eisenhower Parkway
P.O. Box 1346
Ann Arbor, MI 48106-1346

ABSTRACT

Gap junctions are sites of direct communication between adjacent cells where clusters of channels in the membrane of one cell contact clusters of channels in the membrane of the neighbouring cell. Six constituent proteins, known as connexins (Cx), make up each hemi-channel. The channels allow the passage of small metabolites (up to 1200 Daltons in size), ions, and second messengers between cells, coupling them both electrically and chemically. This provides a means for signalling between the cells that enables co-ordinated activity of cells in a tissue and may permit one cell to trigger a response in its neighbour.

Mutations of several connexin genes have been associated with deafness and the inner ear is richly endowed with gap junctions. A review of freeze fracture replicas, obtained from various species, illustrates the unusually large size and number of gap junction plaques throughout cells of the inner ear.

A comprehensive analysis of the gap junctions and connexin expression in the inner ear has been performed. Using a variety of techniques these communication channels have been observed and their constituent protein isoforms characterised. Initial screening of cochlear and vestibular tissue with rt-PCR primers established which connexin isoforms might be present; immunohistochemical follow-up with an array of antibodies enabled spatial and temporal localisation of the proteins. It has been established that Cx26 and Cx30 are the major isoforms expressed in mature inner ear whilst isoforms Cx31, Cx43, Cx45 and Cx50 play a role in development of the cochlea. Isoforms Cx26 and Cx30 appear to be co-localised within the same junctional plaques and may form heteromeric gap junctions unique to the inner ear.

Acknowledgements

I would like to thank my supervisor, Professor Andy Forge, for his advice and support and my second supervisor Dr. David Becker for help and guidance. Thanks to Dr. Stefano Casalotti and Graham Nevill for their expertise and advice with experimental procedures. Thanks to all who kindly donated antibodies for use in this study; in particular Professor W.H. Evans, Cardiff, Professor N. Severs, Imperial College London and Professor K. Willecke, Bonn, Germany.

Thank-you to all members of the laboratory of the late Bernie Gilula at the Scripps Research Institute, La Jolla, California for their patience and help during my visit and for allowing me to use their antibodies and knockout animals. Thanks to all members of the ILO, past and present, and many thanks to Wendy and Jenny for necessary sympathy and distraction.

Special thanks to Dr. Victoria Camp for advice, discussions and help particularly during the final stages of my thesis. I am also extremely grateful to Eugene Battini for his help in editing and printing the final version of the thesis.

Finally, thanks to all of my family and friends, especially Peter, for their constant support and encouragement.

This work was supported by the Ferens Endowment Fund.

Table of Contents

| | |
|--|-----------|
| <i>ABSTRACT</i> | 2 |
| <i>Acknowledgements</i> | 3 |
| <i>Table of Contents</i> | 4 |
| <i>Table of Figures</i> | 6 |
| CHAPTER ONE | 7 |
| <u>INTRODUCTION</u> | 7 |
| <i>Overview</i> | 8 |
| <i>Gap Junction structure</i> | 9 |
| <i>Molecular Components of a Gap Junction</i> | 12 |
| <i>Life Cycle of a Gap Junction</i> | 20 |
| <i>Physical Properties of Gap Junctions</i> | 22 |
| <i>Gap Junctions in vivo</i> | 23 |
| <i>Invertebrate Gap Junctions</i> | 25 |
| <i>Connexins in Development</i> | 26 |
| <i>The Ear</i> | 27 |
| <i>Development of the inner ear of the mouse</i> | 34 |
| <i>Deafness</i> | 35 |
| <i>Connexin mutations and deafness</i> | 35 |
| <i>Aims of this thesis</i> | 40 |
| CHAPTER TWO | 42 |
| <u>MATERIALS AND METHODS</u> | 42 |
| <i>Mice</i> | 43 |
| <i>Immunocytochemistry</i> | 45 |
| <i>RT-PCR</i> | 47 |
| <i>Western Blot</i> | 51 |
| <i>Freeze fracture technique</i> | 53 |
| <i>Dye Transfer</i> | 54 |
| <i>In vitro connexin expression system</i> | 54 |
| <i>Processing tissue for immunogold staining</i> | 55 |
| <i>LacZ method</i> | 55 |
| <i>Plastic sections</i> | 57 |
| <i>Clearing</i> | 57 |
| CHAPTER THREE | 58 |
| <u>IDENTIFICATION OF INNER EAR GAP JUNCTIONS USING FREEZE- FRACTURE</u> | 58 |
| <i>Introduction</i> | 59 |
| <i>K⁺ ion-recycling hypothesis</i> | 63 |
| <i>Results</i> | 64 |
| <i>Discussion</i> | 78 |
| CHAPTER FOUR | 83 |
| <u>CONNEXIN EXPRESSION IN THE MATURE MOUSE INNER EAR</u> | 83 |
| <i>Introduction</i> | 84 |
| <i>Results</i> | 88 |

| | |
|--|------------|
| <i>Immunostaining</i> | 93 |
| <i>Discussion</i> | 112 |
| CHAPTER FIVE | 119 |
| <u>CONNEXIN EXPRESSION IN THE DEVELOPING MOUSE INNER EAR</u> | <u>119</u> |
| <i>Introduction</i> | 120 |
| <i>Results</i> | 123 |
| <i>Discussion</i> | 142 |
| CHAPTER SIX | 149 |
| <u>EXPERIMENTAL CLARIFICATION: HELa CELLS AND IMMUNOGOLD</u> | |
| <u>LABELLING</u> | <u>149</u> |
| <i>Introduction</i> | 150 |
| <i>Results</i> | 152 |
| <i>Discussion</i> | 158 |
| CHAPTER SEVEN | 160 |
| <u>STUDIES WITH KNOCKOUT MICE</u> | <u>160</u> |
| <i>Introduction</i> | 161 |
| <i>Results</i> | 163 |
| <i>Discussion</i> | 175 |
| CHAPTER EIGHT | 178 |
| <u>GENERAL DISCUSSION</u> | <u>178</u> |
| <i>Summary of the findings of this thesis</i> | 180 |
| <i>Why do Cx26 mutations cause deafness?</i> | 184 |
| <i>Future studies</i> | 186 |
| REFERENCES | 188 |
| APPENDIX 1 | 203 |
| APPENDIX 2 | 204 |
| APPENDIX 3 | 205 |
| APPENDIX 4 | 207 |

Table of Figures

| | | |
|-----------------------|--|-----|
| Figure 1.1(a): | TEM of the septilaminar appearance of a gap junction | 11 |
| Figure 1.1(b): | Diagrammatic representation of freeze fracture technique | 11 |
| Figure 1.1(c): | Freeze fracture replica of a supporting cell gap junction | 11 |
| Figure 1.2: | Gap junction structure | 14 |
| Figure 1.3: | Phylogenetic tree of the human connexins | 16 |
| Figure 1.4: | Possible arrangements of gap junction connexons | 19 |
| Figure 1.5: | Sketch diagram of the ear | 29 |
| Figure 1.6: | The cochlea duct | 31 |
| Figure 1.7: | The vestibular system | 33 |
| Figure 3.1: | Freeze fracture electron microscopy of gap junctions | 61 |
| Figure 3.2: | Inner sulcus gap junctions | 65 |
| Figure 3.3: | Gap junctions between pillar cells | 66 |
| Figure 3.4: | Gap junction plaques in Deiters' cells | 68 |
| Figure 3.5: | Hensen's cells and outer sulcus gap junctions | 69 |
| Figure 3.6: | Lateral wall gap junctions | 71 |
| Figure 3.7: | Gap junctions of the crista ampullaris | 73 |
| Figure 3.8: | Vestibular macula gap junctions | 74 |
| Figure 3.9: | Summary diagram of plaques throughout the organ of Corti | 76 |
| Figure 3.10: | Summary diagram of plaques throughout the vestibular system | 76 |
| Figure 3.11: | E16.5 freeze fracture by J. Edwards | 77 |
| Figure 3.12: | Sketch diagram summarising the general distribution of gap junction plaques within sensory epithelia | 79 |
| Figure 4.1: | Reverse transcriptase polymerase chain reaction | 90 |
| Figure 4.2: | Western blots | 92 |
| Figure 4.3: | Immunostaining of Cx26 in wholemount organ of Corti | 95 |
| Figure 4.4: | Diagram to show the organ of Corti cells in wholemount view | 96 |
| Figure 4.5: | Pillar cell junctions | 98 |
| Figure 4.6: | FITC-labelled Cx26 in the adult organ of Corti | 99 |
| Figure 4.7: | Immunostaining in the cochlear lateral wall | 101 |
| Figure 4.8: | Cx26 immunostaining in the vestibular system | 103 |
| Figure 4.9: | Cx30 in wholemount organ of Corti | 105 |
| Figure 4.10: | Cx30 expression in organ of Corti frozen section | 106 |
| Figure 4.11: | Cx30 expression in the vestibular system | 108 |
| Figure 4.12: | Cx43 immunostaining | 110 |
| Figure 5.1: | RT-PCR with various connexin primers through development | 125 |
| Figure 5.2: | Organ of Corti at E17.5 showing diverse connexin expression | 127 |
| Figure 5.3: | Connexin 26 in developing mouse cochlea | 129 |
| Figure 5.4: | Connexin 26 during development | 131 |
| Figure 5.5: | Connexin 30 in postnatal cochlea | 133 |
| Figure 5.6: | Connexin 31 in mouse organ of Corti during development | 135 |
| Figure 5.7: | Connexin 43 expression during development | 137 |
| Figure 5.8: | Connexin 45 expression during development | 139 |
| Figure 5.9: | Connexin 50 expression during development | 141 |
| Figure 6.1: | HeLa cell experiment to show specificity of antibodies | 153 |
| Figure 6.2: | Immunogold labelling of gap junction structures | 155 |
| Figure 6.3: | Successive immunogold sections | 157 |
| Figure 6.4: | Double immunogold labelling of Cx26 and Cx30 | 157 |
| Figure 7.1: | Testing for Cx46 | 164 |
| Figure 7.2: | Positive staining of Cx50 in an E18.5 lens | 166 |
| Figure 7.3: | Cx50 in E15.5 otocyst | 168 |
| Figure 7.4: | Study of a Cx50 ^{-/-} mouse inner ear at E18.5 | 169 |
| Figure 7.5: | Morphological comparison of wild-type with Cx43 ^{-/-} otocyst | 171 |
| Figure 7.6: | Comparison of Cx43 ^{-/-} with wild-type inner ear | 172 |
| Figure 7.7: | TEM of wild-type and Cx43 knockouts | 174 |

CHAPTER ONE

INTRODUCTION

Overview

Hearing is an important part of communication that most of us are able to utilise and enjoy. It is therefore not surprising that the cells of the body should want to “talk” to one another.

Communication between cell populations is essential in all tissues, whilst the segregation of cell types can be equally crucial for correct function of an organ. There are several mechanisms by which communication is achieved – secretion, extracellular matrix molecules, and contact via adhesion molecules and intercellular junctions. There are three main types of cell junction: occluding junctions or tight junctions are areas of plasma membrane that squeeze tightly together between adjacent cells creating a selective barrier; anchoring junctions including adherens junctions, desmosomes and hemidesmosomes; and communication junctions which comprise gap junctions and chemical synapses.

The most rapid method of synchronising neighbouring cells electrically and metabolically is by the passage of ions and small molecules through a direct connection that links the cytoplasm of cells; in animals this connection is via an organelle known as the gap junction. The plant equivalent is the plasmodesmata, fine strands of cytoplasm that extend through pores in the cell wall connecting the cytoplasm of two neighbouring cells, thus providing a route for ions and small molecules to move between cells.

Gap junction channels are unique phenomena in that they provide a means for direct exchange of molecules between cells with no secretion into the extracellular space. Nearly all multicellular organisms express some form of intercellular channels (Revel, 1986).

Gap Junction structure

Observation of the Gap Junction

Dewey and Barr (1962) were the first to notice an apparent fusion of cell membranes when studying smooth muscle cells by electron microscopy. They called this region, where the plasma membranes of two excitable cells fused, a nexus. In 1967 Revel and Karnovsky used a new technique of uranyl salt staining prior to thin-section electron microscopy and saw the 2-4nm intercellular space that characterises the structure now known as a gap junction (see Fig.1.1 (a)).

Gap junctions provide a communication system between most cell types, in almost all organisms; in invertebrates the equivalent junctions are known as septate junctions. Using technological advances in high-resolution microscopy, for example negative staining, X-ray diffraction (Makowski *et al.*, 1977), atomic force microscopy (Lal *et al.*, 1995) and cryoelectron microscopy (Perkins *et al.*, 1997; Yeager 1998, Unger *et al.*, 1999), ultrastructure of the gap junction channel was elucidated.

Freeze Fracture Electron Microscopy

Freeze-fracture studies have provided detailed images of these plaques; fracturing along the membranes between cells produces a picture of raised particles when observing the protoplasmic (P)-face or pits on the exoplasmic (E)-face (Fig. 1.1(b)). Each gap junction plaque comprises tens to thousands of intramembranous particles (Fig. 1.1(c)). These particles seen in freeze fracture images were recognised as the individual units of a gap junction and were named “connexons” (Goodenough, 1975). The gap junction plaques comprising many pairs of connexons are variable in size. It was due to the application of freeze fracture techniques that the distinction between gap junctions and tight junctions was made clear.

Figure 1.1(a): Transmission electron micrograph of the septilaminar appearance of a gap junction (from Hertzberg *et al.*, 1982)

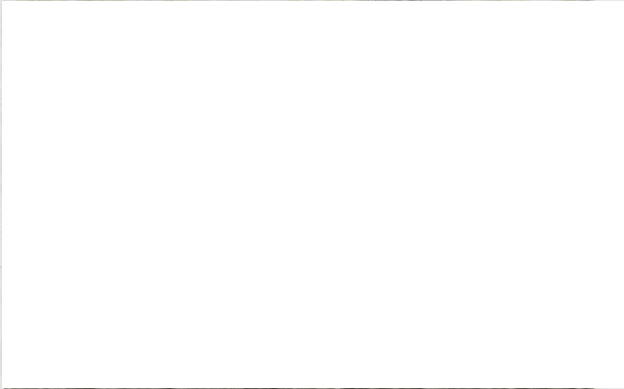


Figure 1.1(b): Diagrammatic representation of freeze fracture technique (from Campbell and Reece, “Campbell Biology text book”, published by Benjamin - Cummings)

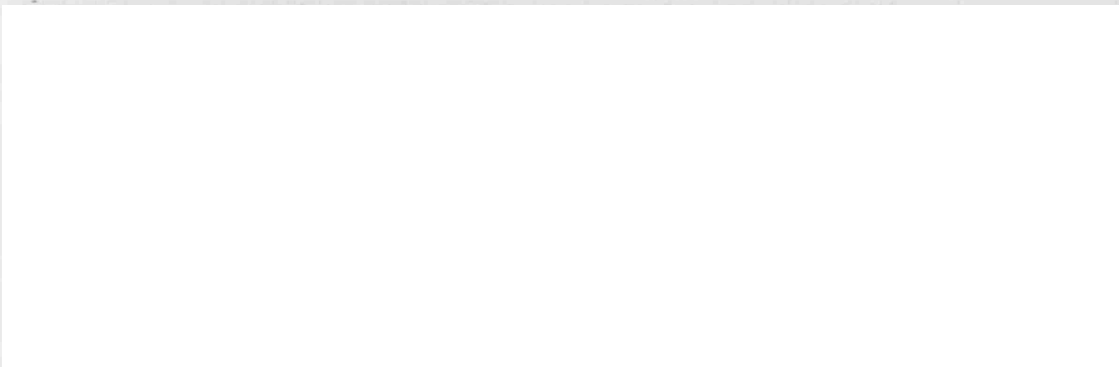


Figure 1.1(c): A freeze fracture replica of a gap junction between supporting cells of the organ of Corti, viewed by SEM (from Prof. A. Forge)



Molecular Components of a Gap Junction

Identification of the Gap Junction Proteins

The gap junction was revealed to be an assembly of membrane-spanning channels whereby connexons from two cells have docked together to form an aqueous pore connecting the cytoplasmic compartments of the cells (see Fig.1.2 (a)). Connexons are comprised of six connexin protein sub-units; two connexons, each embedded in the plasma membrane of a cell, dock together to form a continuous channel between those cells. This channel allows passage of various second messenger molecules, ions and other molecules of less than 1000 Daltons between cells (Lowenstein, 1981). Areas of plasma membranes isolated from liver were shown to exhibit plaques of “hexagonally arranged subunits” (Benedetti and Emmelot, 1968; Revel and Karnovsky, 1967).

The first gap junction protein was cloned from rat hepatic cells (Paul, 1986) and was soon followed by the identification of human and murine homologous sequences (Kumar and Gilula, 1986; Heynkes *et al.*, 1986) with a predicted molecular mass of 32kiloDaltons (kDa).

Subsequent sequences coding for other gap junction proteins were found by using PCR with oligonucleotide primers to the most conserved domains among the previously characterised gap junction proteins (White and Bruzzone, 1996). These protein sub-units are now known to belong to a multigene family called connexins.

Structure of the Connexin Molecule

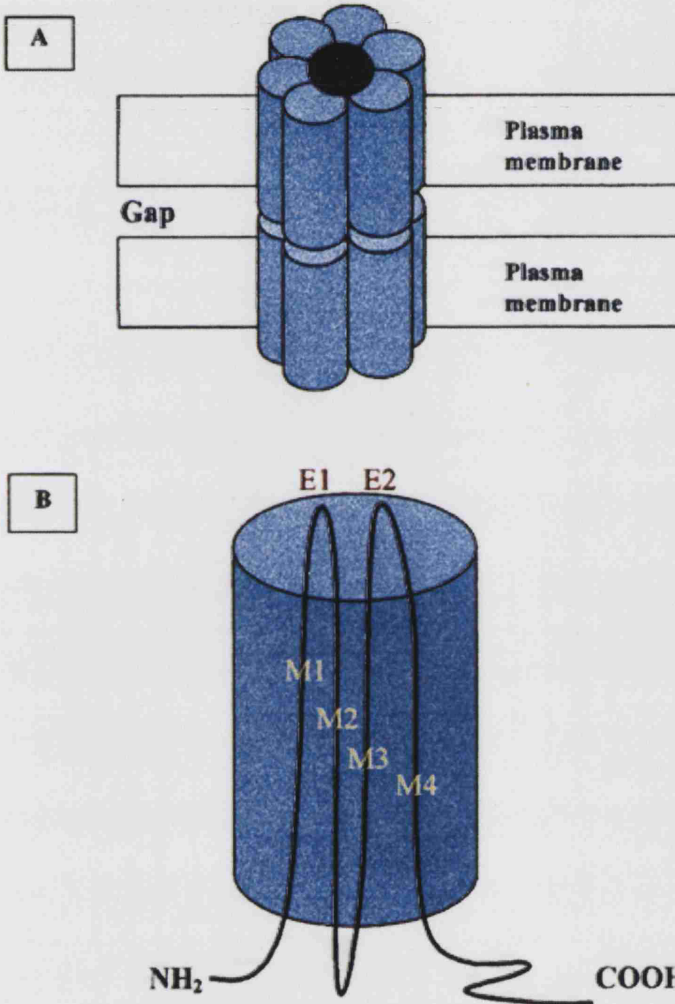
There are several different isoforms of connexin protein but all have four transmembrane domains (named M1-M4 sequentially starting at the amino-terminus end), two extracellular loops (E1 and E2) and one intracellular loop; the amino-terminus and carboxy-tail are located cytoplasmically (Fig. 1.2(b)). Despite the similar topology of all the connexin proteins they also have divergent regions, which produces gap junction channels with distinct properties (Veenstra, 1996; Evans and Martin, 2002). The C-terminal end of the protein is the most variable domain and specific antibodies are usually directed at this cytoplasmic tail.

The length of the carboxy tail largely determines the molecular weight of each individual connexin isoform. The most commonly used nomenclature system for connexin proteins is the one that refers to each on the basis of molecular weight.

Figure 1.2: Gap junction structure

(a) Connexons are composed of six connexin molecules. Two connexons dock together to form a gap junction channel.

(b) Structure of an individual connexin protein.



E1 and E2 are extracellular loops.
M1-M4 are transmembrane domains.
COOH is the carboxy tail end of the protein.
NH₂ is the amino terminal of the protein.

Nomenclature of the Connexins

There are two nomenclature systems currently used to identify the connexin proteins. The most common is that which refers to each isoform on the basis of molecular mass, for example the connexin protein whose molecular mass is 43 kDa is referred to as connexin43 (Cx43) (Beyer *et al.*, 1987). Additionally, a prefix letter can be used to specify the species being referred to, for example, mCx for mouse connexin but hCx for the human protein. An alternative, phylogenetic nomenclature system (Fig. 1.3), which separates the isoforms into three different classes according to their primary sequence and predicted topology, is also in use (Risek *et al.*, 1990; Bennett *et al.*, 1991). Neither of these nomenclature systems is entirely satisfactory; the mass system became somewhat confusing as further connexin isoforms with similar molecular mass were discovered, the latter system has never had clearly defined criteria for categorization into each of the classes and some more recently cloned connexins have not been grouped. Throughout this thesis the more widely utilised molecular mass nomenclature system will be used, refer to Table 1.1 for the relationship of the two nomenclatures.

The extracellular loops are highly conserved between isoforms whereas variations occur in the intracellular loop and carboxy-tail regions. Cx26 is notable in that it has a very short carboxy-tail meaning that it has no phosphorylation sites that are known to regulate other connexins. In all isoforms reported to date, except Cx31, there are three cysteine residues conserved in each extracellular loop; Cx31 only has two of the characteristic cysteines. These structural similarities and differences have not yet been correlated with any specific biological function. It is perplexing to think why so many different isoforms of gap junction-forming protein may be required.

Figure 1.3: Phylogenetic tree of the human connexins

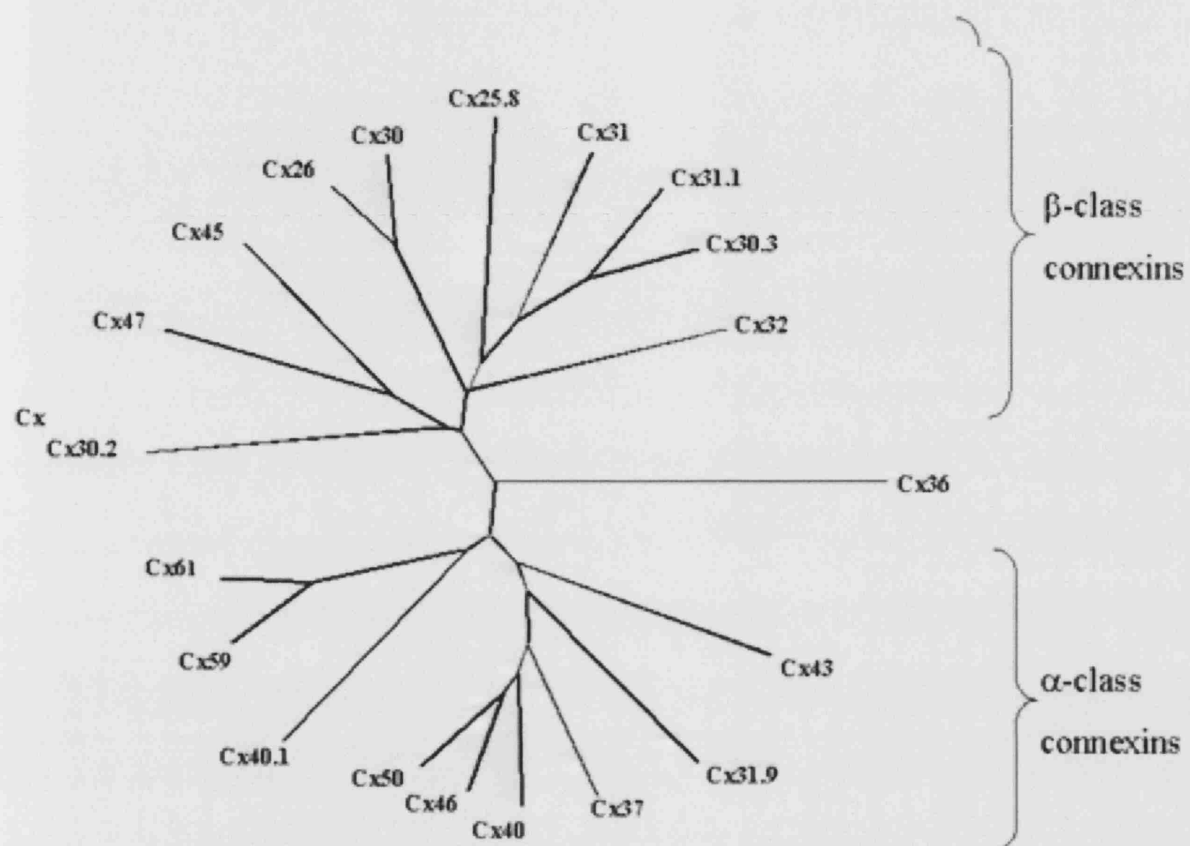


Table 1.1: Nomenclature of connexin proteins (revised from Willecke *et al.* 2001)

| MOUSE | | | | HUMAN | | | |
|--------------|--------------|----------------------|---------------------------|--------------|--------------|----------------------|----------|
| Gene Symbol | Current name | Molecular mass (kDa) | Group name | Gene symbol | Current name | Molecular mass (kDa) | Group |
| | — | — | — | | hCx25 | 25.89 | — |
| <i>Gjb2</i> | mCx26 | 26.41 | β 2 | <i>GJB2</i> | hCx26 | 26.20 | β |
| | mCx29 | 28.98 | — | | hCx30.2 | 30.31 | — |
| <i>Gjb6</i> | mCx30 | 30.37 | β 6 | <i>GJB6</i> | hCx30 | 30.40 | β |
| | mCx30.3 | 30.39 | β | | hCx30.3 | 30.42 | β |
| <i>Gjb3</i> | mCx31 | 30.90 | β 3 | <i>GJB3</i> | hCx31 | 30.82 | β |
| | mCx31.1 | 31.19 | β | | hCx31.1 | 31.09 | β |
| | mCx30.2 | 30.22 | β | | hCx31.9 | 31.93 | β |
| <i>Gjb1</i> | mCx32 | 32.00 | β 1 | <i>GJB1</i> | hCx32 | 32.02 | β |
| <i>Gja7</i> | mCx33 | 32.86 | α 7 | | — | — | — |
| | mCx36 | 36.08 | — | | hCx36 | 36.25 | — |
| <i>Gja4</i> | mCx37 | 37.60 | α 4 | <i>GJA4</i> | hCx37 | 37.41 | α |
| <i>Gja5</i> | mCx40 | 40.41 | α 5 | <i>GJA5</i> | hCx40 | 40.38 | α |
| | mCx39 | 39.99 | — | | hCx40.1 | 40.14 | — |
| <i>Gja1</i> | mCx43 | 43.00 | α 1 | <i>GJA1</i> | hCx43 | 43.01 | α |
| <i>Gja6</i> | mCx45 | 45.67 | α 6 (or γ) | <i>GJA6</i> | hCx45 | 45.48 | γ |
| <i>Gja3</i> | mCx46 | 46.30 | α 3 | <i>GJA3</i> | hCx46 | 47.43 | α |
| <i>Gja10</i> | mCx46.6 | 46.60 | α 10 | <i>GJA10</i> | hCx47 | 46.66 | γ |
| <i>Gja8</i> | mCx50 | 49.60 | α 8 | <i>GJA8</i> | hCx50 | 48.17 | α |
| | — | — | — | | hCx58 | 58.84 | — |
| | mCx57 | 57.11 | α | | hCx62 | 61.87 | α |
| <i>Gja9</i> | mCx60 | — | α 9 | | — | — | — |

Composition of Gap Junctions

In addition to different cells expressing individual connexin isoforms each cell can also express more than one isoform. Therefore there is a wide range of possibilities for the composition of gap junctional plaques. If the connexons of each coupled cell are identical the junction is homotypic, if the connexons from each cell are different the junction is heterotypic. If the connexin isoforms within a connexon are the same this is a homomeric connexon, if the connexon contains different connexin isoforms it is heteromeric (Kumar and Gilula, 1996; Fig. 1.4). Falk (2001) has recently described individual plaques that contain separate areas of different homomeric-homotypic connexons. This study also noted that a cell could express a particular isoform in specific areas so that junctions with one cell may be composed of different connexins than those with another neighbour.

There is a general tendency for the α class of connexins to pair with each other and for the β connexins to pair with themselves (see Table 1.1 or Figure 1.3 for the α and β groupings of connexins). Exceptions to this rule are Cx30.3 which is a β connexin but pairs with α isoforms, and Cx50 which is an α connexin but prefers to pair with β connexins. There are some connexin isoforms that do not appear to pair with any other connexins, Cx31 only pairs with itself for example.

Evaluation of connexon pairing is by the use of oocyte pairs that express different connexins. The coupling efficiency between the oocyte pair is measured to assess whether the connexons are compatible.

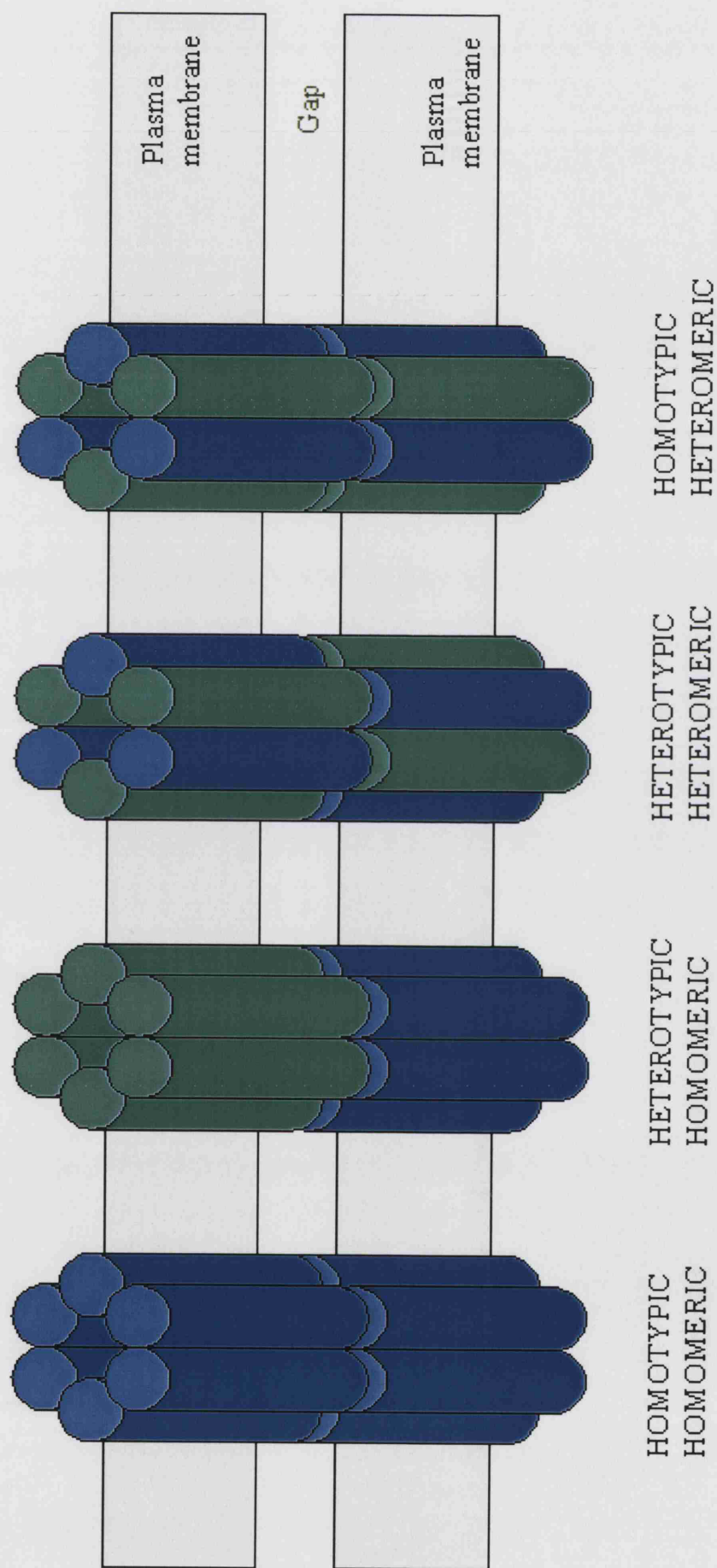


FIGURE 1.4: Possible arrangements of gap junction connexons

Life Cycle of a Gap Junction

Since most tissues express more than one connexin, it is feasible that the expression of these proteins may be controlled by various regulatory mechanisms, such that connexins with different functional properties may be expressed as and when needed by the tissue.

Oligomerisation

Establishment of connexin topology occurs in the Endoplasmic Reticulum (ER). From there the connexin sub-units must oligomerise into a connexon hexamer. This assembly commences in the ER and continues during trafficking via tubulovesicular networks and in the Golgi apparatus (Pfeffer and Rothman, 1987), with the exception of Cx26 which appears to take a different route to the plasma membrane.

The trafficking of Cx26 appears to be unaffected by brefeldin A treatment, a compound which disrupts the Golgi apparatus, indicating no involvement of this organelle (Evans *et al.*, 1999). However, the Cx26 pathway is affected by nocodazole suggesting a microtubule-dependant route (George *et al.*, 1999). This suggests that Cx26 traffics directly from the ER to the membrane without passing through the Golgi.

Several lines of evidence suggest that the extracellular loop domains are involved in the docking together of two connexons. Oocyte cell pairs, transfected with Cx32 cDNA, pre-incubated with synthetic peptides to the extracellular loops showed a reduction in functional coupling (Dahl *et al.*, 1992). Also, disruption of the cysteine residues that have been shown to be conserved between all known connexin

isoforms resulted in loss of functional coupling (although these altered connexins were shown to get to the plasma membrane (Nicholson *et al.*, 1999)).

Using Novikoff cells expressing Cx43 and exposing them to antibodies against the extracellular loops has also been shown to block gap junction formation (Meyer *et al.*, 1992). Cell-adhesion molecules such as the cadherins may facilitate this docking process. When cultured cells have been treated with anti-cadherin antibodies dye transfer has been suppressed (Kanno *et al.*, 1984) and assembly of gap junctions inhibited (Meyer *et al.*, 1992). E-cadherin and β -catenin have been shown to co-localise with connexins during assembly of gap junctions (Fujimoto *et al.*, 1997).

Degradation

Gap junctions are dynamic structures and have a short half-life (as little as two hours) undergoing constant turnover (Laird, 1996). Structures known as annular gap junctions are thought to form as part of the lysosomal pathway for internalisation and degradation of gap junctions. These annular gap junctions are cytoplasmic, bimembranous vesicle-like structures that are derived from whole or parts of gap junctions from apposing cells that invaginate and are internalised into one of the cells (Jordan *et al.*, 2001). It is likely that other methods of gap junction degradation exist as annular junctions are rarely seen in some cell types. Several lines of evidence from Laing and Beyer (1995) suggest that degradation of Cx43 is via an ubiquitin-mediated proteasome proteolysis, which occurs at the cell surface.

Physical Properties of Gap Junctions

Properties of gap junction channels are often studied by measuring dye transfer between cells (Elfgang *et al.*, 1995) or by dual-cell voltage-clamp techniques, which measure electrophysiological characteristics (Salomon *et al.*, 1992). It has been shown that channels composed of different isoforms have particular transfer abilities, for example Cx45 channels do not readily pass Lucifer yellow dye whereas many other channels (including Cx31, Cx32 and Cx43) are permeable to Lucifer yellow (Valiunas, 2002). The molecular weight and charge of the specific dyes are the important factors that mean some isoforms will allow them to pass through and others do not. HeLa cells transfected with Cx30 formed gap junctions that were unable to transfer Lucifer Yellow (Manthey *et al.*, 2001) or Cascade Blue (the molecular weight of these two dyes is similar). Cx30 junctions formed between HeLa cells are capable of neurobiotin transfer (Manthey *et al.*, 2001), which has a smaller molecular weight.

Gating

Opening and closing of the channels can be altered by changes in transjunctional voltage, intracellular pH, and cytoplasmic calcium concentration.

The conductance of connexins can be altered by a variation of potential between cells; a wide range of voltage-gating characteristics exists among the connexin multigene family (Verselis and Bargiello, 1991; Veenstra *et al.*, 1992).

Closure of gap junction channels can be observed in response to both pH (Turin and Warner, 1977) and calcium concentration (Rose and Loewenstein, 1976).

Intracellular acidification reversibly decreases gap junction intercellular communication (Spray *et al.*, 1991). Increased Ca^{2+} levels also decrease the permeability of gap junctions (Spray and Bennett, 1985); the effects of Ca^{2+} may be mediated by protein kinase C (Lazrak and Peracchia, 1993).

Phosphorylation of Connexins

The other main factor responsible for chemical gating is connexin phosphorylation. The first report of connexin phosphorylation was that of Cx32 in hepatocytes (Traub *et al.*, 1987). Many other connexins have since been observed to have phosphorylation sites, with the notable exception of Cx26 (Saez *et al.*, 1990). Some are differentially phosphorylated in a tissue-specific manner; an example of this is Cx43 (Kadle *et al.*, 1991). Phosphorylation sites are usually the serine and threonine residues of the carboxy tail. It is possible that phosphorylation of connexins is involved with their degradation (Laing & Beyer, 1995) but it is also thought to have an effect on channel gating (Lampe and Lau, 2000).

Gap Junctions *in vivo*

Gap junctions contribute to the regulation of numerous functions, including contraction of cardiac and smooth muscle (Spray and Burt, 1990); transmission of neuronal signals at synapses (Bennett and Verselis, 1992), and pattern formation during development (Guthrie and Gilula, 1989; Warner, 1992). Appendix 1 gives examples of the specific connexins present in different tissues.

Passage through a Gap Junction

Many different molecules are able to pass through gap junction channels; these include second messenger molecules, inorganic ions, nucleotides, neurotransmitters, small metabolites and small steroid hormones (Loewenstein, 1981; Vaney *et al.*, 1998). Only ions and molecules less than 1.5nm in diameter and up to 1 – 2 kDa of molecular mass can traverse a gap junction channel (Simpson *et al.*, 1977).

Function of Gap Junction Intercellular Signalling

To fully understand gap junctional communication between cells, it is important to characterize all functional channels and type the connexin isoforms present. Identification of connexin isoforms can provide information relevant to understanding the functioning of tissues, and may possibly be used to monitor changes in a tissue, or as a marker to identify particular cell types.

Studies of spontaneous or targeted mutations in connexin genes have contributed to the understanding of gap junction function. Inactivation of genes by targeted deletion in animal models, ‘knockouts’, has provided interesting results. Cx43 knockout mice die shortly after birth due to a morphological defect of the heart (Reaume, *et al.*, 1995). Cx32 knockout mice are viable and fertile but develop abnormalities of myelin after four months of age (Scherer *et al.*, 1998) and are more susceptible to liver tumours than wild-type littermates. Cx26-deficient mice do not survive past eleven days *in utero* (Gabriel *et al.*, 1998), as placental gap junctions must be dependant on Cx26 for passage of nutrients. The human placenta differs from mouse placenta in that it has a single membrane (mouse has a double placental membrane), which may explain why

humans with mutations in their Cx26 gene survive. The targeted deletion of Cx26, in mice, from the supporting cells of the organ of Corti causes death of outer hair cells (Cohen-Salmon *et al.*, 2002). Mice with a deletion of Cx30 are deaf and do not generate an endocochlear potential (Teubner *et al.*, 2003). Cx37 knockout mice are viable but females are infertile (Simon *et al.*, 1997) due to incomplete development of oocytes. Cx40-deficient mice survive and are fertile but often develop heart arrhythmias and have reduced conduction velocity in the heart (Kirchhoff *et al.*, 1998). Cx36 is expressed in beta cells of the pancreas and in mice lacking Cx36 these beta cells are seen to develop and differentiate normally but they do not secrete as wild-type beta cells do (Calabrese *et al.*, 2001). Gong and colleagues (1997) showed Cx46 knockout mice are viable but develop lens cataracts after two weeks of age. Cx50 knockout mice also have eye defects with smaller eyes, smaller lenses and nuclear opacity of the lens appearing one week after birth (White and Paul, 1999). Analysis of these varied knockout study results and with knowledge of human diseases caused by connexin mutations (see later) has led to considerable insights into the diverse function of gap junction intercellular signalling.

Invertebrate Gap Junctions

Direct intercellular communication through gap junctions appeared early in evolution with the conversion from unicellular to multicellular organisms. Connexins have been demonstrated in mammals, chicks, amphibians and fish but with the full genomic sequences of *Caenorhabditis elegans* and *Drosophila melanogaster* complete (The C.

elegans Sequencing Consortium, Science 1998: 282, 2012-2018; Adams *et al.*, 2000) it is apparent that no invertebrate connexins exist.

Through genetic screens of *C. elegans* and *Drosophila* mutant genes were discovered that are essential for the formation of electrical synapses (Shak-B in *Drosophila*) and synchronised muscle contraction (EAT-5 in *C. elegans*). Loss of electrical and dye coupling in these mutants suggested that these genes may code for gap junction proteins (Starich *et al.*, 1996; Phelan *et al.*, 1996). Expressing these proteins in *Xenopus* oocytes and observing the formation of functional intercellular channels verified this suggestion (Phelan *et al.*, 1998). These invertebrate connexin analogues have been named innexins (Phelan *et al.*, 1998).

Despite the lack of sequence homology between innexins and connexins they are topologically and functionally similar. Much research is ongoing to further investigate how and why invertebrates and vertebrates have evolved two different protein families to form their gap junctions.

Connexins in Development

In 1966 it was reported that all cells in the early squid embryo could communicate (Potter *et al.*, 1966). This was the first proposal that suggested gap junction communication as a feature of early embryos.

Studies of cell-to-cell communication in other developing embryos and tissues, using ionic coupling or dye coupling experiments, showed that gap junction communication starts at a very early stage in most embryos. In the mouse embryo dye coupling has been observed from the late eight-cell stage (Lo and Gilula, 1979).

As development progresses the gap junctional coupling becomes compartmentalised, indicating that some cell populations need to be segregated during embryonic development. By E7.5 in mice, the embryo and tissue of the placenta are completely separate from each other, yet there is gap junctional communication between the placenta and maternal tissues. These findings suggest that gap junction communication plays an intrinsic role in normal development.

Studies using antibodies to block gap junctions in amphibians, mice and chicks have created embryos with developmental defects (Warner *et al.*, 1984; Becker *et al.*, 1995; Allen *et al.*, 1991).

The Ear

The mammalian ear comprises three parts (Fig. 1.5). The outer ear consists of a cartilaginous pinna whose function is to channel sound waves into the ear canal (external auditory meatus) and onto the tympanic membrane, which is where the middle ear begins. The middle ear contains the ossicles. These are small bones that amplify the force of movements of the tympanic membrane and transfer the wave energy to the oval window and into the fluids of the cochlea. The inner ear houses the cochlea (the

hearing organ of mammals) and the vestibular system that is involved in balance. The inner ear is a membranous labyrinth encased in bony channels. A fluid known as perilymph surrounds the membranous ducts. This has a composition similar to that of most extracellular fluids. The membranous labyrinth is filled with a fluid called endolymph. This is unusual in that it has a high K^+ concentration and low Na^+ content. In the cochlea, but not the vestibular system, this endolymph has a high electrical potential, known as the endocochlear potential, of +80mV (Wangemann and Schacht, 1996).

Mature vestibular and auditory sensory epithelia are similar in their general organisation; a mosaic of hair cells separated by intervening supporting cells. Hair cells are so called because of thin, rigid stereocilia that project from their apical surface. Stereocilia extend into an extracellular matrix material that overlies the sensory epithelium. Displacement of this structure by sound vibrations or head movements causes deflection of the stereocilia, opening ion channels leading to depolarisation of the hair cell. Depolarisation stimulates release of neurotransmitter consequently generating neural impulses that pass along nerve fibres to the brain.

Figure 1.5. Sketch Diagram of the Ear



OUTER EAR

- 1 Pinna
- 2 External auditory meatus

MIDDLE EAR

- 3 Tympanic membrane
- 4 Ossicles
- 5 Oval window

INNER EAR

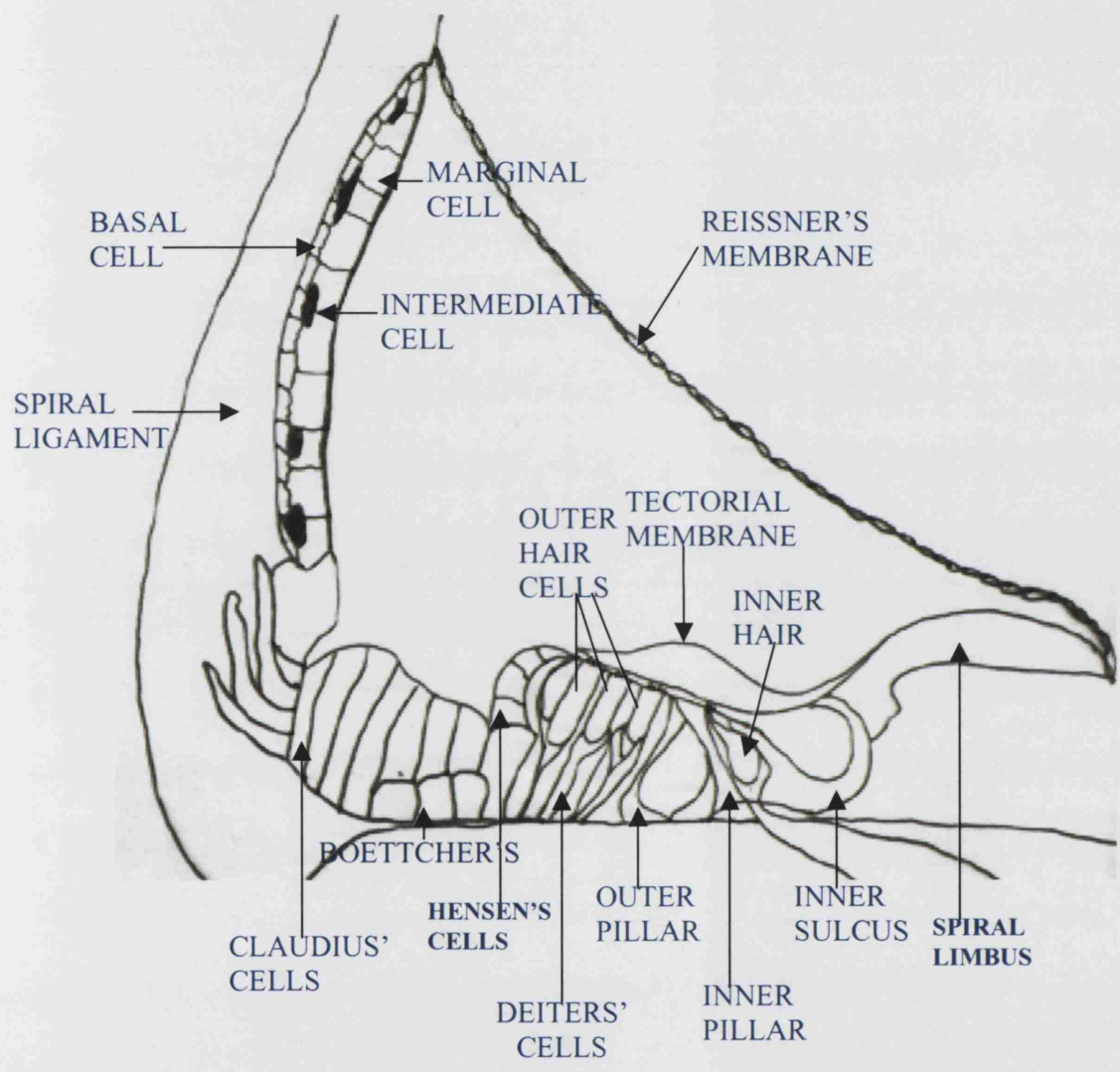
- 6 Semi-circular canals
- 7 Cochlea
- 8 Nerves

Auditory structure

The sensory epithelium of the cochlea is known as the organ of Corti. This is a strip of cells coiled along the length of the cochlea (Fig. 1.6). There are two types of hair cell, inner and outer, and five different supporting cell populations in the organ of Corti.

Endolymph composition is maintained by the ion-transporting epithelia of the cochlea that is the stria vascularis which comprises three different kinds of cell – marginal, intermediate and basal cells and blood capillaries. Marginal cells are epithelial cells and border the endolymph. Intermediate cells are melanin-containing cells that originate from the neural crest and form a discontinuous layer between the marginal and basal cells. Basal cells are of mesenchymal origin and separate the stria vascularis from the underlying spiral ligament via a tight junctional network, which provides a barrier to ionic diffusion between the perilymph of the spiral ligament and the stria vascularis. Basal cells are connected to each other and to the fibrocytes of the lateral wall of the cochlea via gap junctions (Forge, 1984; Kikuchi *et al.*, 1995). Endolymph of the cochlea has a characteristic highly positive electrical potential of approximately 80mV known as the endocochlear potential; the stria vascularis generates the endocochlear potential and maintains the endolymph composition.

Figure 1.6: The Cochlea Duct



Vestibular structure

There are five areas of sensory epithelium in the vestibular system, the cristae of the three semi-circular canals, the utricular macula (utricle) and the saccular macula (sacculè). A single layer of dark cells at the base of each crista and around the utricular macula serves as the ion-transporting epithelia for regulation of endolymph (Fig 1.7). There is a difference between the vestibular and auditory endolymphatic compartments in that the vestibular endolymph does not have the high +80mV potential that is a feature of the cochlear endolymph.

Figure 1.7: The Vestibular System

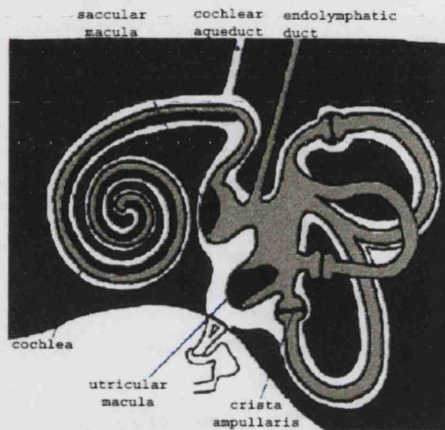


Figure 1.7(a). Diagram depicting the membranous labyrinth of the inner ear and showing position of the cochlea and vestibular sensory organs.

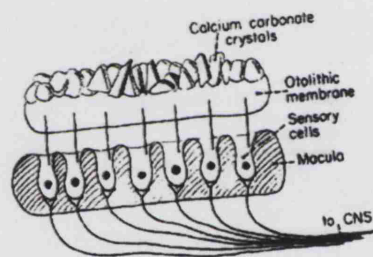


Figure 1.7(b). Schematic diagram of a macula organ that detects linear acceleration and head tilt.

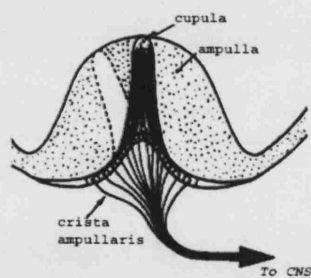


Figure 1.7(c). Illustration of a crista ampullaris. The three cristae, within the semi-circular canals, detect head rotation and angular acceleration.

Development of the inner ear of the mouse

The inner ear originates from a thickening of the ectoderm in the region of the developing hindbrain known as the otic placode. Neural crest also contributes to form the melanocytes of stria vascularis, cells of the ganglion and mesenchymal tissue. Between embryonic days (E) eight and twelve the otic placode invaginates to form the otic vesicle, the tectorial membrane starts to form and the semi-circular canals begin to take form in the lateral portion of the otocyst. In the following two days the three semi-circular canals are seen to form completely and the cochlea begins to coil as it extends (Morsli *et al.*, 1998). By E17 the membranous labyrinth has attained its mature shape and the cochlea has coiled to its full one and three-quarter turns. Sensory cells at the basal end of the cochlea show arrangement into three rows of outer and one row of inner hair cells. The stria vascularis also starts to differentiate on the seventeenth day of gestation. By postnatal day 4 (P4) Reissner's membrane has differentiated along the entire length of the cochlea. Between P8 and P10 the tunnel of Corti widens although the stria vascularis is still not entirely mature (Sher, 1971). In mice auditory function is initiated around P8 and the structure is adult-like by P14 (Forge *et al.*, 1997).

Studies of cochlear development have found evidence consistent with the theory that a gap junction population is involved in the ion circulation, which is essential for the maintenance of the ionic composition of the cochlear fluids. In gerbils the onset and rise of endocochlear potential, between ten and eighteen days after birth, coincides with the appearance of large areas of gap junctions on the apical membranes of basal cells in the stria vascularis (Souter and Forge, 1998).

Deafness

Deafness is generally divided into two categories: conductive, whereby sound cannot pass through either the outer or middle ear, and sensorineural whereby a problem either with the cochlea or the auditory nerves causes deafness. Diseases, noise, drugs and ageing, can cause hearing impairment but most congenital deafness is due to genetic factors. Approximately one in one thousand babies are affected by congenital deafness with about 60% in developed countries being due to genetic factors (Rabionet *et al.*, 2000).

If hearing impairment is accompanied by other clinical features it is known as a syndromic deafness, if deafness is the only phenotype expressed then it is a non-syndromic hearing impairment. Most non-syndromic hearing loss is due to an autosomal recessive mutation but there are also autosomal dominant forms and some X-linked cases.

Connexin mutations and deafness

Several connexins have been implicated in various disease conditions. The initial human genetic disorder shown to be caused by a connexin gene mutation was the X-linked form of Charcot-Marie-Tooth disease (Bergoffen *et al.*, 1993). Mutations in the gene for Cx32 cause demyelination of the Schwann cell, which in turn causes wasting of muscles and decreased sensation in limb extremities; the phenotype of this syndrome also includes late-onset hearing loss.

The major cause of inherited sensorineural deafness is mutations in *GJB2*, the gene for Cx26. To date more than 60 recessive mutations in this gene have been reported to cause deafness (Rabionet, Gasparini, Estivill. Connexins and deafness homepage; <http://www.iro.es/deafness/>). Several dominant forms of deafness have also been associated with *GJB2* mutations, namely, M34T (Kelsell *et al.*, 1997); W44S (Gasparini *et al.*, 1997); W44C (Denoyelle *et al.*, 1998); R75W (Richard *et al.*, 1998); G59A (Heathcote *et al.*, 2000) and D66H (Maestrini *et al.*, 1999). The latter three mutations are syndromes being associated with skin disease as well as deafness. There is controversy over whether the M34T mutant is dominant or not; M34T has been variously reported to be dominant, recessive or a polymorphism. The discovery of individuals heterozygous for the M34T mutation with normal hearing suggested either autosomal recessive or a neutral polymorphism (Scott *et al.*, 1998). More recently it was reported as recessive as homozygote individuals with mid-to-high-frequency hearing loss were identified (Houseman *et al.*, 2001).

GJB2 was the first non-syndromic human deafness gene to be reported (Kelsell *et al.*, 1997) and is responsible for up to 50% of childhood deafness in some populations. One mutation has a particularly high frequency, 30delG (also known as 35delG), which is a deletion of one guanine base in a sequence of six guanine residues at position 30. This deletion truncates the protein at this position before the first transmembrane domain therefore making it effectively a knockout. Another mutation, 167delT, also leads to truncation of the Cx26 protein and subsequently a loss of function (Zelante *et al.* 1997).

The clinical phenotype of Cx26 hearing loss is variable even within families ranging from mild to profound (Murgia *et al.*, 1999). The frequency of Cx26 mutations varies between populations, with the prevalence related to the ethnicity of a particular population. For example the 235delC mutation has only been discovered in Japanese individuals (Fuse *et al.*, 1999).

To date, four other connexin genes have also been reported to be involved in deafness. These are *GJB1* (codes for Cx32), which as mentioned above is responsible for X-linked Charcot-Marie-Tooth disease; *GJB6* (Cx30) has been linked to a dominant form of hereditary deafness (Grifa *et al.*, 1999); *GJB3* (Cx31) is implicated in cases of deafness and the skin disorder erythrokeratoderma variabilis (Xia *et al.*, 1998; Richard *et al.*, 1998); and *GJA1* (Cx43) mutations, found in an African American population have also been shown to cause non-syndromic deafness (Liu *et al.*, 2001).

Various connexin mutations have been studied using an *in vitro* expression system whereby the mutated connexin is introduced into cultured cells that do not have endogenous connexins (Elfgang *et al.*, 1995). Five deafness-causing mutations in Cx26 have been investigated using this method; M34T was trafficked to the membrane but did not form functional channels capable of transferring Lucifer Yellow dye (Martin *et al.*, 1999). G59A and D66H mutants were retained in the cytoplasm close to the nucleus, whilst W44S and W44C were trafficked to the membrane but at reduced levels in comparison to wild-type Cx26 (Marziano *et al.*, 2003). Four of these mutant proteins (G59A, D66H, R75W, W44S) were functionally defective as shown by non-transfer of Cascade Blue dye between the cells. Further *in vitro* experiments whereby mutant Cx26

proteins were expressed together with wild type Cx26 and wild type Cx30 allowed dominant effects to be studied too (Marziano *et al.*, 2003).

Functionality of Cx30 mutations associated with skin disease and deafness has also been studied (Common *et al.*, 2002). T5M is a dominant non-syndromic hearing loss mutant of Cx30, which was shown by this study to traffic to the plasma membrane in the same way as wild-type Cx30 protein, but did not form functional intercellular channels.

The following table (Table 1.2) shows the identified chromosomal locations of connexin genes; connexins highlighted in blue have been studied in this thesis.

Table 1.2: This table shows each connexin gene whose chromosomal location is known. The blue font indicates that the protein has been investigated in the inner ear.

| GENE NAME | CHROMOSOME LOCATION | NAME OF PROTEIN |
|--------------|---------------------|-----------------|
| <i>GJA1</i> | 6q21-q23.2 | Cx43 |
| <i>GJA3</i> | 13q11-q12 | Cx46 |
| <i>GJA4</i> | 1p35.1 | Cx37 |
| <i>GJA5</i> | 1q21.1 | Cx40 |
| <i>GJA7</i> | 17p13.2 | Cx45 |
| <i>GJA8</i> | 1q21.1 | Cx50 |
| <i>GJA10</i> | 1p34 | Cx59 |
| <i>GJB1</i> | Xq13.1 | Cx32 |
| <i>GJB2</i> | 13q11-q12 | Cx26 |
| <i>GJB3</i> | 1p34 | Cx31 |
| <i>GJB4</i> | 1p35-p34 | Cx30.3 |
| <i>GJB5</i> | 1p35.1 | Cx31.1 |
| <i>GJB6</i> | 13q12 | Cx30 |

Aims of this thesis

It is not known what the precise role of gap junctions is within the inner ear. That they are present and that defects in their constituent proteins causes deafness suggests they are important but there have been no proven theories of their exact function to date. It is intriguing how mutations in a protein that is present throughout the body cause deafness as the sole phenotype. This project set out to identify the location of gap junction plaques and to analyse the connexin isoforms present in the inner ear throughout development and into maturity in the mammalian inner ear using mice as a model. It was hoped that results of these studies might clarify the functions of gap junction in the inner ear and that the mechanisms by which connexin mutations cause deafness may be elucidated.

The work presented in this thesis illustrates a thorough analysis of connexin expression and gap junction structures in the auditory and vestibular systems of the mouse inner ear. Initially an in depth analysis of freeze fracture images of the membranes of all inner ear cell types in Chapter 3 is shown to ascertain the location and relative sizes of gap junction plaques; these results are discussed in relation to the theories of gap junction function in the inner ear. Several experimental procedures were implemented throughout the progression of this project. Initial investigations described in chapters 4 and 5 utilised immunolabelling techniques and the molecular biology approaches of RT-PCR and Western blotting to determine the connexin isoforms present in mature and developing ears. It became apparent through advances in the field of gap junction study that proof of antibody specificity and experimental techniques would be required

to corroborate the results obtained through immunolabelling research, Chapter 6 explains the methods used and results obtained from testing the anti-connexin antibodies. Chapter 7 focuses on the role that knockout mice can play in understanding the effects of connexin mutations; there is an investigation of the inner ears of mice that have had a specific connexin gene “knocked-out”.

CHAPTER TWO

MATERIALS AND METHODS

Mice

Husbandry

For the majority of these studies an inbred strain of pigmented mouse, CBA/Ca, was used. For the more experimental parts of the project mice with either their Cx46 or Cx50 or both genes interrupted were used. These were on a background of the C57BL/6J strain.

Mice were kept on a scheme of 12 hours of light, 12 hours of dark cycle in a temperature-controlled environment. Females, aged older than eight weeks and of weight more than 20g, were monitored for signs of being in oestrus, when the vagina becomes slightly pink and swollen, to aid successful mating. Each female mouse that was in oestrus in the early evening was mated with a male of the same strain. The following morning the females were checked for a vaginal plug, which is usually white and hard. The presumed time of conception was at midnight, the mid-point of the dark period, with the day the vaginal plug was observed considered as embryonic day 0.5 (E0.5).

Dissection

Postnatal mice

The mice were killed by cervical dislocation. Mice more than six weeks of age were killed singly, for those between P0 and P14 two at a time were taken. After decapitation, the head was bisected sagittally, the brain removed and bulla taken out. The outline of the bulla was clearly visible after removal of the brain, and can be traced

through from the entrance of the auditory meatus. The bulla was carefully dissected away from the temporal bone and to allow thorough penetration of the fixative a small hole was made in the apex of the protective bony covering of the cochlea. Prior to sectioning the bulla was carefully opened to expose the cochlea.

Alternatively after dissection of the bulla the bony capsule was carefully removed to expose the cochlea and vestibular organs. These were dissected out separately into fixative if they were to be subsequently used for sectioning.

For molecular biology procedures the dissection was performed on ice and the cochlea and vestibular organs were transferred to cold eppendorff tubes. This was particularly important when the tissue was to be used for RT-PCR or western blots.

Embryonic mice

The time-mated female mouse was killed either by cervical dislocation or in a carbon dioxide chamber. The abdomen was opened to expose the bicornate uterus. The uterus was removed by cutting its attachments at the ovaries and the cervix, and placed in a petri dish containing cold phosphate buffered saline (PBS; Oxoid). The uterus was rinsed twice in PBS before being cut along its anti-placental border to remove the embryos. The embryos were then carefully freed of their deciduas and subsequently delivered from their yolk sacs, by cutting away the yolk sac where it joins the placenta. After the final membrane, the amniotic membrane, had been carefully peeled away, the embryos were decapitated with heads being immersed immediately in 4%

paraformaldehyde for one hour for fixation. If the embryos were to be used for RT-PCR or Western blot analysis they were stored immediately in liquid nitrogen prior to further dissection and processing as detailed later.

An alternative fixation was used prior to labelling with the Willecke Cx31 antibody. Tissue was fixed immediately after dissection in cold 100% ethanol for 30 minutes. Embedding and blocking proceeded as with paraformaldehyde-fixed tissue.

The embryos were staged according to Kaufman (1998) and Martin (1990), using the development of the forelimbs and hindlimb buds as indicators.

Immunocytochemistry

In sections

After the tissue was fixed for one hour at room temperature it was washed in PBS. Otoliths were dissected out from the embryo heads and placed in 30% sucrose solution at 4°C overnight. Bullae from older animals were first decalcified in a 1% ascorbic acid, 0.8% sodium chloride solution (pH 2.5-2.6) for seven days in the dark; the solution was changed every second day (Merchan-Perez *et al.*, 1999), prior to immersion in 30% sucrose. Specimens were embedded in 1% low-gelling temperature agarose in 18% sucrose, mounted on chucks with OCT compound, frozen in liquid nitrogen, sectioned at 10-15µm thickness on a cryostat between -21 and -24°C and mounted on polylysine coated slides then stored at -20°C. Pre-incubation in block solution (100mM L-lysine, 10% dried skimmed milk in PBS) with 0.15% triton X-100

(Sigma) was followed by incubation overnight at 4°C in affinity-purified anti-connexin antibodies diluted appropriately for each individual antibody in block solution. Sections were washed six times over 40 minutes in PBS, and then the relevant biotinylated secondary antibody was applied for one hour at a dilution of 1:150 in PBS. After washes in PBS the sections were left in FITC-conjugated streptavidin in the dark for an hour, then washed with equilibration buffer for 10 minutes and mounted using “Slowfade Light” antifade glycerol mountant (Molecular Probes). Free radicals are produced when fluorescent molecules are excited by light. These have the effect of degrading the fluorescent molecules and cause fading. The antifade reagent acts as a free-radical scavenger and so slows the fading. Observation and photography of the sections was performed using either fluorescence or confocal microscopy (Nikon Optiphot-2 or Leica TCS4D Confocal Laser Scanning Microscope). Liver, heart and brain tissue from adult mice was used as a positive control; omission of primary antibodies from some sections provided a negative control.

A total of 26 adult mice were used for immunocytochemistry sections.

In wholemounts

The same methodology as for frozen sections was used but processing took place in a 72-microwell plate. When mounting the specimens either specially designed slides were used or a protective nail varnish boundary was painted onto the slide prior to sealing with a coverslip to prevent squashing the tissue. 9 adult mice were taken for wholemount studies.

Propidium iodide (Sigma) stains nucleic acids and therefore labels nuclei. In some wholmount tissue propidium iodide was applied at the same time as the secondary antibody to observe double-labelling of connexin and cell nuclei. This was used at a concentration of 1µg/ml with 100µg/ml DNase-free ribonuclease A (Sigma) in PBS.

Antibodies

When more anti-connexin antibodies became available for use it was soon apparent that some antibodies are more efficient and some more specific than others. For all immunostaining experiments a relevant positive control tissue was used (see appendix 1). The negative control was a cochlea section processed alongside other sections and using the same protocol but with the omission of a primary antibody. It was also necessary to check the specificity of the Cx26 and cx30 antibodies due to the colocalisation seen and in the knowledge that these two isoforms have a very similar sequence (see Chapter Six).

RT-PCR

Polymerase chain reaction (PCR) is a technique used to amplify a specific sequence of DNA. Oligonucleotide primers are designed that flank this specific sequence so when added to the DNA with DNA polymerase and deoxyribonucleoside triphosphates synthesis of a complementary DNA strand occurs between the primers. The three steps involved are denaturation of the DNA to be amplified, annealing of the primers and synthesis of the new strands. After the second cycle of this process the strands

produced can themselves act as templates for production of more DNA which leads to an exponential accumulation of product in each successive cycle. Addition of a reverse transcriptase to extracted RNA provides the cDNA.

The cochlea and vestibular sensory epithelia from postnatal mice were dissected out separately and RNA extracted for RT-PCR analysis, for embryonic mice RNA was extracted from the whole otocyst. For each preparation, 8-10 auditory bullae were dissected on ice. RT-PCR was performed at least three times for each primer.

Oligonucleotide primers were designed for Cx26, Cx30, Cx32, Cx43 and Cx46.6 using the Primer3 program.

Connexin 26 U1 5' -TTCAGACCTGCTCCTTACCG-3'
 L1 3' -GGAAGTGGTGGTCGTAGCAT-5'

Connexin 30 U1 5' -AGGAAGTGTGGGGTGATGAG-3'
 L1 3' -AGGTAACACAACCTCGGCCAC-5'

Connexin 32 U1 5' -CAGACACGCCTGCATACATT-3'
 L1 3' -CCTCAAGCCGTAGCATTTTC-5'

Connexin 43 U1 5' -AATGAGGCAGGATGAACTGG-3'
 L1 3' -CATGAAGACAGCCTCGAACA-5'

Connexin 46.6 U1 5' -AACGTCTGCTATGACGCCTT-3'
 L1 3' -GGCAGCTGACCACGTACATA-5'

Primers for five other isoforms were constructed according to data from Davies *et al.* (1996).

| | | |
|-----------------------------|----|-----------------------------|
| <i>Connexin 30.3</i> | U1 | 5' -TCAAACATGGGCCCAATG-3' |
| | L1 | 3' -CGAACGAGACACTGAGGG-5' |
| <i>Connexin 31</i> | U1 | 5' -AGAAGCACGGGGAGCAAT-3' |
| | L1 | 3' -GTCACGCGGTTCGTATCAT-5' |
| <i>Connexin 37</i> | U1 | 5' -GGCTGGACCATGGAGCCGGT-3' |
| | L1 | 3' -CGGGGGGTCCCACCGGCTTT-5' |
| <i>Connexin 45</i> | U1 | 5' -AATGCTAAGATTGCCTACA-3' |
| | L1 | 3' -AATCATCGTTTAGTCCCC-5' |
| <i>Connexin 50</i> | U1 | 5' -CATCCTGCCCCTCTATC-3' |
| | L1 | 3' -TTCACCTCGCCCTTCTC-5' |

Alignments were performed on each set of primers with all connexin isoforms to exclude cross-reactivity.

PCRs were run with initial denaturation at 94°C, followed by 35 cycles of 94°C for 30 seconds, 60°C for 30 seconds, and 72°C for 45 seconds, with a final extension at 72°C for 7 minutes. PCR products were run on a 2% agarose gel with ethidium bromide at

80mV for 1 hour. Glyceraldehyde-3-Phosphate Dehydrogenase (GAPDH) primers were used as a positive control, nucleotide-free water used as a negative control in each PCR experiment. The GAPDH primer sequences are shown below;

| | |
|--------|----------------------|
| GAP-U1 | AACTTTGGCATTGTGGAAGG |
| GAP-L1 | TGTGAGGGAGATGCTCAGTG |
| GAP-U2 | ACTCACGGCAAATTCAACG |
| GAP-L2 | ATGCAGGGATGATGTTCTGG |

Optical densities at 260nm and 280nm wavelengths were measured to assess the quantity and purity of the RNA from each sample.

Western Blot

Polyacrylamide gel electrophoresis (PAGE) is a method by which proteins can be separated according to their size. Larger molecules are impeded more than smaller molecules as they migrate through the pores of the gel. Proteins need to be treated with sodium dodecyl sulphate (SDS) detergent prior to the electrophoresis to remove their secondary and tertiary structures; this also coats them with a negative charge to aid the movement through the gel.

A process, known as blotting, enables the proteins to be transferred onto a nitrocellulose membrane for identification with specific antibodies.

Dissected tissue from 10 to 12 auditory bullae was homogenised in a mixture of 1mM NaHCO₃, 5mM ethylene diamine tetra acetate (EDTA), 1mM PMSF, 1mM sodium

orthovanadate (NaV) and 10mM sodium fluoride (NaF) that acted as protease inhibitors. To 40µl of each sample was added 40µl of 2x sample buffer (100mM Tris base, 20% glycerol, 4% SDS, 10% 2-mercaptoethanol, 0.2% bromophenol blue adjusted to pH6.8) before brief sonication. 10µl was then loaded into the individual wells of the acrylamide gel (see appendix 2). A lane of rainbow molecular weight markers was also loaded so progress of the gel could be monitored and approximate weights of proteins could be estimated after visualisation of the proteins. Gels were typically run at 100-150 Volts for 90-120 minutes.

Some gels were stained with Coomassie blue to check the migration and separation of the proteins. Coomassie blue stain was made up as 50% methanol, 0.05% Coomassie blue (Biorad), 10% acetic acid, and 40% water. The gel was placed in Coomassie blue stain for two hours, then into destaining solution in a container lined with tissue to absorb the stain for five hours on a rocking platform. The destaining solution was 7% acetic acid, 5% methanol, and 88% water.

Blotting onto a nitrocellulose membrane was via electrophoresis at 30 Volts overnight. The membrane with proteins bound to it was now blocked in 5% skimmed milk powder in TBS-T for an hour prior to incubation in primary antibody solution for a further hour (dilutions ranged from 1:1000 to 1:5000 in block solution according to the antibody). Three 10-minute washes in TBS-T (tris-buffered saline with Tween) removed any unhybridised primary antibody before incubation in horseradish peroxidase (HRP) conjugated secondary antibody at 1:10000 in block solution. After another wash series

the blot was developed using a commercial kit (ECL Amersham Pharmacia Biotech) that utilises the chemiluminescence resulting from the HRP-catalysed breakdown of luminol. This chemiluminescence was detected by exposing a piece of X-ray film to the blot in the dark for a length of time determined by the strength of the signal, usually between 30 seconds and 5 minutes.

Sometimes the blot could be stripped without affecting the bound proteins and re-incubated with a different primary antibody then processed with HRP-conjugated secondary antibody and developed. To strip a blot it was placed in 0.2M sodium hydroxide for an hour then washed in TBS-T solution for 30 minutes.

Freeze fracture technique

Bullae were rapidly removed and fixed with 2.5% glutaraldehyde in 0.1M cacodylate buffer (pH7.3) for 1.5 hours. Following rinsing in cacodylate buffer, samples were dissected into separate pieces of basal and apical cochlea, stria vascularis and spiral ligament, and vestibular organs whilst in cacodylate buffer. The pieces were then infiltrated with 25% v/v glycerol in 0.1M sodium cacodylate in distilled water, at room temperature, under gentle rotation for 45 minutes. Individual pieces of tissue were packed between two specimen holders using a yeast/glycerol paste then rapidly frozen in liquid nitrogen-cooled propane:isopentane 4:1. Fracturing took place at 115°C in a Balzers BAF400 high vacuum freeze-etch unit. Samples were then shadowed with platinum-carbon from 45° and backed with carbon from 90°. The replicas were cleaned

in 40% chrome-sulphuric acid. Freeze fracture replicas were observed on a scanning electron microscope.

Dye Transfer

Strips of organ of Corti and tissue from the cochlear lateral wall were attached to coverslips with BD Cell-TakTM Cell and Tissue Adhesive immediately after dissection. The tissue was bathed in Hanks' balanced salt solution (HBSS) with 0.1M HEPES as the injections were performed using Lucifer Yellow dye.

In vitro connexin expression system

HeLa cells were cultured at 37°C in medium made up as 10% Foetal Calf Serum, 1% Penicillin, 1% Anti PPLO (an antibiotic against mycoplasma and Gram positive bacteria), 0.5% Fungizone and 87.5% Dulbecco's modified Eagle's medium (DMEM). Plasmids were microinjected in to HeLa cells with an Eppendorf microinjection system 500µg/ml for 0.2 seconds at 100hPa. Howard Evans, Cardiff, kindly donated the rat Cx26 cDNA clone in PCDNA3. To obtain mouse cDNA for connexin 30 primers were designed using the Primer3 program and the Cx30cDNA clone was also in PCDNA3 (Invitrogen).

Twenty-four hours after microinjection cells were fixed with 4% paraformaldehyde and then immunostained with either antiCx26 or antiCx30 antibodies as described for frozen sections and wholemounts in the immunocytochemistry section earlier in this chapter.

Processing tissue for immunogold staining

Immunogold staining

Cochleae from mice and guinea pigs were fixed in 2% paraformaldehyde, alone or supplemented with 0.025% glutaraldehyde in PBS, pH7.3, for 1 hour then rinsed in PBS. Tissue was then dehydrated in an alcohol series and embedded in LR Gold plastic. The plastic was polymerised with UV light at -30°C . Sections were cut onto nickel 200 mesh grids, pre-coated with 'grid glue'. Grids were then blocked for 30 minutes in a solution of 10% horse serum and 100mM l-lysine in PBS. The incubation in primary antibody, diluted 1:50 in PBS, was overnight in a moist chamber at 4°C . After three washes in PBS with 0.15% tween grids were incubated in the appropriate gold-labelled secondary antibody at a dilution of 1:50 for one hour. Three washes in PBS with 0.15% tween followed by three washes in distilled water preceded a post-label fixation in 0.25% glutaraldehyde in PBS. Grids were stained lightly with uranyl acetate and lead citrate prior to observation of the sections by transmission electron microscopy.

LacZ method

β -galactosidase is the product of the lacZ gene from *Escherichia Coli*, it is this that can be detected as indigo blue staining following reaction with 5-bromo-4-chloro-3-indolyl β -D-galactopyranoside (X-gal).

Mice with Cx46, Cx50 or both isoform genes knocked-out from two different strain backgrounds have been studied using the LacZ expression system. A portion of DNA responsible for encoding the four transmembrane domains of connexin was removed

from the exon and replaced by a lacZ-nls gene (Bonnerot *et al.*, 1987) followed by a PGK *neo* gene to create a targeting vector. This vector is then transfected into embryonic stem cells and their mutated DNA subsequently used to generate male chimeras. Genotype of offspring was determined using PCR techniques. The knockout mice (Cx46^{-/-} and Cx50^{-/-}) used for experiments included in this thesis were kindly donated by the laboratory of the late N.B. Gilula (TSRI, La Jolla, USA). Three adult Cx46^{-/-} and Cx50^{-/-} mice were studied to look for expression in mature mouse inner ear. Four littermates from three different litters were taken at stages E15.5, E18.5, P0 and P4 for the developmental study of Cx50^{-/-} mice.

After dissection tissue was fixed in 2% PFA for 3 hours then washed three times in PBS. This fixation protocol was shown to preserve histology whilst giving good signal. The X-gal reaction was allowed to occur overnight at 37°C in the dark. The X-gal reaction mix is 1mg/ml of X-gal in 1x reaction buffer (35mM potassium ferricyanide, 2mM MgCl₂ in 1x PBS). Tissue was then washed thoroughly in PBS and left in 30% sucrose overnight prior to embedding in low gelling temperature agarose for sectioning as described earlier.

Plastic sections

The laboratory of Dr. D. Becker donated $cx43^{-/-}$ mice; these mice do not survive postnatally so tissue was taken at either E18.5 or P0 (immediately after birth). Five littermates were taken from three different litters, genotyping was carried out in Dr. Becker's laboratory. Tissue was fixed in 2.5% glutaraldehyde in 0.1M cacodylate for 1-2 hours then washed in 0.1M cacodylate buffer for 20 minutes. Samples were immersed in 1% osmium tetroxide in cacodylate buffer for 1 hour then washed well in buffer. Dehydration through a series of alcohols preceded overnight treatment with uranyl acetate stain. Tissue was then placed in propylene oxide for two sessions of 15 minutes prior to immersion in Agar 100 resin (Agar Scientific) made up as 3:1 propylene oxide to resin for 2 hours then transferred to 1:1 propylene oxide to resin mix overnight. The resin was polymerised for 24 hours at 60°C.

Clearing

Otocysts from five littermates were dissected out into Bodian's fixative (75% ethanol, 15% water, 5% formalin, 5% glacial acetic acid) and left for 24 hours at room temperature. Dehydration through a graded series of ethanol for 30 minutes each preceded clearing in methyl salicylate overnight. This technique was based on a methodology used for paint-filling cochleae from Martin and Swanson (1993). It is important to use only glass equipment as methyl salicylate dissolves some plastics.

CHAPTER THREE

Identification of Inner Ear Gap Junctions **Using Freeze-Fracture**

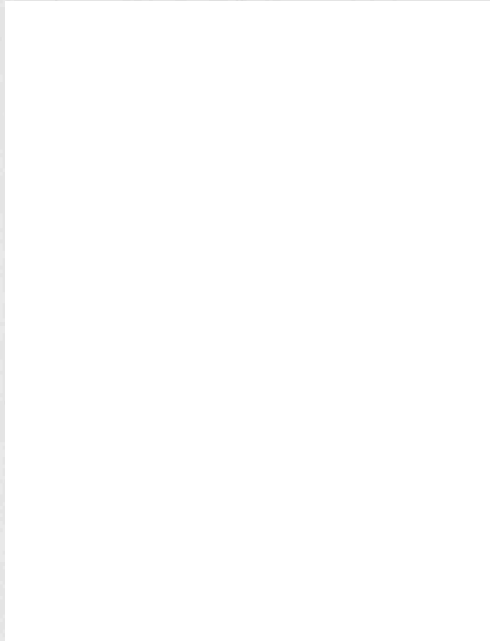
Introduction

This chapter describes work undertaken prior to the start of this project and studies performed alongside the investigations described in the thesis (by A. Forge and G. Nevill) and serves as a second introduction by describing the locations of gap junction plaques throughout the inner ear. The images shown in this chapter are from freeze fracturing by Forge and Nevill then collated by the author; there is one image from freeze-fracturing of an E16.5 cochlea which was produced by the author. Gap junctions are too small to be viewed directly by histological light microscopy. Through advances in thin-section transmission electron microscopy, using lanthanum as an extracellular tracer (Revel and Karnovsky, 1967), and the advent of freeze fracture electron microscopy the details of gap junction structure could be elucidated. Fracturing a frozen tissue sample causes splintering along the hydrophobic interior of the plasma membrane revealing gap junctions in face view as clusters of intramembranous particles, on the protoplasmic faces with matching pits on the exoplasmic faces (Pinto da Silva and Branton, 1970) (see Figure 3.1). Each of these intramembranous particles corresponds to a connexon (Goodenough, 1975). Freeze fracture electron microscopy is invaluable as a technique that allows assessment of the size, shape, contours, layout and general distribution of gap junction plaques (Green *et al.*, 1993). Gap junctions are pleomorphic and can range in size from tens to thousands of intramembrane particles.

Freeze fracture studies in many different species support the demonstration of abundant, often large, gap junctions in the inner ear. In 1975 Jahnke studied the distribution and size of both tight and gap junctions within the guinea pig inner ear. He reported that

many gap junctions of various sizes interconnect the fibrocytes of the spiral ligament to each other and to the basal cells of the stria vascularis, and that all stria vascularis cells express gap junctions. The prominent conclusion was that gap junctions were seen to couple all supporting cells of both the organ of Corti and vestibular epithelia.

Figure 3.1. Freeze fracture electron microscopy of gap junctions



Freeze fracture replica showing intramembranous particles on the protoplasmic face (P) and pits on the exoplasmic face (E).

A detailed study of gap junctions in the chinchilla cochlea (Iurato *et al.*, 1976) also showed gap junctions between all supporting cells, with those between the footplates of inner pillars and outer pillars, and between Deiters' cell bodies being numerous and exceptionally large. Gap junctions were never observed between supporting and sensory cells, between sensory cells and nerve endings, or between nerve fibres. This paper concluded that gap junctions link all supporting cells electrically and metabolically.

Additionally, the basilar papilla of the lizard, *Calotes versicolor*, was found to have gap junctions only between neighbouring supporting cells; sensory hair cells never expressed gap junctions. The size and distribution of the gap junctions varied, but they were reported to "occupy substantial regions of the contact area between the supporting cells" in the basal part of the epithelium (Bagger-Sjöbäck and Flock, 1977).

Gap junctions have been observed on hair cells of the goldfish saccular macula (Hama, 1980). The only other study to observe gap junction-like arrangements between hair cells and supporting cells was by Nadol in 1978. This paper reported these structures in thin sections from human and cat organ of Corti; however, a dense material filled the gap in-between the membranes that is not normally seen suggesting that these structures were not gap junctions.

Another freeze fracture study by Forge (1984) using guinea pigs and gerbils showed a few, small gap junctions on the head region increasing in number towards the base of

Deiters' cells. The body region of pillar cells was shown to be particularly well endowed with gap junctions.

K⁺ ion-recycling hypothesis

Freeze fracture of the stria vascularis has shown gap junctions to occupy up to 16% of the basal cell plasma membrane in rodents (Forge 1984). Analysis of the location of the gap junctions in the organ of Corti led to the hypothesis that they are important in the potassium ion (K⁺) recycling which is essential for normal auditory function (Kikuchi *et al.*, 1995; Forge *et al.*, 1999; Kikuchi *et al.*, 2000; Wangemann, 2002). The apical surface of the epithelium is bathed in K⁺ rich endolymph, and K⁺ current passes through the hair cell along an electrochemical gradient to the low K⁺ environment around the basolateral surface of the supporting cell. The proposal suggested that supporting cells take up K⁺, perhaps through the action of the K-Cl transporter Kcc4 (Boettger *et al.*, 2002); then the ions are passed, via gap junctions, medially through inner sulcus cells or via the fibrocytes of the spiral limbus to interdental cells whereupon they are released back into the endolymph. Recycling of ions after release from outer hair cells is thought to be via a lateral route through Deiters', Hensen's, Claudius' and outer sulcus cells to the fibrocyte populations of the lateral wall from where they pass through the basal cells and to the intermediate cells of the stria vascularis. The following sequence of freeze fracture images demonstrates the location, size and number of gap junctions throughout the inner ear. This chapter is a survey of all gap junctions within the inner ear visualised using freeze-fracture, performed by A. Forge and G. Nevill, and provides a context for the results shown in subsequent chapters.

Results

The membranes of all non-sensory cells of the organ of Corti exhibit gap junction plaques. Starting at the inner edge of the cochlear duct the inner sulcus cells are seen to be connected by large gap junctions. These plaques are often greater than $0.5\mu\text{m}$ in diameter (figure 3.2).

Figure 3.3 shows pillar cell gap junctions as seen by freeze fracture electron microscopy. At the apex of pillar cells, where inner and outer pillar cells are connected, gap junctions are numerous but small (Fig. 3.3(a)). In contrast, those seen more basally between inner pillar cell bodies (Fig. 3.3(b)) are much larger. These smaller gap junction plaques at the apex connect inner and outer pillar cells in the radial direction; junctions between the cell bodies of neighbouring inner pillar cells are extremely large often seen to occupy the majority of the cell body membrane and connect the inner pillars longitudinally.

Figure 3.2: Inner sulcus cell gap junctions



- (a) Arrows show the position of gap junction plaques
- (b) Higher magnification view of the junctions seen in (a)

Figure 3.3: Gap junctions between pillar cells



Boxed area in (i) is shown at a higher magnification in (ii)

Gap junctions exposed by freeze fracturing between Deiters' cell membranes are shown in Figures 3.4(a) and (b). Figures 3.4(a) shows the smaller gap junction plaques at the apex of the cell where the Deiters' cells contact. The gap junction plaques situated more basally in the Deiters' cell bodies are much larger (Fig. 3.4(b)). Gap junctions between Deiters' cells appear to be arranged to enable communication both longitudinally and radially.

Moving laterally across the organ of Corti Figure 3.5(a) shows large gap junctions at the apex of a Hensen's cell. Gap junctions of an outer sulcus cell are shown in Figures 3.5(b)(i) and at higher magnification in 3.5(b)(ii).





In the cochlear lateral wall gap junctions are present between spiral ligament fibrocytes and are associated with basal and intermediate cells of the stria vascularis. There are numerous, large gap junctions between the fibrocytes of the spiral ligament. Basal cells are coupled to other basal cells in both the radial and longitudinal directions in the spaces between the elements of the tight junctions; basal cells are also connected via gap junctions to spiral ligament fibrocytes and to stria intermediate cells where the plaques are seen to be numerous and relatively small. Figure 3.6 shows freeze fracture replicas of gap junctions between stria basal cells, between a basal cell and a cell of the spiral ligament, and between the fibrocyte cells of the spiral ligament. That gap junctions are not present between basal cells and marginal cells is suggested by their absence from both the basal projections of marginal cells and the cell body region of the marginal cells. The marginal cells are a separate population that are not connected to each other or to the rest of the stria vascularis by gap junctions. Figure 3.6(a) shows the gap junctions between a stria basal cell and a spiral ligament fibrocyte. Figure 3.6(b) demonstrates the gap junctions between spiral ligament fibrocytes. Figures 3.6(c, d, e and f) are a collection of gap junctions expressed in basal cells of the stria vascularis in a variety of animal species. Figure 3.6(e) shows the numerous, large gap junctions between a stria basal cell and intermediate cell.



Gap junctions are also present between supporting cells of the sensory organs within the vestibular system. Again, the hair cells of the vestibular sensory organs do not have gap junctions. Figure 3.7 shows several gap junction plaques on the body of a supporting cell of the crista ampullaris. The supporting cells of a vestibular macula also exhibit gap junctions (Fig. 3.8). The gap junctions of the vestibular supporting cells show a similar generalised distribution pattern to that of the organ of Corti non-sensory cells in that there are smaller plaques towards the luminal side and larger ones towards the base in the cell body region.

Figure 3.7: Gap junctions of the crista ampullaris



FIGURE 3.8: Vestibular macula gap junctions (guinea-pig)



Figure 3.9 is a sketch diagram that summarises the relative size and location of gap junctions throughout the organ of Corti. This diagram demonstrates that all supporting cells are linked via gap junctions but that hair cells do not have gap junctions. It also shows the difference between the large junctions seen between cell bodies and the smaller gap junctions at the apices of pillar and Deiters' cells.

Figure 3.10 is a similar diagram showing the gap junctions of the stria vascularis. There are numerous gap junctions between basal cells and fibrocytes of the spiral ligament, between adjacent basal cells and between basal cells and intermediate cells. The marginal cells are isolated from the rest of the stria vascularis; they don't have gap junctions so are not directly coupled to other marginal cells or intermediate cells or basal cells. The distribution of gap junctions within the cochlear lateral wall indicates that the spiral ligament fibrocytes, basal cells and intermediate cells are functionally allied and that the marginal cells are isolated from other marginal cells and separate from this syncytium.

From these two figures it is easy to recognise how the hypothesis that gap junctions play a role in ion recycling was formulated.

FIGURE 3.9



Figure 3.11 is a freeze fracture image from an E16.5 mouse cochlea, produced by the author (J. Edwards). This is from a preliminary study observing gap junction structures in the developing mouse inner ear.

Figure 3.11

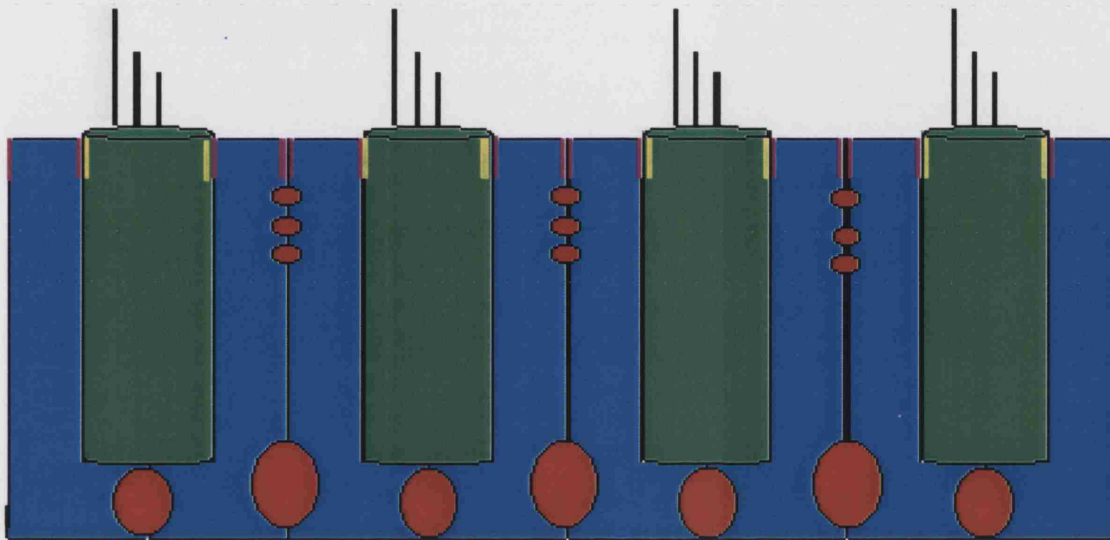


Discussion

Proper functioning of the cochlea is reliant on the properties of cell membranes and intercellular junctions. Membrane properties and specialisations are easily viewed by freeze fracturing the tissue and observing the exposed membranes by transmission electron microscopy. The presence of gap junctions, seen as plaques of large particles, is thought to enable ionic and electrical coupling between cells.

In the ear gap junctions are seen exclusively between supporting cells of the organ of Corti and vestibular sensory organs, and between intermediate and basal cells of the stria vascularis and cells of the spiral ligament. There appears to be a generalised distribution pattern of gap junctions in both the organ of Corti and vestibular sensory patches summarised by a sketch diagram in Figure 3.12. The luminal ends of cells express smaller gap junction plaques whereas there are larger gap junctions in the cell body regions; this pattern is also repeated in avian and reptile basilar papillae and vestibular organs (A. Forge, personal communication). Non-sensory cells of the organ of Corti and of the vestibular system are evidently connected via gap junctions in all directions with the possible exception of the pillar cells. In a theoretical model it was shown that scattered gap junctions have higher communication efficiency than compact plaques with an equal number of connexons (Chen and Meng, 1995).

Figure 3.12: Sketch diagram summarising the general distribution of gap junction plaques within sensory epithelia



This diagram has been constructed using the results from several different freeze fracture replicas. The red oval shapes represent gap junctions showing that plaques at the apex of cells are much smaller than those at the base of the cells; purple lines correspond to tight junctions. The green cells are general sensory cells, which do not express gap junctions, the blue cells are the non-sensory cells connected via gap junctions.

The freeze fracture images in this chapter show gap junction locations correlate well with the theory that supporting cells may provide a route for recycling potassium ions (Kikuchi *et al.*, 1995; Forge *et al.*, 1999; Kikuchi *et al.*, 2000; Wangemann, 2002). It is suggested that supporting cells take up K^+ , perhaps through the action of the K-Cl co-transporter Kcc4 (Boettger *et al.*, 2002) and the gap junctions provide an intracellular route for dispersion of K^+ away from the sensory region to maintain homeostasis. Marcus *et al.*, (2002) showed that mice lacking the potassium channel, KCNJ10 (Kir4.1), in their intermediate cells do not generate an E.P. Their studies on these knockout mice also demonstrated that in conjunction with other transport pathways this K^+ channel provides the molecular mechanism for generation of the E.P.

The ion-transporting epithelia of the inner ear are the dark cell region of the vestibular system and the stria vascularis in the cochlea. The dark cell region of the vestibular system is a single layer of ion transporting cells; their basolateral membranes are infolded and have high levels of Na^+/K^+ ATPase and a $Na^+/K^+/Cl^-$ co-transporter (Wangemann and Schacht, 1996). The dark cells are exposed to perilymph in the extracellular spaces of the underlying connective tissue. The K^+ ions enter the vestibular dark cells via the transporters from the perilymph and diffuse into the endolymph through K^+ channels in the apical membrane. Marginal cells of the stria line the endolymphatic space and, similar to the vestibular dark cells, have extensively infolded basolateral membranes that possess Na^+/K^+ ATPase and a $Na^+/K^+/Cl^-$ co-transporter. It is thought that they actively take up K^+ and circulate it back to the endolymph; these cells do not have gap junctions. Basal cells of the stria are coupled to other basal cells, intermediate cells of the stria and fibrocytes of the spiral ligament. Fibrocytes of the

spiral ligament are coupled to each other via gap junctions and are rich in Na^+/K^+ ATPase (Schulte and Adams, 1989; Schulte and Steel, 1994) suggesting that they may take up K^+ from the perilymph around them. This data indicates that stria and spiral ligament gap junctions play an essential role in providing an intracellular pathway for the K^+ from perilymph to the basolateral membranes of marginal cells. It is also apparent that the endocochlear potential is generated by this K^+ discharge from basal or intermediate cells into the extracellular spaces of the stria vascularis. Evidence for this comes from studies of a mouse mutant, the *viable dominant spotting* mouse, which has no recordable endocochlear potential despite having morphologically normal marginal cells (Steel *et al.*, 1987; Carlisle *et al.*, 1990; Shulte and Steel, 1994). This mutant doesn't have intermediate cells though which indicates that either intermediate cells or the intermediate cell / basal cell complex is the vital factor for endocochlear potential generation. It is possible that some connexin mutations cause only deafness due to the extreme importance of ion homeostasis in the cochlea. A study of cochlear development in gerbils showed endocochlear potential generation correlates with the appearance of gap junction plaques on stria basal cell membranes (Souter and Forge, 1998).

There is also evidence that gap junctions are involved in repair after damage to the sensory epithelia. New gap junctions are seen to form where the lateral membranes of supporting cells come together to close a lesion both in the organ of Corti (McDowell *et al.* 1989) and in the vestibular system (Prof. A. Forge, unpublished observation). It is possible that these gap junctions are required for the passage of signalling molecules necessary for the repair process.

Another suggestion is that the gap junctions may play a role in maintaining the structural integrity of the organ of Corti. This idea is particularly appealing with reference to the huge pillar cell junctions, which cover most of the lateral membrane of these cells that form the arch between the inner and outer hair cells. Further evidence for this possibility comes from immunogold labelling results that showed no annular gap junctions in the pillar cells. Annular gap junctions are formed as a method of gap junction degradation, the absence of these in pillar cells suggests a lower level of gap junction turnover in these particular organ of Corti cells.

CHAPTER FOUR

Connexin Expression in the Mature Mouse **Inner Ear**

Introduction

A comprehensive study of the chicken otocyst by Ginzberg and Gilula in 1979 first described inner ear gap junctions. In the pre-innervation sensory epithelium homogeneous cells are joined at their apices by tight and gap junctions with some smaller gap junctions also found along the lateral membranes. In these early stages the gap junction plaques are small, but were seen to increase in size and number throughout development. At stages just before the first appearance of hair cells, a high incidence of internalised and annular gap junctions was observed. From the presumptive stage through to maturity hair cells of the inner ear do not have gap junctions. One of the earliest noted hair cell specialisations was this absence of gap junctions.

Gap junctions are known as points of intercellular connection, however their presence alone is not proof of electrical and metabolic cell coupling. In the initial study of functional coupling by Santos-Sacchi and Dallos (1983) electrical measurements indicated ionic coupling between Hensen's cells in both *in vivo* and *in vitro* preparations of guinea pig organ of Corti. However, there was no dye transfer of either Lucifer Yellow or 6-carboxyfluorescein between cells observed for an hour after initial injection. It was suggested that dye transfer might be very slow or that the dilution within the cytoplasm meant it could not be visualised. Dye coupling was demonstrated between Hensen's cells and Deiters' and the outer pillar cells of the organ of Corti using fluorescein and 6-carboxyfluorescein (Santos-Sacchi, 1986). It was thought that Hensen's cells had been damaged by photoinactivation when illuminating the intracellular dye in earlier studies, thus preventing any transfer of Lucifer yellow dye.

Subsequently, the effects of changing conditions on the electrical pairing were examined. The effects of altering pH on the electrical coupling of Hensen's cells *in vitro* showed that cytoplasmic acidification decreased the coupling ratio (Santos-Sacchi, 1985). Reversible uncoupling was achieved using CO₂-saturated medium. Injection of hydrogen ions directly into one Hensen's cell was seen to uncouple that cell specifically, with other cells in the tissue remaining coupled.

Temperature had been shown to affect both cochlea electrophysiology (Coats, 1965) and communication through gap junctions (Payton *et al.*, 1969). A study that entailed lowering the temperature of an organ of Corti preparation from 37°C to 15°C gave a positive correlation between temperature reduction and cell uncoupling (Santos-Sacchi, 1986). Membrane potentials and cell coupling returned to normal levels upon warming.

Differences in voltage dependence of gap junctional conductance between supporting cells led to speculation that junctional channels may be heterotypic or heteromeric. The different combinations of connexin isoforms within gap junctions may create directional intracellular pathways through the supporting cell populations (Santos-Sacchi, 2000).

In 1997 the first reports of mutations in a connexin gene causing hereditary non-syndromic deafness were published (Kelsell *et al.*, 1997; Denoyelle *et al.*, 1997). Kelsell and colleagues studied a Caucasian pedigree and found that a change in an amino acid, methionine to threonine, in codon 34 (M34T) of the Cx26 gene segregated with the profound deafness in the family. Screening of a large, consanguineous Pakistani family with recessive non-syndromic profound deafness for mutations in the

Cx26 gene found a substitution in the bases from G-to-A in codon 77 (W77X) in two affected individuals, resulting in premature truncation of Cx26 protein. Analysis of 65 Caucasian families, worldwide, affected by non-syndromic deafness found a probable mutation hotspot, 30delG, accounted for approximately 70% of the Cx26 mutant alleles (Denoyelle *et al.*, 1997). In effect, these mutations are null mutations leading to a complete absence of this connexin protein throughout the body which raised the question, “Why does a lack of functional Cx26 protein cause deafness?” In contrast, dominant Cx26 mutations can also cause syndromic diseases including KID syndrome (van Steensel *et al.*, 2002) and Vohwinkel syndrome (Maestrini *et al.*, 1999).

The fact that mutations which cause hearing loss do not cause a vestibular dysfunction (Cohn *et al.*, 1999) suggests a difference between the auditory and vestibular systems. It is possible that there may be some degree of functional compensation in the vestibular organs by other connexin isoforms. Alternatively the difference in physiology between the systems may account for why the balance organs are not affected.

An examination of guinea pig inner ear, by Prof. A. Forge, prior to the start of my study detected a difference in the isoforms expressed in the vestibular and auditory epithelia which fuelled the hypothesis that compensation via other connexin isoforms may occur in some organs that doesn't operate in the auditory system. The aim of this project was to identify and localise gap junctions and their constituent connexin isoforms throughout the inner ear.

Initial examination of the tissue of the inner ear was via reverse transcriptase polymerase chain reaction (RT-PCR) experiments. Extraction of RNA from whole cochleae allowed a preliminary screen for several connexin isoforms. RT-PCR is a very sensitive method enabling detection of even small amounts of RNA. Results from these experiments aided in the choice of connexin-specific antibodies for use in immunocytochemical and western blotting procedures.

Results

Mature mouse inner ear tissue was examined for ten different connexin isoforms using a variety of different techniques.

RT-PCR

Figure 4.1 shows the results of the RT-PCR experiments using mature tissue. Figure 4.1(a) shows the presence of both Cx30 and Cx43 in mature vestibular and cochlea tissue but proves the absence of Cx32 mRNA in these inner ear tissues. The presence of Cx26 mRNA in the cochlea is shown in figure 4.1(b). Three isoforms, Cx26, Cx30 and Cx43, were the only connexins out of the ten analysed that gave a positive result in RT-PCR experiments in adult inner ear. Figures 4.1(c) and (d) show negative results for Cx30.3, Cx31, Cx32, Cx37, Cx45 and Cx46.6 in mature mouse inner ear.

Table 4.1 gives details of the primers, their locations, the expected band sizes and the positive control tissues used. The expected band sizes are calculated according to the number of base pairs in the amplified region; the larger the amplicon, the heavier the product will be and therefore it will run through the gel more slowly than a smaller product. Alignments were performed on each set of primers with all connexin isoforms to exclude cross-reactivity. All mRNA preparations were tested with gapdh primers, which will give a positive band if RNA is present. Gapdh primers with nuclease-free water provided a negative control.

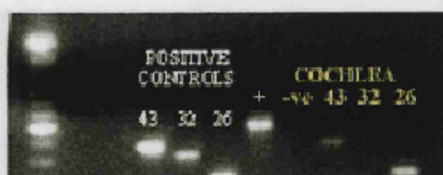
| CX | FORWARD | REVERSE | GENE | START | END | EXPECTED SIZE | POSITIVE CONTROL TISSUE |
|--------------------------|---------------------------------|----------------------------|------------------------------------|---------------|----------------|------------------|-------------------------------|
| 26 | β2 TTCAGACCTGCTC CTTACCG | GGAAGTGGTGGT CGTAGCAT | BC013634.1 | 134 | 439 | 305 | Liver |
| 30 | β6 AGGAAAGTGTGGG GTGATGAG | AGGTAACACAA CTCGGCCAC | BC013811.1 | 394 | 910 | 516 | Skin |
| 30.3 | β4 TCAAACATGGGCC CAATG | GGGAGTCACAG AGCAAGC | NM_008127.1 | 320 | 504 | 184 | Skin |
| 31 | β3 AGAAGCACGGGG AGCAAT | TACTATGCTGGC GCACTG | BC024387.1 | 382 | 549 | 167 | Skin |
| 32 | β1 CAGACACGCCCTGC ATACATT | CCTCAAGCCGTA GCATTTTC | AJ271753.1 (685- 749 7537-9004) | 685 exon 1 | 7880 exon 2 | 407 | Liver |
| 37 | α4 GGCTGGACCATGG AGCCGGT | TTTCGGCCACCC TGGGGGGC | NM_008120.1 | 532 | 953 | 421 | Heart |
| 43 | α1 TACCACGCCACCA CCGGCCCA | AAGGACTGCTG TCGGTTTACGG | NM_010288.2 | 825 | 1323 | 498 | Heart |
| 45 | α7 AATGCTAAGATTG CCTACA | CCCCTGATTTC TACTAA | NM_008122.1 | 1372 | 1621 | 249 | Heart |
| 46.6 | α12 AACGTCTGCTATG ACGCCTT | GGCAGCTGACCA CGTACATA | BC035840.1 Human seq | 260 | 896 | 636 | Whole embryo |
| 50 | α8 CATCCTGCCCCCTC TATC | CTCTTCCCGCTC CACTT | NM_008123.1 | 549 | 1026 | 677 | Lens |
| POSITIVE CONTROL PRIMERS | | | | | | | |
| GAPDH | AAC TTTGGCATTG TGGAAGG | TGTGAGGGAGAT GCTCAGTG | M32599 | 539 | 1138 | 599 | |
| GAPDH | ACTCACGGCAAAT TCAACG | ATGCAGGGATG ATGTTCTG | M32599.1 | 194 | 669 | 475 | |

Table 4.1: RT-PCR primers used with mature mouse RNA

Figure 4.1: RT-PCR of Mature Tissue



a) RT-PCR of mature vestibular and cochlea tissue. The positive controls used were liver and heart RNA. Water with GAPDH primers acted as a negative control, GAPDH primers were also used with the vestibular and cochlea RNA, represented by +.



b) RT-PCR of mature cochlea tissue. Positive controls were liver and heart RNA. GAPDH with cochlea RNA is represented by +. GAPDH with water is the negative control, -ve.



c) RT-PCR of mature mouse vestibular and cochlea tissue.

1 is water with GAPDH as a control
2 is GAPDH with vestibular RNA
3 is GAPDH with cochlea RNA
4 is Cx37 with heart RNA
5 is Cx37 with vestibular RNA
6 is Cx37 with cochlea RNA
7 is Cx32 with liver RNA
8 is Cx32 with vestibular RNA
9 is Cx32 with cochlea RNA
10 is Cx31 with skin RNA
11 is Cx31 with vestibular RNA
12 is Cx31 with cochlea RNA
13 is Cx30 with skin RNA
14 is Cx30 with vestibular RNA
15 is Cx30 with cochlea RNA



d) RT-PCR of mature cochlea tissue

1 is Cx46.6 with cochlea RNA
2 is Cx46.6 with whole embryo RNA
3 is Cx30 with skin RNA
4 is Cx30 with cochlea RNA
5 is Cx30 with cochlea RNA
(repeated because of problems loading sample into well 4)
6 is Cx45 with heart RNA
7 is Cx45 with cochlea RNA
8 is Cx30.3 with skin RNA
9 is Cx30.3 with cochlea RNA

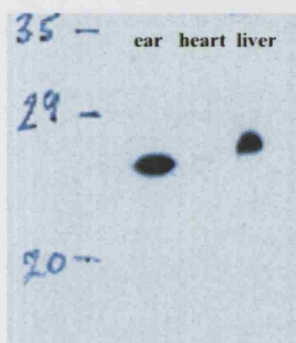
Western Blots

Figure 4.2 shows positive results from western blots with preparations of mature vestibular and cochlear tissue combined (labelled as “ear” in fig.4.2). Positive bands appear at the appropriate molecular weight position after incubation in anti-connexin antibodies. Figure 4.2(a) shows Cx26 is present in inner ear tissue and liver but not heart. Cx30 is present in inner ear tissue and kidney but not lens (fig.4.2(b)). Figure 4.2(c) shows Cx43 is present in inner ear tissue and heart tissue. No other isoform gave a positive result with mature inner ear tissue using this immunoblotting technique, Cx32 is shown here as being present in liver but giving a negative result with inner ear tissue (fig.4.2(d)).

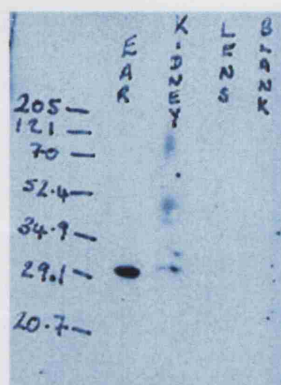
Table 4.2: Summary of Western Blot results in mature mouse ear

| Connexin isoform and antibody used | Present in mature ear? | Positive control tissue |
|---|-------------------------------|--------------------------------|
| Cx26 β2J and Gap28H | YES | Liver |
| Cx30 Anti-Cx30 (Zymed) | YES | Kidney |
| Cx31 β3S | NO | Skin |
| Cx32 β1J | NO | Liver |
| Cx43 α1J and α1S | YES | Heart |
| Cx45 α6J | NO | Heart |
| Cx46 α3J and α3S | NO | Lens |

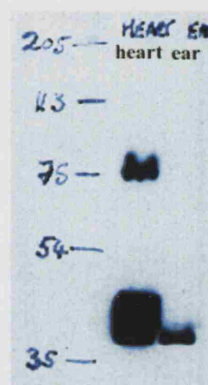
Figure 4.2: Western Blots



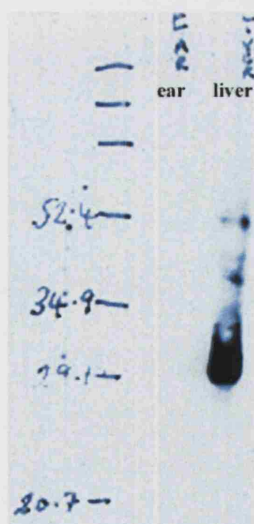
a) Western blot incubated in anti-Cx26 antibody



b) Western blot incubated in anti-Cx30 antibody



c) Western blot incubated in anti-Cx43 antibody



d) Western blot incubated in anti-Cx32 antibody

These western blots show preparations of mature tissues incubated in different anti-connexin antibodies then labelled via chemiluminescence. The numbers written on the side of the blots represent the positions of known molecular weight proteins in kiloDaltons.

Connexins are named according to their molecular weight so the positive bands would be expected to be at the level of the number within their name, for example Cx26 at the level of 26kiloDaltons.

Dye Transfer

Several attempts at *in vitro* dye transfer experiments were performed to assess functional coupling of the cells in the inner ear. The experiments with cochlear lateral wall cells showed a fibrocyte injected with Lucifer Yellow dye did not transfer the dye to neighbouring cells. It has since been reported that Cx30 gap junction channels do not pass Lucifer Yellow so this result cannot be properly interpreted. It would be valuable to repeat this dye transfer with other dyes, such as neurobiotin, to ascertain the functional coupling between cells of the inner ear. Attempts to study transfer between supporting cells of the organ of Corti were unsuccessful probably due to deterioration of the tissue prior to the injections. There was obvious injury caused by the dissection and attachment process. The methodology for this technique would need to be improved to ensure the tissue under investigation was well maintained and undamaged to accurately reflect the coupling *in vivo*.

Immunostaining

Using anti-connexin antibodies gap junction plaques are seen as dots (smaller junctions) or lines (large gap junctions) at the cell membranes where two cells are joined.

Connexin 26

Organ of Corti

Cx26 is expressed abundantly throughout the cochlea; however there is a distinctive pattern of immunostaining that suggests the absence of this isoform in some cell populations is also important to cochlear function.

In the organ of Corti Cx26 can be seen in the supporting cells and is notably absent from the sensory hair cells in accordance with the freeze fracture replicas shown in Chapter 3. This pattern of labelling can be seen in wholemount preparations with Cx26 between sulcus cells, Hensen's, Deiters' and pillar cells with notable absence of staining in the hair cell regions. Figure 4.3 is a wholemount labelled for Cx26 that displays extensive staining between all supporting cells of the organ of Corti, the hair cells do are not labelled. The inner sulcus region and Hensen's cells have been highlighted in Figure 4.3. To aid with locations of supporting cell populations Figure 4.4 is a diagram that relates the organ of Corti structure seen in cross section to the organ of Corti viewed as a wholemount preparation.

Figure 4.3: Immunostaining of Cx26 in a wholemount preparation of organ of Corti



Indicates the Hensen's cells region



Indicates the inner sulcus

ohc is the location of the outer hair cells

Figure 4.4: Diagram to show cells of the organ of Corti as seen in wholemount view



From freeze fracture replicas it is obvious that gap junctions between pillar cell bodies are extremely large. The previous immunostaining of a wholemount preparation (Fig.4.3) was not focussed at a level that shows these pillar cell junctions labelled with the Cx26 antibody. The immunostaining in Figure 4.5(a) shows that there are large, Cx26 containing junctions between pillar cells, the arrowhead highlights the pillar cell region, which correlates with the freeze fracture images. Figure 4.5(b) demonstrates extensive labelling of Cx30 between all supporting cell populations, including the pillar cells. Figures 4.5(c) and (d) show phalloidin-labelled hair cells, seen as red labelling of the actin, alongside staining for connexin, labelled green, to show that it is the supporting cell bodies that contain large gap junctions. Figure 4.5(d) shows Cx30 present around the cell bodies of Deiters' cells at the level of the actin bundles at the base of the cell.

The pattern of immunolabelling within cells is more obvious in frozen sections. There tends to be smaller punctate labelling at the apices of supporting cells, with larger plaques labelled between the cell bodies. The boxed area in figure 4.6(a) shows more intense labelling at the base of the supporting cells with punctate staining around the apices. Figure 4.6 (a) gives an overview of the Cx26 distribution in a cochlea turn. It is obvious that Cx26 is abundant in the organ of Corti, and in the fibrocytes of the spiral ligament. The position of the hair cells in fig.4.6(a) is notable by the absence of staining.

Figure 4.5: Pillar cell junctions



Figure 4.6: FITC-labelling Cx26 in a section of the adult organ of Corti



Immunolabelling in the cochlear lateral wall

There appears to be a lack of Cx26 present in the basal part of the lateral wall and in the stria vascularis, whereas the fibrocytes of the spiral ligament are profusely stained (Fig.4.7 (a)). The same distribution of staining was seen with the polyclonal anti-Cx26 antibodies (Gap28H, Des3 and Zymed anti-Cx26) and with the monoclonal β 2J antibody.

Initially the profusion of Cx26 staining in the spiral ligament fibrocytes masked the subtle lack of Cx26 in the stria vascularis. Only after closer observation of sections of lateral wall did it become apparent that Cx26 staining appears to be contained mainly between the fibrocytes with very small amounts, if any, in the stria vascularis. The plates in Figure 4.7 show the same section photographed under Nomarski imaging and under fluorescence microscopy for Cx30 and Cx26 respectively. They indicate differences between Cx26 and Cx30 expression in the stria, which is discussed in more detail later in this chapter. The arrowhead in Fig 4.7(c) and (d) points to the position of the same cell in both images, there is no connexin staining in this intermediate cell region. This figure is presented to show the differences between Cx26 and Cx30 staining in the lateral wall of the cochlea using sections showing the same region but from different cochleae.

Figure 4.7: Immunostaining in cochlear lateral wall



c) Nomarski image of a section through the cochlear lateral wall, arrowhead shows pigmented cell

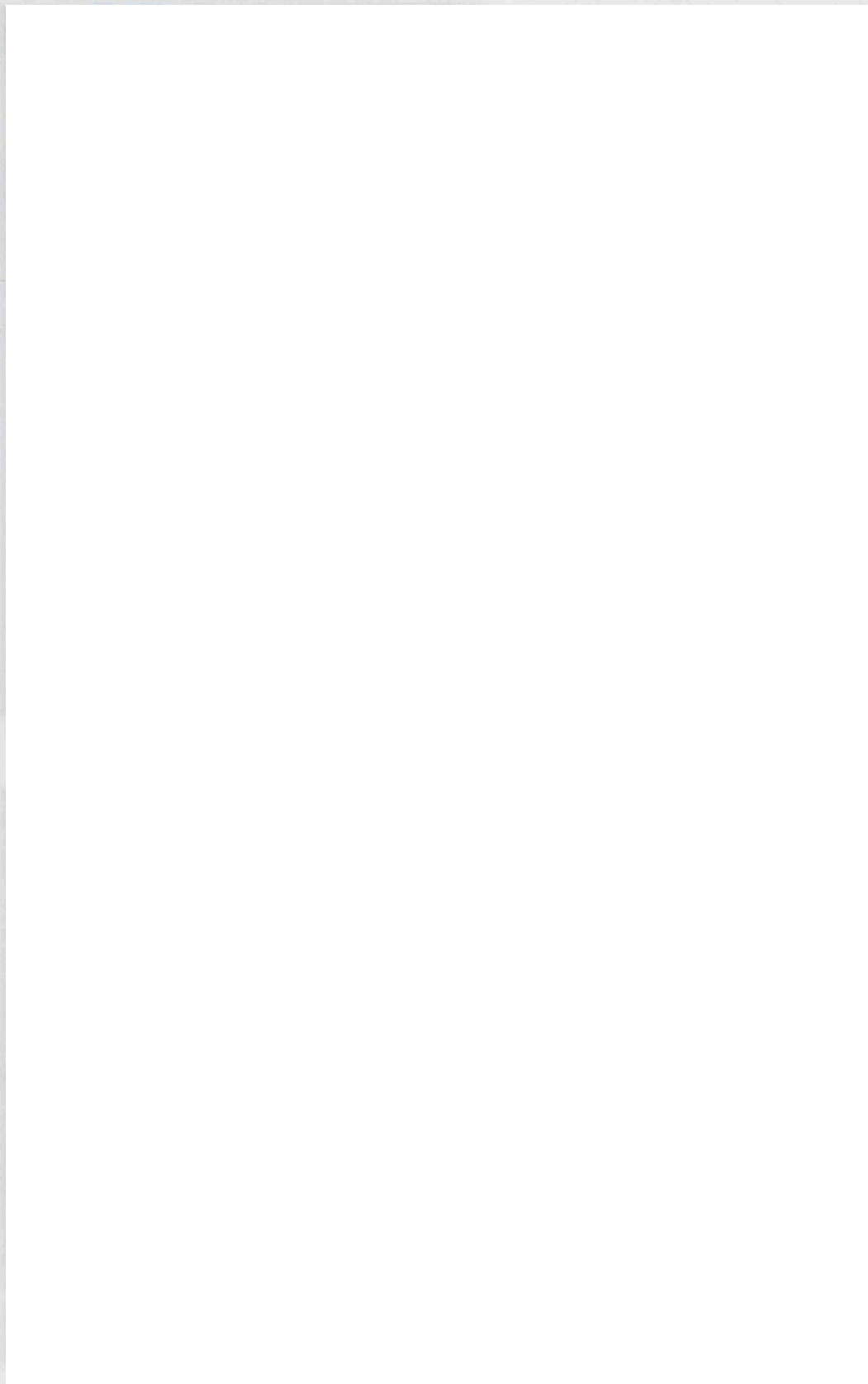
d) Same area as in c) under fluorescence microscopy showing FITC-labelled Cx26, arrowhead corresponds to same cell as that in c)

Vestibular system

Freeze fracture replicas in Chapter 3 indicated that gap junction plaques are present between vestibular supporting cells but absent from vestibular hair cells. Connexin staining results show that these supporting cell gap junctions contain Cx26 and that there is no Cx26 expression in hair cells. The immunostaining pattern also correlates with the freeze fracture survey, showing larger gap junction plaques at the base of the supporting cells than at the apex. Figure 4.8(a) shows FITC-labelled Cx26 between the supporting cells of the crista ampullaris. In Figure 4.8(b) the gap junctions expressing Cx26 between supporting cells of the utricular macula can be clearly seen. The position of the hair cells is noticeable due to the absence of staining.

Connexin 26 is abundant in many cells of the inner ear and has stained profusely in both the cochlea and vestibular organs using four different antibodies.

Figure 4.8 : Cx26 immunostaining in vestibular system



Connexin 30

Organ of Corti

Staining using a commercially produced anti-Cx30 antibody (Zymed) showed positive staining to be prolific throughout the cochlea and vestibular organs in agreement with RT-PCR experiments. Staining of wholemount preparations of the organ of Corti proved Cx30 to be present in all cochlear supporting cells but absent from the hair cells (Figure 4.9). The similarity in expression pattern of this isoform to that seen in Figure 4.3 of Cx26 is obvious. Cx26 and Cx30 seem to be co-localised throughout the supporting cells of the organ of Corti. Two plates in Figure 4.5, (a) and (b), demonstrate further the similarity in staining patterns for Cx30 and Cx26. The large gap junctions between pillar cells, not obvious in wholemount Figures 4.3 and 4.9, have been focussed upon. Both Cx26 and Cx30 clearly label in these pillar cell junctions.

The results from wholemounts are confirmed by staining observed in frozen sections (Fig.4.10). A Nomarski image (Fig. 4.10(a)) shows the same section as the Cx30-FITC-labelled image (Fig. 4.10(b)) to facilitate identification of organ of Corti structures. It is apparent from the FITC-labelling that Cx30 is expressed between all supporting cells, between cells of the spiral limbus and the fibrocytes of the spiral ligament.

Figure 4.9: Cx30 in wholemound organ of Corti



Figure 4.10: Cx30 expression in organ of Corti frozen section



Cochlear lateral wall

Earlier in this chapter the presence of Cx26 in the lateral wall fibrocytes but not in the stria vascularis was documented. There is a significant difference in this area between Cx26 and Cx30 expression, whereas in the organ of Corti and vestibular organs these two isoforms are colocalised. Figure 4.7 shows the comparison of Cx26 and Cx30 in the stria vascularis. Cx30 appears to be expressed in basal and intermediate cells of the stria as punctate staining can clearly be seen in the areas that correlate to these cell types shown in the Nomarski image (Fig. 4.7(b)).

Cx26 staining was noted to be less or absent from the more basal part of the spiral ligament. Cx30 immunostaining shows that this isoform is still present in this area but appears to be reduced in comparison to the staining seen through the upper part of the spiral ligament (shown in Fig. 4.10(b)).

Vestibular system

The presence of Cx26 and Cx30 is obvious in the vestibular end-organs. The expression pattern of Cx30 in vestibular organs is similar to that of Cx26. Figures 4.11(a) and (b) show positive staining of Cx30 between supporting cells of the crista ampullaris and utricular macula respectively; abundant punctate FITC-labelling represents the presence of Cx30. Again, the expression patterns of Cx26 and Cx30 are analogous in the vestibular sensory organs, as they appear to be throughout the organ of Corti. The expression of these connexin isoforms also corresponds to the gap junction plaques seen in freeze fracture replicas in Chapter 3.

Figure 4.11 : Cx30 expression in the vestibular system

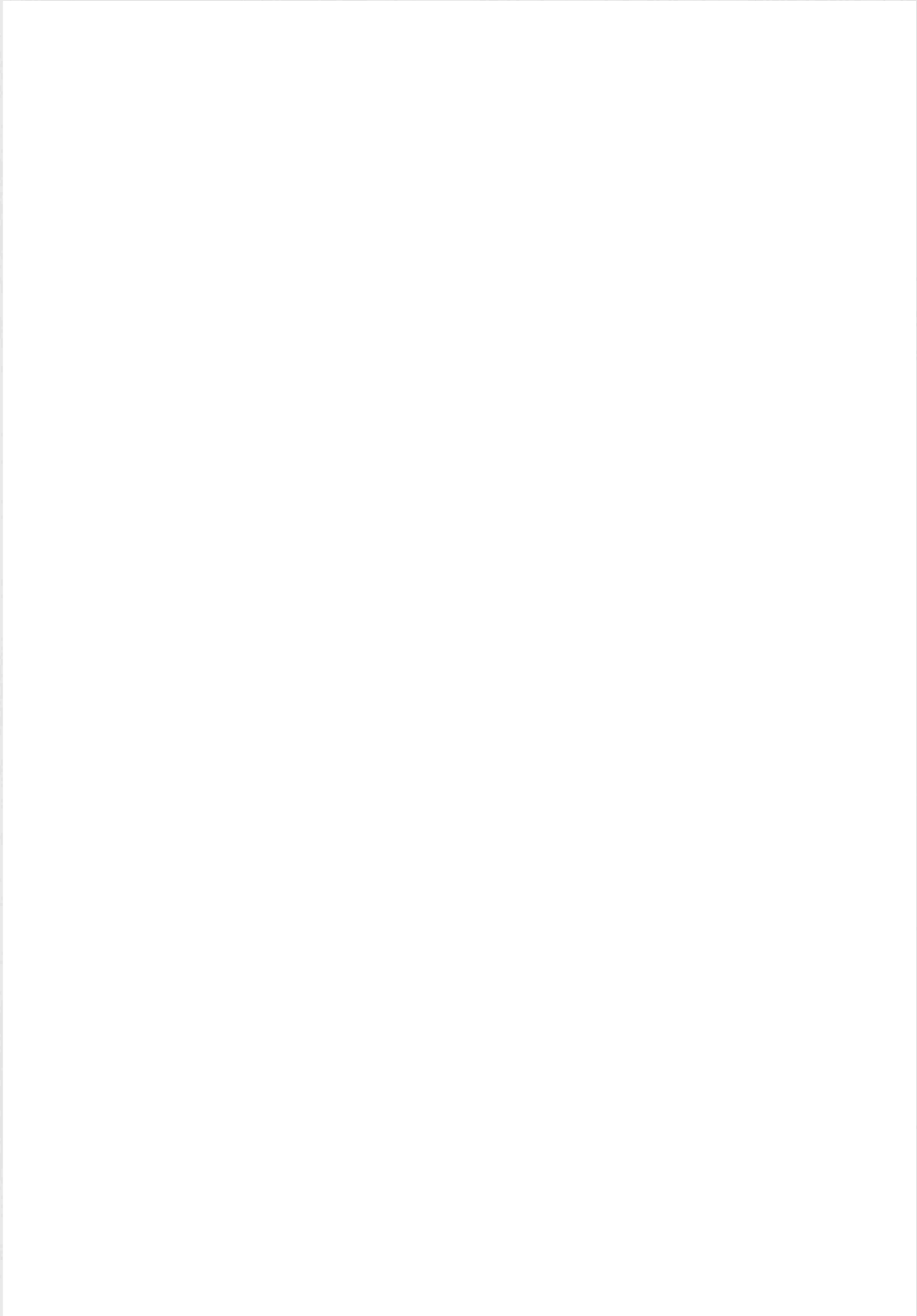


Connexin 43

The presence of Cx43 in the mouse inner ear was demonstrated by RT-PCR results (see Fig. 4.1). However, immunostaining for Cx43 has produced variable results dependant on the antibody used. There were five anti-cx43 antibodies used in this study all of which gave positive staining in some part of the inner ear but there were discrepancies in the amount and location of the stain. The results from each antibody were verified by careful analysis of positive and negative control sections. By analysis of Cx43 expression seen in heart sections and through study of previously published results the more reliable antibodies were ascertained. The results obtained using the $\alpha 1J$ and $\alpha 1S$ antibodies are shown here, these antibodies stained heart sections well with very little background staining and discrete punctate staining seen at the gap junction plaques. Figure 4.12(a) shows an area of the lateral wall that expresses Cx43 between the fibrocytes. The sketch diagram, Figure 4.12(b), outlines the area of the cochlea lateral wall in which this Cx43 staining is seen. Cx43 does not appear to be expressed between any of the organ of Corti supporting cells. This Cx43 staining is very specific and is interesting in that it appears to be in an area of the lateral wall that does not express Cx26.

Two different Cx43 mutations have been shown to cause a form of non-syndromic autosomal recessive deafness in African Americans (Liu *et al.* 2001). These findings show that despite a low level of Cx43 present in the cochlea the specific expression of this connexin isoform is vital in the physiology of hearing.

Figure 4.12: Cx43 immunostaining



Cx43 in the vestibular system

Figure 4.12(c) shows some staining with an anti-Cx43 antibody ($\alpha 1$, TSRI) in a wholemount preparation of an adult utricular macula. That the staining appears specifically along the borders between cells also indicates that the antibody is labelling gap junction plaques. In the vestibular system supporting cells surround the hair cells at their apices, the staining seen in Figure 4.12(c) is between these supporting cells.

Negative immunostaining

The negative immunostaining results are not shown in the thesis as the figures would show as black images. Positive controls were used for all antibodies and some immunostaining was demonstrated in the control tissues. Only positive results in the inner ear tissues have been included in the thesis.

Discussion

Table 4.3: Summary of mature connexin expression

| <u>Connexin isoforms</u> <u>studied</u> | <u>Result with RT-</u> <u>PCR</u> | <u>Result with</u> <u>immunostaining</u> |
|--|--|---|
| Cx26 | + | + |
| Cx30 | + | + |
| Cx30.3 | | ND |
| Cx31 | | |
| Cx32 | | |
| Cx37 | | |
| Cx40 | ND | |
| Cx43 | + | + |
| Cx45 | | |
| Cx46 | ND | |
| Cx46.6 | | ND |
| Cx50 | | |

+ Indicates a positive result seen

Blank space indicates a negative result seen

ND Means not done, the isoform was not investigated using this method

Gap junctions are numerous in the inner ear tissues and previous work has demonstrated Cx26 expression in both the auditory and vestibular systems of rats (Kikuchi *et al.*, 1994; Kikuchi *et al.*, 1995). Freeze fracture studies, as summarised in Chapter 3, have shown the size and location of the many gap junction plaques seen in the mammalian inner ear.

Connexin 26

All immunocytochemistry work in this thesis shows results from mouse inner ear. The results shown in this thesis agree with previously published results that showed Cx26 to be present in non-sensory epithelial cells and connective tissues within the adult cochlea (Kikuchi *et al.* 1994; Lautermann *et al.* 1998). All antibodies to Cx26 gave intense immunoreactivity throughout the supporting cell populations of both auditory and vestibular organs, as well as labelling fibrocytes in the lateral wall. These immunostaining results associate very well with the freeze fracture results analysed in the previous chapter; gap junction plaques containing Cx26 seen using antibody staining are located between all non-sensory cell types with larger plaques seen more basally in each cell type. Kikuchi and colleagues (2000) observed immunostaining with an anti-Cx26 antibody in all areas of gap junctions in the cochlea with the only areas not expressing Cx26 being the hair cells, spiral prominence, stria marginal cells and Reissner's membrane.

The presence of Cx26 in mature ear is shown by Rt-PCR and immunoblotting (Fig's 4.1 & 4.2) with localisation throughout the cochlea and vestibular systems demonstrated in Figures 4.3 through to 4.8. There is a general pattern of Cx26 expression throughout the auditory and vestibular parts of the ear in that the

supporting cells all have Cx26-containing gap junctions with more Cx26 seen more basally within these cells.

The result in Figure 4.7 suggests that there is either a low-level or no expression of Cx26 in the cells of the stria vascularis. There also appears to be an absence or reduction of Cx26 in the central and subcentral regions of the spiral ligament just below the stria vascularis, which raises intriguing questions about the exact function of this specific region of the cochlea. This result differs from that reported by Kikuchi *et al.*, 1994 who reported Cx26 presence in basal and intermediate cells of the stria vascularis and in all cells of the spiral ligament, and Lautermann *et al.*, 1998 who found Cx26 in the basal cells of the stria vascularis but only a low level of Cx26 expression in the fibrocytes of the lateral wall. The research in both of these papers was performed on rats and used different fixation techniques and antibodies to those used in this thesis. Either the species difference or the methodology difference could account for the difference in staining patterns identified in the lateral wall.

Connexin 30

Results with PCR primers showed that Cx30 was also present in the inner ear and upon acquisition of a Cx30 antibody (Zymed) profuse immunostaining was also seen (Fig. 4.5, 4.7, 4.9, 4.10 & 4.11). Lautermann *et al.*, 1998 found Cx30 to be co-expressed with Cx26 throughout the mature rat cochlea; results in this thesis using mouse tissue agree with this result in that Cx30 is expressed in cochlear supporting cells and in the lateral wall.

This isoform has been shown to form heterotypic junctions readily in *Xenopus* oocytes with Cx26, Cx30.3, Cx40, Cx43, Cx45 and Cx50 (Manthey *et al.*, 2001). It is known to colocalise with Cx43 in adult rat astrocytes (Kunzelmann, 1999). Cx26 and Cx30 have been observed together in the spiral limbus, spiral ligament, and between all non-sensory supporting cells of the organ of Corti. The similarity in staining patterns of Cx26 and Cx30 suggests the possibility of Cx26 / Cx30 heteromeric connexons or a mixture of homomeric Cx26 and homomeric Cx30 connexons within the same gap junction plaque. Again the results observed with anti-Cx30 antibody correspond well with the freeze fracture results reported in Chapter 3. From these immunostaining results it would seem that many gap junction plaques within the cochlea contain Cx30 as staining is seen in the areas where the freeze fracture replicas exposed gap junction plaques.

Connexin 31

There has been considerable debate about the presence of Cx31 in the cochlea. Using the Cx31 antibody from the laboratory of Klaus Willecke abundant staining was initially seen throughout cells of the cochlea. Several different fixation and blocking techniques were tried with this antibody. None of the immunostaining seemed specifically to be localised along cell borders and often the stain was not of the punctate nature expected when labelling gap junction plaques. Results from RT-PCR with primers did not support this positive immunostaining result either. This prompted the search for another Cx31 antibody. An antibody that had been utilised in a study of rat skin and hair development (Risek *et al.*, 1992) was kindly donated by TSRI, La Jolla. This antibody gave no positive result in mature inner ear by either immunoblotting or immunostaining procedures whilst skin samples gave

positive results in both techniques with this antibody. This result reflects the findings of Plum and colleagues in 2001, who carried out studies on mice whose Cx31 gene had been replaced by a LacZ reporter gene. No β -galactosidase product could be seen in the inner ears of these knockout mice. The Cx31-knockout mice had apparently normal auditory responses determined by brainstem-evoked potentials and the morphology of their inner ears appeared the same as control mice.

Connexin 32

Although Cx32 has been linked to deafness in X-linked Charcot-Marie Tooth disease there was no evidence of its presence in the peripheral auditory system. Experiments using PCR primers and four different antibodies for immunocytochemistry in wholemount and frozen section preparations all gave negative results for the presence of Cx32. One antibody did suggest the presence of Cx32 in the utricle but this must be considered a false positive when compared with the negative results from other experiments. The β 1J anti-Cx32 antibody was also used in a Western blot on mature cochlea tissue and indicated that this isoform is not present. Deafness caused by a mutation in *GJB1*, the gene for Cx32 protein, must be due to a more central cause possibly involving demyelination of nerves.

Connexin 43

This isoform is well documented in gap junction literature. Its presence is important from early stages of embryonic development through to birth and is vital for postnatal heart development; Cx43 knockout mice die shortly after birth due to a lethal cardiac malformation. Several antibodies are available against this isoform, some proven to be more reliable than others (Coppen *et al.*, 1998). Weak bands on

both RT-PCR and western blots with some anti-Cx43 antibodies indicate the presence of this isoform within the inner ear (Figs. 4.1 and 4.2); however, immunostaining of this isoform could easily be overlooked due to the low level of expression. In 1998 Lautermann *et al.*, stated that they found small amounts of Cx43 in the spiral ligament and stria vascularis but not in the spiral limbus. They also saw Cx43 between the supporting cells of the organ of Corti but this was not shown in any figure and therefore could not be compared to immunostaining results seen in mouse cochlea shown in this chapter. Very recent results using a LacZ reporter gene in mice have shown Cx43 present only in the bony capsule (Cohen-Salmon, unpublished data).

The expression of Cx43 in the mature mouse cochlea seen in this chapter is restricted to a small region of the lateral wall (Fig. 4.12). This specific expression pattern is particularly interesting when compared with Cx26 and Cx30 expression. This specific area of the spiral ligament has a reduced level of both Cx26 and Cx30 in comparison to the more apical spiral ligament. The question arises, “Why does this one population of cochlear cells need Cx43 when all other cell types of the cochlea only express Cx26 and Cx30?”

The presence of Cx43 in the supporting cells of the vestibular system introduces a difference between the auditory and vestibular systems. If this expression pattern is the same in humans it may contribute to the normal functioning of the balance system in patients with deafness caused by Cx26 mutations.

No labelling for any other connexin isoform was detected in either the auditory or vestibular systems of the mature mouse inner ear.

CHAPTER FIVE

Connexin Expression in the Developing Mouse Inner Ear

Introduction

Ear Development

The inner ear begins as a thickened patch of ectoderm, known as the otic placode, next to the imminent hindbrain during neural tube closure. In mice it is between embryonic (E) days 8 and 12 that the otic placode invaginates to form the otic vesicle or otocyst. The endolymphatic duct projects from the medial part of the otocyst; the semicircular canals begin to form in the lateral part of the otocyst and the utricle appears as a bulge at the anterior end of the otocyst.

The neural crest is a group of embryonic cells that separate from the neural plate and migrate to give several different lineages of adult cells including the spinal and autonomic ganglia, the glial cells of the peripheral nervous system and nonneuronal cells, such as chromaffin cells, and some haemopoietic cells. The pigmented intermediate cells of the stria vascularis are derived from the neural crest.

Neurons develop from neuroblasts that migrate out from the ventral part of the otocyst. One neurite is extended back to the otic epithelium and one out to the hindbrain via the eighth cranial nerve; the Schwann cells of this nerve derive from the neural crest (Corwin, 1997).

Between E13 to E15 the three semicircular canals are formed and the entire membranous labyrinth thins. The distal part of the cochlea starts to coil as the proximal tip extends. By E17 the membranous labyrinth has achieved its mature form and the cochlea has curled to the complete one and three-quarter coils.

The sensory epithelia of the inner ear are a mosaic of hair cells and supporting cells. In the presumptive epithelia all cells are potential hair cells then when one cell becomes a hair cell it inhibits its neighbours from becoming hair cells. The Delta-Notch signalling pathway mediates this lateral inhibition; the Delta protein acts as the ligand in the nascent hair cell with the Notch protein a transmembrane receptor in the cell receiving inhibition which then develops as a supporting cell (Eddison *et al.*, 2000; Corwin *et al.*, 1991; Lewis, 1991). In mice the terminal mitosis of basal cochlear hair cells is at E15-E16 (Ruben, 1967) hair cells at the apical end of the cochlea leave the mitotic cycle before this. Hair cell maturation proceeds in the other direction with basal coil hair cells maturing before the apical hair cells. Deiters' and pillar cells elongate to support the outer hair cells and the tunnel of Corti space is formed between P8 and P10 (Sher, 1971).

Mice, rats and gerbils are all altricial animals, which are born deaf and maturation of the cochlea continues postnatally. In mice auditory function is initiated at about P8, and is adult-like by P14.

Connexins in Development

Many different connexin isoforms are expressed during development. The study of squid embryos (Potter *et al.*, 1966) was the first to propose gap junction communication as a feature of early embryos. Later studies noticed that gap junction communication is separated into multicellular divisions, termed communication compartments (Lo and Gilula, 1979); these compartments often correspond to developmentally important domains.

Gap junctions are important during patterning, differentiation and development of embryos, and during growth and proliferation given that these membrane channels can mediate the transmission of second messengers and cell signalling molecules (Lo, 1996). In addition to the presence or absence of specific connexins the precise regulation and expression levels are also significant during development.

In the preimplantation mouse embryo Cx43 mRNA and protein have been detected at the 4-cell stage (Nishi *et al.*, 1991) but the gap junctions do not get inserted into the membrane until the 8-cell stage. Functional dye coupling at this 8-cell stage has been described indicating gap junctional communication (Lo and Gilula, 1979).

Gap junctions connect all cells of the presumptive sensory epithelia of the developing vestibular organs of chicks. Cells that then differentiate into hair cells internalise and lose their gap junction plaques, whilst cells whose fate is to function as supporting cells remain connected via gap junctions (Ginzberg and Gilula, 1979). This finding is consistent with a study that shows gap junctions are not associated with hair cells of any sensory organs of the inner ear of the rat (Kikuchi *et al.*, 1994). Results shown in Chapters 3 and 4 of this thesis show that mouse hair cells do not have gap junctions but that all supporting cells do. This situation is reflected in other mammals; supporting cells express extensive gap junction plaques whilst there is an absence of gap junctions in the hair cells (Jahnke, 1975; Iurato *et al.*, 1976).

It is well established that intercellular communication via gap junctions is crucial for normal tissue development; specific isoforms are expressed at particular developmental stages. In a study by Souter and Forge (1998) gerbil cochleae, aged

from 2 days after birth (DAB) to 20DAB, were processed for freeze fracture prior to observation by electron microscopy. Endocochlear potential was measured from gerbils aged 8DAB to 20DAB. A strong correlation between maturation of strial gap junctions and onset and rise of endocochlear potential was shown.

As connexin isoform expression levels fluctuate throughout the developmental process it seems that the precise regulation of gap junctions and their constituent protein isoforms is important. This study has shown several connexins to be implicated during inner ear development.

Results

RT-PCR

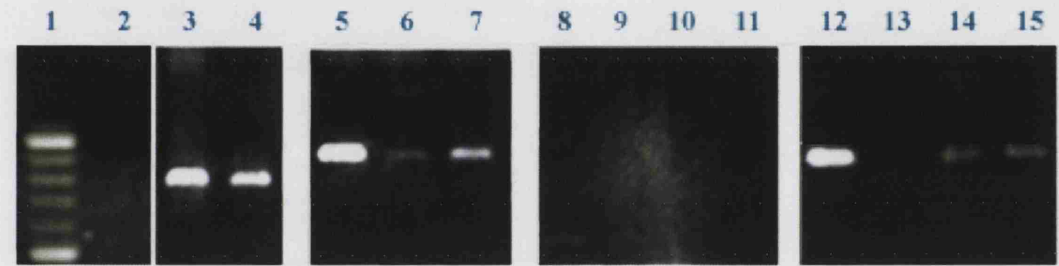
Figure 5.1 is an RT-PCR gel in which tissue from the developing inner ear is tested for the presence of different connexin isoforms. A total of ten isoforms were investigated in the developing ear using this RT-PCR technique. Initially RNA extracted from both E15.5 otocysts (6 embryos used for each preparation) and whole P4 cochleae (8 cochleae per preparation) was tested with the ten connexin primers (see Chapter 2 for the primer sequences). Any primer that produced a positive band with the positive control tissue and the inner ear tissue, yet with no band in the negative control column, was used on otocyst and cochlea RNA extracted from other developmental stages. There was found to be RNA of connexins 26, 30, 31 and 43 present during various developmental stages of the mouse inner ear. Cx26 is shown here as present in E15.5 otocyst and P4 cochlea; Cx30 is also present in E15.5 and P4 and there is an additional positive result shown in E13.5 otocyst. Cx43 is shown as present at E15.5, P0 and P4. Cx31 can be seen to be present at the

embryonic stages of E13.5 and E15.5 but must be down-regulated as there is no positive band seen at either P4 or in mature ear. Results that are not shown in this figure show Cx26 and Cx30 to be present through development from E11.5 to adult. Other isoforms investigated using RT-PCR but mRNA not be detected in developing inner ear were Cx32, Cx30.3, Cx37, Cx45 and Cx46.6.

It is important to realise that Figure 5.1 does not show a quantitative PCR and therefore the intensity of the bands seen on the PCR gel cannot be correlated with the amount of connexin RNA present in the cochlea. All results presented in this thesis indicate only the presence or absence of the connexin RNA.

Figure 5.1: RT-PCR with various connexin primers through development

PCR primers designed to ten different connexins were used first on E15 otocysts and P4 cochlea. If these two stages gave a positive result further stages were tested. All other primers used but not shown here gave negative results.



- 1 Molecular weight marker
- 2 Negative control
- 3 Connexin 26 in P4 cochlea
- 4 Connexin 26 in E15 otocysts
- 5 Connexin 30 in P4 cochlea
- 6 Connexin 30 in E13 otocysts
- 7 Connexin 30 in E15 otocysts
- 8 Connexin 31 in E13 otocysts
- 9 Connexin 31 in E15 otocysts
- 10 Connexin 31 in P4 cochlea
- 11 Connexin 31 in adult cochlea
- 12 Connexin 43 in E15 otocysts
- 13 Negative control in Cx43 PCR
- 14 Connexin 43 in P0 cochlea
- 15 Connexin 43 in P4 cochlea

Expected band sizes:

| | |
|------|-----|
| Cx26 | 305 |
| Cx30 | 516 |
| Cx31 | 167 |
| Cx43 | 507 |

Immunostaining

Antibodies to ten different connexin isoforms were utilised on tissue from mouse inner ear throughout stages of development. The total number of different antibodies used was 27; some have been shown to be more reliable than others (as explained in Chapter 6).

Figure 5.2 is a plate of images from E17.5 otocysts showing expression of the five isoforms found to be involved in development. Figures 5.2(a), 5.2(c) and 5.2(d) show that connexins 26, 31 and 43 are fairly evenly distributed around the developing cochlear duct in most differentiating cell populations whereas Figure 5.2(b) and Figure 5.2(e) show specific areas of intense connexin expression. In Figure 5.2(b) Cx30 appears only in the areas under the presumptive organ of Corti and on one side of the duct, which is the developing spiral limbus. In Figure 5.2(e) Cx45 expression is in a small area of the developing epithelial ridge but is distinctly different from the area of Cx30 expression, Cx45 is seen more laterally in the epithelial ridge and is seen in the connective tissue below the developing spiral limbus. The sketch diagram (Fig. 5.2(f)) indicates the important structures in the E17.5 cochlear duct. The spiral limbus begins differentiation on E17 in the axial portion of the caudal wall in the basal coil only. The developing stria vascularis at E17.5 is seen as a dense area of mesenchyme rich in capillaries adjacent to the rostral wall of the cochlear duct. Pillar cell differentiation, inner sulcus differentiation and tectorial membrane formation do not begin before E19.

**Figure 5.2. Mouse organ of Corti at E17.5
showing diverse connexin expression**



Connexin 26

Connexin 26 expression has been seen at every stage studied during development, from E11.5 to P10 and into adulthood; there is more Cx26 in the adult cochlea than during development.

At E13.5 Cx26 is evenly distributed around the cochlear duct. At stages E15.5 to E19.5 the expression of Cx26 becomes more specifically localised with labelling only seen in the presumptive lateral wall and epithelial ridge regions. At E19.5 there are particularly large Cx26-containing plaques between cells of the differentiating lateral wall (Fig. 5.3(a)). By postnatal day 2 large amounts of Cx26 can be seen in the supporting cells of the organ of Corti but the hair cell regions are distinguishable by their lack of Cx26-labelling (Fig. 5.3(b)). In the P9 cochlea, Figure 5.3(c), plaques can be seen at junctions between supporting cells, the staining is adult-like in both distribution and amount. A sketch diagram which relates to the mature cochlear duct can be used to identify cells in the P2 and P9 figures (Fig. 5.3(e)). The region shown in Figure 5.3 (a) is that of the spiral limbus. The onset of cochlear function in the mouse is at P9 or P10 (Pujol *et al.*, 1986).

Figure 5.3 Connexin 26 in developing mouse cochlea

- a) shows Cx26 expressed in E19.5 cochlear duct
- b) shows Cx26 expression in P2 cochlea
- c) shows Cx26 expression in P9 cochlea



The pattern of Cx26 expression was an even distribution around the E11.5 and E13.5 cochlear duct, followed by a more specific distribution in the later otocyst development which remained into the postnatal cochlea. The specific sites of Cx26 are the developing stria vascularis and spiral ligament, spiral limbus and the epithelial ridge. This isoform is also present in developing vestibular organs. In late embryonic stages of development a base to apex gradient of Cx26 expression can be seen (Fig. 5.4). The basal coil of the cochlea is more developed than the apical coil at embryonic day 20.5 and more Cx26 can be observed in the basal coil.

Figure 5.4: Example of the specific expression of Cx26 during development



(a) Cx26 in the developing spiral limbus of the apical coil in an E20.5 cochlear duct

(b) Cx26 in the developing spiral limbus region of the basal coil in an E20.5 cochlear duct

Connexin 30

This isoform was also found to be present throughout development of the mouse inner ear. Cx30 is abundantly expressed throughout the mature inner ear but its pattern of expression during development is more specialised. Specific populations of cells label with anti-Cx30 antibody in the developing otocyst, Figure 5.2(b) shows this specialised expression pattern in the otocyst at E17.5, labelling is seen in the epithelial ridge and developing spiral limbus.

Expression levels increase gradually from E13.5 through to P4, the labelling starts in the root region of the spiral ligament at E17.5, moving to the basal cells of the stria and the limbus by P4. In the P4 cochlea Cx30 is strongly expressed in the basal and intermediate cells of the stria vascularis, as it is in the mature cochlea, but there is no Cx30 seen in the spiral ligament fibrocytes at this stage. Figure 5.5 is a plate showing Cx30 in the developing cochlea at P4. Figure 5.5(a) is an overview of the Cx30 expression where a Nomarski image has been overlayed with the fluorescence to create a 3D-representation of protein location within the cochlea duct. Figure 5.5(b) is a FITC fluorescence image of Cx30 showing intense expression in the spiral limbus, epithelial ridge and in the stria vascularis. Figure 5.5(c) is a close-up of the Cx30 expression in the stria vascularis demonstrating the presence of this connexin in stria basal cells and possibly intermediate cells but not the marginal cells of this structure. Cx30 is notable in its absence from the spiral ligament prior to E.P. generation. Labelling of this isoform increases after P4 and is extensive in the mature spiral ligament fibrocytes.

Figure 5.5: Connexin 30 in postnatal cochlea

a) Connexin 30 in P4 cochlea



Connexin 31

Connexin 31 is present only during development of the mouse cochlea. Results in Chapter 4 show that this isoform is not expressed in the mature mouse inner ear. At the earliest stages of development studied Cx31 labelling was extensive around the border of the developing cochlear duct (Fig. 5.6(a)). In these early stages (E13.5 to E17.5) Cx31 is present in all cells surrounding the lumen of the developing cochlear duct, including the future hair cells and supporting cells. As development progressed the Cx31 labelling was seen to be gradually downregulated. At E17.5 the Cx31 is still present around the entire cochlear duct but there is more seen in the area of the developing sensory epithelia (see Fig. 5.2). Cx31 is still present in the early postnatal stages as the cochlea continues its maturation however the expression is greatly reduced in comparison to the expression patterns seen embryonically. At P0 the Cx31 labelling is limited to cells in the developing organ of Corti but is not seen in the hair cells (Fig. 5.6(b)) and by P4 it appears to be restricted to one population of supporting cells, thought to be the Hensen's cells (Fig.5.6(c)). By P9 there was no Cx31 expressed in the inner ear.

Figure 5.6: Connexin 31 in mouse organ of Corti during development



Connexin 43

Widespread Cx43 staining can be seen at the earlier developmental stages, Figure 5.7 (a) shows Cx43 expression at E15.5 in the otocyst. This isoform is widely expressed throughout development (Fig. 5.2(d)) and is still seen postnatally but is downregulated as the cochlea reaches maturity. The expression of Cx43 at E15.5 and E17.5 appears mainly along the greater epithelial ridge and in the developing spiral limbus area (see figure 5.7). It does not appear to be present in the developing stria vascularis or lateral wall area. By postnatal day 4 the expression of Cx43 has reduced greatly in comparison to the otocyst at E15.5 (Fig.5.7 (a)). This isoform is only present in the greater epithelial ridge at P4, as can be observed as puncta along cell borders in Figure 5.7(b). In the adult mouse cochlea Cx43 is not present in the organ of Corti but can still be seen in a discrete area of the lateral wall.

Figure 5.7: Connexin 43 expression during development



Connexin 45

Two developmental stages have been tested with an antibody for Cx45. Cx45 does not appear to be present in adult ear tissue but these preliminary results with a new antibody show its involvement during development.

In an early stage of development, E17.5, there is some Cx45 expression seen in the epithelial ridge, which is the area of the developing organ of Corti (Fig. 5.8(c) and (d)). Later in development, P10, this isoform is still present in small amounts in the supporting cells of the organ of Corti and is also seen in the spiral ligament region of the lateral wall (Fig. 5.8(a)). Figure 5.8(b) is a sketch diagram of the organ of Corti features shown in figure 5.8(a) to show the orientation of the section and to aid in localisation of the corresponding FITC-staining of Cx45 in P10 cochlea.

Figure 5.8: Connexin 45 expression during development



Connexin 50

It has been difficult to find a reliable antibody for Cx50. Results discussed later in this thesis (see Chapter 7) prove the presence of this isoform in cochlear development using mice whose Cx50 gene has been replaced by a LacZ reporter gene. Some results from two Cx50 antibodies used have suggested this too. Labelling with a FITC-conjugated polyclonal antibody has shown punctate staining along the borders of cells but there was also high background fluorescence with this antibody. Figure 5.9(a) indicates the presence of Cx50 in the supporting cells of the P4 organ of Corti.

Immunolabelling has also indicated the presence of Cx50 in the vestibular supporting cells during development (Fig. 5.9(b)). Again this staining is not as clear as that obtained with antibodies for other isoforms but the punctate staining is in accordance with the cell borders suggesting the puncta are representing gap junction plaques. No Cx50 labelling has been observed in the mature mouse inner ear.

Figure 5.9: Connexin 50 expression during development



Discussion

Variations in expression levels and differences in distribution of connexin isoforms indicates that gap junctions are not simply passive channels for movement of molecules less than 1000Daltons in size. These channels provide a selective signalling route between specific cells that is carefully regulated throughout development.

The role of individual isoforms is difficult to establish because there is multiple isoform expression in most cell types and it has been shown that the expression levels do not necessarily correlate with gap junction communication levels (Sia *et al.*, 1999). Connexin isoforms show uneven distribution throughout the developing cochlea.

Cx26

Xia and colleagues, in 1999, studied Cx26 expression in the developing mouse cochlear lateral wall from 0 days after birth to 30 days after birth. Tissue was fixed in paraformaldehyde and embedded in paraffin wax for sectioning then visualised using 3,3'-diaminobenzidine (DAB) -H₂O₂. At P0 they observed small amounts of Cx26 in connective tissue cells just lateral to future strial marginal cells and in outer sulcus cells. At ages P3-P6 Cx26 was also expressed in the strial basal cell region but was not present in the lateral wall fibrocytes until P10. Expression of Cx26 had increased in the fibrocytes at P12 and the staining had reached an adult-like pattern at P15.

Also in 1999, Lautermann *et al.* described the developmental expression patterns of Cx26 and Cx30 in rat cochlea from gestational day 15 (15GD) to 30 days after birth. This study did not detect any Cx26 in the cochlea at 15GD but described Cx26 in the lateral wall and neurosensory epithelium at 17GD and 19GD. The expression of Cx26 then gradually increased postnatally.

A study performed by Frenz and Van De Water in 2000, on mice aged between E12.5 and P3, reported no Cx26 expression in E12.5 and E14.5 otocysts with mild expression at E16.5. A stronger signal seen in E18.5 and P0 cochleae was graded from higher intensity staining in the basal turn to weaker immunostaining at the apex. This study used a methacarn fixation technique and paraffin sections but no details of the anti-Cx26 antibody were given.

The experiments in this thesis have shown there to be less Cx26 staining during development than in mature organ of Corti with an up-regulation of Cx26 protein in late embryonic and early post-natal cochlea. However, contrary to some of the published studies, both RT-PCR experiments and immunolabelling of frozen sections with Cx26 antibodies in this project have shown the presence of Cx26 in the developing inner ear from E11.5. All of the researchers quoted above used an alternative methodology with paraffin sections and different antibodies. These experiments also used either rats or a different strain of mouse (C57/BL6 females with CBA-J males). These differences in strain, methodology and possibly in the antibodies used must account for the discrepancy between the studies.

Cx30

This isoform has been noted as the most abundantly expressed in the mature mouse cochlea but appears to have restricted boundaries of expression during development. This is further evidence that the segregation of particular cell types during development may be as important as the connections between other cell populations.

The findings in this thesis show Cx30 to be present from E13.5 and at E15.5 (RT-PCR result shown in figure 5.1), which differs from the findings published about the developing rat cochlea (Lautermann *et al.*, 1999). This study did not detect staining for Cx30 until gestational day 17, which may indicate a difference in the development of the cochlea between the species. However, Cx30 expression was observed in discrete cell populations during development and then seen to increase postnatally which is similar to the results shown here in the developing mouse cochlea. Another reason for the discrepancy could be that RT-PCR is more sensitive than immunostaining and if there is only a small amount of Cx30 present this may not be seen in sections but can be detected using molecular biology methods.

Xia *et al.*, 2001, have also performed a study of Cx30 during development of the mouse cochlea starting from postnatal day 0. Cx30 was seen to be present in small amounts from P0 then seen to increase to an adult-like pattern of expression by P15.

There is an increase in Cx30 expression during development of the cochlea with the isoform being arguably the most widely expressed in adult mouse cochlea. During development it is interesting to observe that Cx30 is absent from the spiral ligament

prior to E.P. generation up to postnatal day 4. Labelling of this isoform increases after P4 and is extensive in the mature spiral ligament fibrocytes.

Cx31

Cx31 presence has been reported during the early stages of both rat and mouse embryonic development (Reuss, 1997; Dahl *et al.*, 1996; Davies, 1996). In the rat Cx31 expression pattern appeared to correlate well with that of Cx43.

Cx31 expression has been studied in the developing cochlea of CBA/N mice from 0 days after birth to 60 days after birth (Xia *et al.*, 2000). The results show that there is no expression of Cx31 from P0 to P10 with the initial weak signal seen at P12. Between P12 and P30 there is an increase in the expression pattern, reaching adult pattern by P60. In the mature mice (older than P60) the study reports intense immunoreactivity in the spiral ligament and weak immunoreactivity observed in the spiral limbus. No Cx31 was seen in the organ of Corti or in the stria vascularis. This study also described a difference in Cx31 expression between the basal and apical turns of the cochlea with more being observed in the basal part of the cochlea. The first detection of Cx31 at P12 and the increase in expression to P60 fits well with the observed phenotype in humans with Cx31 mutations who have a progressive hearing loss. Unfortunately these results could not be replicated in this thesis, perhaps due to different fixation techniques and the particular antibodies used.

The studies in this thesis have shown the highest expression levels of the Cx31 isoform at stages E13.5 and E15.5. Cx31 is then seen to be down-regulated during the later stages of development with no expression of the protein observed in the

mature cochlea. At P2 and P4 Cx31 is restricted to a supporting cell population in the developing organ of Corti, by P9 there is no Cx31 expression.

Cx43

Cx43 expression is well documented and appears to be the most widely observed isoform during embryonic development with significant levels seen in many tissues; down regulation of Cx43 often occurs as the tissues mature (Becker *et al.*, 1992; Dermietzel *et al.*, 1989; Green *et al.*, 1994; Rozental *et al.*, 1998). A similar phenomenon is seen during development of the mouse cochlea. Cx43 is abundant in the early otocyst and its expression is seen to decrease as the postnatal cochlea matures. It is possible that Cx43 expression decreases in accordance with the notable increase in Cx26 and Cx30 expression through cochlea development. These isoforms may serve different purposes and therefore change in relation to one another as the inner ear matures. The gap junctions comprised of Cx43 and Cx26 may fulfil alternative functions and therefore a conversion is required for various maturational events associated with either anatomical or physiological function of the ear.

Neural crest cells are highly coupled by gap junctions expressing Cx43 (Lo *et al.*, 1997). Analysis of Cx43 function during migration and proliferation of neural crest cells *in vitro* by Huang and colleagues (1998) showed over-expression of Cx43 increased the rate of neural crest migration whereas migration decreased with inhibition of gap junction communication or reduction or loss of Cx43. The intermediate cells of the stria vascularis are of neural crest origin and Cx43 staining is seen in the developing spiral ligament and stria vascularis of the cochlea this

study. Cx43 is not seen in the stria vascularis by postnatal day 4 although it is still present in the cochlear lateral wall and greater epithelial ridge (see Chapter 7 for further analysis of Cx43 in development of the cochlea).

Cx45

Mouse Cx45 gene is different from most other isoforms in that it has two introns and three exons and that exon 3 contains the coding region (Kumai *et al.*, 2000). The Cx45 protein is unusual in that it has a remarkably long cytoplasmic loop domain. Cx45 has been found in various mature tissues and is significant during development, particularly in early embryos (Jacob and Beyer, 2001). Levels of this isoform are seen to decrease through development. Cx45 deficient mice die around E10.5 from heart failure (Lo, 2000).

Expression of this isoform has not been investigated in detail in this study. Preliminary results show that the protein is not expressed in mature mouse cochlea but the two developmental stages that have been studied have shown this isoform to be specifically expressed in the early organ of Corti. It would be appropriate to track the expression of this connexin in both the cochlea and vestibular organs through all stages of development to discover Cx45 location and possible interaction with other isoforms.

Cx50

This isoform is present during development in both the auditory and vestibular portions of the mouse inner ear. The Cx50 antibodies available for use gave a

pattern of staining which indicates that there are gap junctions containing Cx50 in both the development of the cochlea and vestibular organs.

This study has shown there are distinct differences between connexin expression in the developing and mature mouse cochlea. It is interesting to observe that some connexin isoforms are down regulated as development of the cochlea progresses (for example Cx31 and Cx43) whilst others are up regulated and remain important in the mature cochlea. This introduces the idea that particular connexin isoforms perform very specific roles during inner ear development.

Further study is required to elucidate the complete pattern of connexin isoform expression in the developing vestibular system. Results in this chapter have shown Cx26 and Cx30 to be present in the vestibular organs. Cx50 is not present in vestibular organs at E18.5 but earlier stages have not yet been investigated. RT-PCR results show positive bands for Cx26, Cx30, Cx31 and Cx43 (Fig. 5.1) but these results were obtained from whole otocyst material and therefore give no indication as to whether these isoforms are involved in vestibular development. More immunostaining concentrating on the vestibular organs through several developmental stages should clarify the exact isoform distribution.

CHAPTER SIX

Experimental Clarification: HeLa Cells and Immunogold Labelling

Introduction

To investigate connexin expression in the inner ear several anti-connexin antibodies have been used (see appendix 3). Many of these antibodies are commercially available whilst others have been designed and raised by individual researchers for specific use within their laboratories. Studies throughout this thesis have used a combination of commercially produced antibodies, donations of aliquots from various sources and antibodies produced within University College London. In each instance peptide antigens are designed to match isotype-specific sequences of the connexin protein of interest.

It is important that each antibody used has been screened for specificity; all those obtained by donation had been tested within the laboratory from which they originated. In all immunohistochemical and immunoblotting experiments controls were used to ensure that each antibody labels in a tissue known to express the relevant connexin (see appendix 1).

Results shown in earlier chapters of this thesis have demonstrated connexins 26 and 30 to be the dominant connexin isoforms expressed in the inner ear, often appearing to be co-localised. There is 77% amino acid sequence identity between Cx26 and Cx30 increasing the possibility that an antibody thought to be specific for one of these isoforms may also recognise the other isoform. To determine antibody specificity and exclude cross-reactivity of the antibodies used for identification of Cx26 and Cx30 an *in vitro* expression system was developed by Dr. Nerissa Marziano with whom this work was conducted. Separate populations of HeLa cells

were transfected with either Cx26 or Cx30 plasmid constructs then fixed and incubated in either Gap 28h (anti-Cx26) or anti-Cx30 antibodies.

Further to recent questions within the gap junction research community regarding the specificity of some anti-connexin antibodies it was necessary to include extra experiments within the thesis to validate results found using antibodies.

Immunogold labelling allows verification that a particular antibody binds to a gap junction structure. In this technique connexin antibodies are conjugated to gold particles and applied to thin sections; subsequent electron microscopic examination illustrates the gold particles bound to structures morphologically distinct as gap junctions. It is imperative that the antibody is tested via this method, particularly if the expression level is low, to verify that immunofluorescent labelling can be associated with a gap junction. Graham Nevill performed the immunogold labelling experiments included in this thesis.

Results

In Vitro antibody testing

HeLa cells, which do not endogenously express connexins (Elfgang *et al.*, 1995), were microinjected with either Cx26 or Cx30 constructs. The cells were then fixed; anti-connexin antibodies were applied, and then processed for observation by confocal microscopy. In Figures 6.1(a and d) cells have been transfected with Cx26 and Cx30 respectively and incubated in the appropriate antibodies for each isoform; bright spots are obvious where the connexin proteins have reacted with the antibody and are labelled with TRITC. In Figure 6.1 (b) cells transfected with Cx30 have been incubated in anti-Cx26 antibody and there is no positive staining. Figure 6.1(c) shows cells injected with Cx26 construct, which have been incubated in anti-Cx30 antibody, again there is no positive staining. That the Cx26 transfected cells positively stained with Gap 28h and not with anti-Cx30 antibody, whereas Cx30 transfected cells showed no staining with Gap 28h but did stain positively with anti-Cx30 antibody provides evidence that the antibodies are isoform-specific.

Figure 6.1: HeLa cell experiment to show specificity of anti-cx26 and anti-cx30 antibodies

- a) HeLa cells transfected with cx26 cDNA incubated in anti-cx26 antibody
- b) HeLa cells transfected with cx30 cDNA incubated in anti-cx26 antibody
- c) HeLa cells transfected with cx26 cDNA incubated in anti-cx30 antibody
- d) HeLa cells transfected with cx30 cDNA incubated in anti-cx30 antibody



Immunogold labelling

This is an important technique that verifies immunostaining results. A fluorescent spot may not necessarily represent a connexin protein. Immunogold labelling, performed by Graham Nevill, with the same antibodies used in the immunofluorescence and immunoblotting experiments showed the antibody labelling connexin proteins integrated within structures identifiable as gap junctions under transmission electron microscopy.

Initial immunogold experiments used only the anti-Cx26 antibody Gap28h. Specific gold-labelling of gap junctions throughout the inner ear was observed using this antibody. Cx30 Zymed polyclonal antibody also specifically labels gap junction structures throughout the inner ear. Figures 6.2 (a) shows a gap junction gold-labelled with the anti-Cx26 antibody, Gap28h; Figure 6.2 (b) shows a gap junction specifically gold-labelled with Cx30 antibody. When a monoclonal Cx26 antibody became available to us the possibility of double-labelling gap junction structures with the polyclonal Cx30 and monoclonal Cx26 antibody arose. Figure 6.2 (c) shows the monoclonal Cx26 antibody exclusively labelling the gap junction plaque, although it does not seem as efficient as the polyclonal Cx26 antibody. That the gold particles label only the structure identifiable as a gap junction and are not present elsewhere demonstrates that this antibody specifically recognises the connexin protein constituents of the gap junction.

Figure 6.2: Immunogold labelling of gap junction structures



Figure 6.3 shows gold-labelling specifically for Cx30 (Fig. 6.3(a)) and Cx26 (Fig. 6.3(b)), of a gap junction between inner pillar cells. These are serial sections and therefore show the same gap junction labelled with both Cx30 and Cx26. It may appear from these images that the antibodies label only on one side of the gap junction, this is an artefact, which arises from the fact that the antibody doesn't penetrate the plastic section, and only labels where the epitope is exposed by the sectioning on the face that was in contact with the labelling solutions. The gold-labelling results correspond with the freeze fracture and immunostaining results showing gap junctions containing both Cx26 and Cx30 are expressed throughout the inner ear. Figure 6.3 is a good example of the large gap junction plaques between inner pillar cell bodies.

By using secondary antibodies raised in different species and conjugated to different sized gold particles double labelling of gap junctions was achieved. In Figure 6.4 small gold particles label Cx26 and the large gold particles label Cx30 in a Deiters' cell junction. Both sets of gold labels are evenly distributed along the junction profile and on both sides of the junction. Immunogold labelling has indicated that in every non-sensory cell type from the inner sulcus to the outer sulcus both Cx26 and Cx30 are present in the same junctions. That the immunogold staining demonstrates the presence and even distribution of Cx26 and Cx30 in the same gap junction plaques suggests that these junctions may be heteromeric.

Figure 6.3: Successive immunogold sections



Discussion

Antibodies

As this project progressed more anti-connexin antibodies became available for use and it was soon apparent that some antibodies are more efficient and some more specific than others. Antibodies initially thought to be specific to a particular isoform have subsequently been found to label other connexin proteins; it is possible that the isoform that has been labelled was not discovered at the time of antibody production. This factor led to misinterpretation of results in some early experiments. Further checking with rt-PCR primers and other antibodies eliminates this problem. Other researchers have also reported specificity problems with commercially supplied antibodies (Severs *et al.* 2001).

In addition to various checks of antibody specificity it is also necessary to realise that different antibodies may require different fixation and staining protocols. All antibodies used in this study were tested with two different protocols and at different dilutions (for an alternative blocking protocol used for some antibodies see appendix 4).

In particular, antibodies designed to specifically recognise either Cx43 or Cx32 have been found to be non-specific. Thorough testing of each Cx43 antibody, performed in the laboratories of N. Severs and D. Becker, allowed determination of those that are isoform-specific. With Cx32 antibodies both positive and negative immunostaining results were achieved in the inner ear; however, RT-PCR results have shown that this isoform is not present in the peripheral auditory system of mice (see chapter 4, figure 4.1).

Immunogold labelling results have proved that the antibodies used label gap junction structures throughout the non-sensory cell populations of the inner ear. The immunogold results also support the evidence from immunohistochemistry that these two isoforms co-localise in the same junction plaques.

CHAPTER SEVEN

Studies With Knockout Mice

Introduction

To gain further insight into the possible functions of connexins within the inner ear knockout mice, with targeted deletion or replacement of particular connexin genes, have been studied. Unfortunately neither a Cx26 knockout (Cx26^{-/-}) nor a Cx30 knockout (Cx30^{-/-}) mouse had been generated at the time of these studies. Cx26^{-/-} mice do not survive *in utero*, as the mouse placenta is reliant on gap junctions that contain Cx26 to function properly. These two knockouts would be particularly interesting to study, as Cx26 and Cx30 are by far the most abundant connexin isoforms present within the mouse inner ear.

A conditional knockout of Cx26 in the ear has now been produced (Cohen-Salmon *et al.*, 2002), and findings from this mouse should add significantly to our understanding of the function of this isoform within the inner ear.

Development of the lens, in vertebrates, is reliant on three connexin isoforms, Cx50, Cx46 and Cx43 (Beyer *et al.* 1987; Paul *et al.* 1991; White *et al.* 1992). Cx43 is restricted to lens epithelial cells and the newly differentiating cells in the bow region of the lens. Cx50 is also found in the lens epithelial cells; Cx50 and Cx46 have been observed to be colocalised in the lens fibre cells (Benedetti *et al.* 2000). Knockout of Cx50 causes reduction in growth of the lens and cataracts (Rong *et al.* 2002). Cx46 knockouts develop cataracts to varying degrees dependant on the genetic background of the mouse strain (Gong *et al.*, 1997; Gong *et al.* 1999).

Mice that have been generated with a targeted replacement of either the Cx46

(Cx46^{-/-}), Cx50 (Cx50^{-/-}) or both (double-knockout) of these coding regions with a lacZ-reporter gene were studied at The Scripps Research Institute, La Jolla, USA.

Following a report that a mutation in Cx31 causes high frequency hearing loss in humans (Xia *et al.*, 1998), the expression of Cx31 in the mouse inner ear was investigated. Initially Cx31 appeared to be abundantly expressed throughout the ear using a polyclonal anti-Cx31 antibody, though this result was not confirmed by RT-PCR (see Chapter 4 for result). When Cx31^{-/-} mice were produced they did not differ in appearance, weight, fertility or viability and their inner ears were morphologically normal (Plum *et al.*, 2001).

Mice with a targeted deletion of their Cx43 gene are not viable and die quickly after birth due to a heart defect (Reaume *et al.*, 1995). Cx43 is known to be associated with migration of neural crest cells; locomotion of the neural crest is reduced with Cx43 inhibition (Lo, International Gap Junction Conference, Hawaii, 2001). That neural crest cells contribute the intermediate cells of the stria vascularis in the inner ear and that Cx43 is expressed in the ear (see Chapters 4 and 5) introduced the possibility that a Cx43^{-/-} mouse may have inner ear defects. Cx43^{-/-} mice from the laboratory of David Becker, UCL, London were genotyped by Stefano Casalotti and studied by either embedding in plastic and sectioning or dehydrating and clearing with methyl salicylate (see Chapter 2 for methods).

Results

The morphology of the inner ears of the Cx31^{-/-}, Cx43^{-/-}, Cx46^{-/-} the Cx50^{-/-} and of the double-knockout (Cx46^{-/-} / Cx50^{-/-}) all appeared normal under light microscopy.

The laboratory of Klaus Willecke in Bonn, Germany, kindly donated mice with a lacZ reporter gene replacing their Cx31-coding region to further investigate Cx31 expression in mouse inner ear. The tissue from these mice had been fixed in 4% paraformaldehyde so no X-Gal staining was performed in this study. LacZ staining by Plum and colleagues (2001), in the Cx31^{-/-} mice was reported to give no staining in the inner ear.

Frozen sections and wholemounts were studied after X-gal staining of the Cx46^{-/-} and Cx50^{-/-} otocysts and mature inner ears. Any blue staining indicates the location of the LacZ reporter gene that has replaced the connexin genes in these knockouts, thereby illustrating the presence and location of these connexins in wild-type animals.

Cx46

Figure 7.1 shows the results of testing for the presence of Cx46. Figure 7.1(b) indicates the absence of Cx46 in wild-type mouse organ of Corti as FITC-staining with an anti-Cx46 antibody is negative. Figure 7.1(a) is a light microscope view of the section shown in 7.1(b) to aid with identification of the organ of Corti structures. A positive control section of wild-type mouse lens is shown (Fig. 7.1(e)) stained using the same Cx46 antibody applied to the section in figure 7.1(b).

Figure 7.1: Testing for Cx46 expression



Figures 7.1(c) and (d) show sections of Cx46^{-/-} mouse organ of Corti and utricle respectively; no blue X-gal staining is seen. None of the sections from the Cx46^{-/-} mice showed positive staining with X-gal. This indicates that Cx46 is not present in the mouse inner ear. As a negative control for these experiments wild-type ears were subjected to the X-gal staining. No positive, blue staining was ever seen in the wild-type ears.

Cx50

Upon observation of the adult cochlea and vestibular organs of both wholmount preparations and sections, no X-gal staining was seen in the mature Cx50^{-/-} mouse ears. X-gal staining was seen in the lens this acted as a positive control (see Figure 7.2).

Figure 7.2: Cx50 in lens



Positive staining of Cx50 in an E18.5 lens

Studies of immature ears from the Cx50^{-/-} mice did provide evidence that Cx50 is involved in inner ear development. Figure 7.3 shows obvious blue staining of β -galactosidase in both the apical and basal regions of the E15.5 otocyst where Cx50 would normally be expressed. The presence of the LacZ gene product represents the normal location of Cx50 and can be seen along the lower edge of the developing cochlear duct in the region of the epithelial ridges (Fig. 7.3 (a) and (b)) at E15.5. That there is less blue staining in the basal coil than the apical coil may be significantly related to the fact that the cochlea develops from base to apex, whereby there is less Cx50 in the more mature coil. This idea is further supported by the expression of the LacZ reporter gene product seen in the E18.5 otocyst. At this stage the blue β -galactosidase stain is only seen in the apical coil of the developing cochlea (Fig. 7.4 (a)), there is no blue stain in the basal coil (Fig. 7.4 (b)) indicating the down-regulation of Cx50 at this stage of otocyst development. In Figure 7.4 a sketch diagram indicates the area of the differentiating cochlear sensory cells in a late embryonic otocyst. With reference to this it is clear that the Cx50 expression correlates with this developing sensory area (Fig. 7.4). The vestibular system matures earlier than the cochlea so the absence of β -galactosidase staining, demonstrated in figures 7.4(c) and (d), may mean that either there is no Cx50 expressed in the vestibular organs during development or that Cx50 is expressed earlier than the stages studied here.

Figure 7.3: Cx50 in E15.5



(b) LacZ staining representing Cx50 location in the basal coil of an E15.5 mouse

FIGURE 7.4: Cx50^{-/-} E18.5 mouse



Cx43

Early postnatal cochleae and late embryonic otocysts were studied from *Cx43*^{-/-} mice and compared to those from wild-type littermates. Upon morphological comparison the size and shape of both late otocysts and early cochleae appeared the same in both knockouts and wild-type mice (Fig. 7.5). The shape of the cochlea and the structure of the semicircular canals were normal in *Cx43*^{-/-} mice. One ear from each mouse was cleared to allow this morphological comparison the other was embedded in plastic and sectioned to allow analysis of the inner ear at a cellular level (Fig. 7.6). By assessment of sections from both cochlear duct and vestibular epithelia the wild-type and knockout mouse inner seem analogous in their development.

In both the wild-type and knockout P0 cochlear duct and vestibular sections the development of all structures can be seen. The otolithic and tectorial membranes can be seen, the hair cells and supporting cells are arranged normally and Reissner's membrane is forming. The sections in Fig. 7.6 show that the knockout inner ear and wild-type inner ear are at the same stage of maturation. The cochlear duct sections show the same coil to allow direct comparison of the developmental stage.

Figure 7.5: Morphological comparison of wild-type with Cx43 knockout otocyst



Figure 7.6: Comparison of Cx43 knockouts with wild-type mouse inner ear



Some of the plastic sections were observed by TEM. The pigmented intermediate cells are difficult to see in both the wild-type and knockout strial sections at this stage of development. The presence of pigmented cells is more obvious at this stage in the dark cell region of the vestibular system. This dark cell region is the ion-transporting epithelia of the vestibular organs. Pigmented cells can be seen in the normal region in the vestibular epithelia of Cx43^{-/-} ears (Fig. 7.7 (a)). By directly comparing the wild-type (Fig. 7.7 (b)) and Cx43^{-/-} (Fig. 7.7 (a)) sections there does not appear to be a developmental delay in the inner ear of the knockout mice.

Figure 7.7: Plastic sections viewed by transmission electron microscopy



(a) Vestibular organ showing pigmented cells in the dark cell region of an E18.5 Cx43 knockout mouse



(b) Vestibular organ showing pigmented cells in the dark cell region of an E18.5 wild-type mouse

Discussion

The phenotypic consequences of alterations in different connexin genes are diverse. It is apparent through the difference in viability of Cx26-deficient mice and humans that defective connexin genes can cause different effects in different species. Throughout this thesis mainly mice have been studied and one has to be aware that results seen are not necessarily comparable between mammalian species. However the study of knockout mice does provide valuable insight into *in vivo* functioning of the connexin proteins.

Study of knockout mice in this thesis has demonstrated the presence of a connexin protein not previously identified in the mouse cochlea, Cx50. This isoform is not present in the mature mouse cochlea, but is involved during development as demonstrated by the presence of the LacZ gene product in animals where the LacZ gene has replaced the Cx50 gene. For all of the results from Cx 50^{-/-} mice the β -galactosidase staining is thought to represent Cx50 expression in wild-type mice, therefore Cx50 is involved in development of the mouse cochlea. The results show that there is less Cx50 in the basal coil than the apical coil at E15.5, this could be related to the base to apex development of the cochlea. This is again demonstrated by the presence of Cx50 in the apical coil but absence of Cx50 in the basal coil of the E18.5 otocyst; the Cx50 has been down-regulated in the more mature cochlea.

It is possible that the developing vestibular organs do not ever express Cx50 or that they require Cx50 at a stage earlier than those studied; E15.5 was the earliest time that Cx50^{-/-} mice were examined. This result, obtained by a gene replacement

method, has not been easily demonstrable using immunohistochemical methods as the only Cx50 antibody available gave high levels of background fluorescence.

Mice whose Cx46^{-/-} gene had been replaced with a LacZ reporter gene showed no β -galactosidase staining demonstrating that Cx46 is not present in the mouse inner ear at any stage. This result was corroborated using an anti-Cx46 antibody, which gave no positive staining in the wild-type mouse inner ear.

Observation of embryos from mice heterozygous for Cx43 allowed assessment of the effect of knocking-out connexin 43. Whole otocysts and cochleae from Cx43^{-/-} mice looked morphologically normal at E18.5 and P0 compared with wild-type littermates by using clearing techniques. Inner ears from the same mice were observed as sections after embedding in plastic. There did not appear to be any developmental delay at the cellular level in the ears of Cx43^{-/-} mice. The eyes from the same Cx43^{-/-} animals did show retarded development. Eyes from knockout mice were smaller and less differentiated than those of the wild-type littermates.

The presence of the pigmented cells in the dark cell region and the apparently normal development of the stria vascularis of the Cx43^{-/-} mice suggest that cells of neural crest origin are present and functional within the Cx43^{-/-} inner ears. The involvement of Cx43 in neural crest migration had required that these inner ear neural crest-derived cells be investigated.

Knocking out the connexins present within the inner ear would be a valuable study but as seen with Cx26 knockout mice some gene deletions can be lethal. The

dysfunction due to a gene knockout may be difficult to identify and may be missed altogether if the altered phenotype is age dependant, for example a gene deletion causing progressive deafness. A gene deletion may also cause no effect because there is compensation by another gene. Although knockout mice have provided interesting results it is necessary to remember that any phenotypic changes seen may be indirectly related to the gene deletion.

CHAPTER EIGHT

General Discussion

Unlike tight and adherens junctions, gap junctions do not seal membranes together, nor do they restrict the passage of material between membranes. Gap junctions are clusters of channels that allow the passage of small molecules from one cell to another, thereby connecting the interior of adjacent cells. Gap junctions enable electrical and metabolic coupling amongst cell populations; a signal initiated in one cell can readily extend into the adjoining cells via these junctions. Separation of cell populations by an absence of these gap junctions or by junctions that are selectively opened and closed in specific conditions can be just as important for correct functioning. Defects in gap junction proteins expressed in the cochlea cause deafness due to the breakdown in this coupling.

Summary of the findings of this thesis

Table 8.1: Summary of spatiotemporal analysis of connexin isoforms in the inner ear

| | DEVELOPING LATERAL WALL | | DEVELOPING ORGAN OF CORTI |
|------------------------------------|--------------------------------|-------------------------|--|
| E11.5 | 26 30 31 43 | | 26 30 31 43 |
| E15.5 | 26 30 31 43 | | 26 30 31 43 50 |
| E18.5 | 26 30 31 43 | | 26 30 31 43 45 50 |
| | LATERAL WALL | | ORGAN OF CORTI |
| | Spiral ligament | Stria vascularis | Supporting cells |
| P0 | 26 30 43 | 26 30 | 26 30 31 43 |
| P4 | 26 30 43 | 30 | 26 30 31 43 |
| ADULT (>6 weeks old) | 26 30 43 | 30 | 26 30 |

This thesis set out to determine why a defect in or an absence of one of these connexin proteins can cause deafness by analysis of the presence, location and expression patterns of all connexins within the inner ear. Analyses of a large collection of freeze fracture replicas from inner ear tissues provided an overview of gap junction plaque sizes and location in the inner ear (freeze fracture experiments were performed by Prof. A. Forge and G. Nevill). Investigations using molecular biology and immuno-histochemical techniques allowed resolution of the individual connexin isoforms present in mature tissue and throughout development. Immunogold staining also established that the antibodies stain structures recognisable as gap junction plaques.

The immunogold labelling of gap junctions within inner ear tissues corresponded both in size and distribution with the results from freeze fracture replicas. The patterns of connexin expression seen by immunostaining anti-connexin antibodies matched with the location of gap junction plaques seen by freeze fracturing the ear tissues and corresponded with the immunogold labelling. All non-sensory cells of the organ of Corti, supporting cells in the vestibular organs and all cells of the cochlear lateral wall except marginal cells of the stria vascularis have gap junctions. The sensory hair cells do not have gap junctions in either the cochlea or vestibular system.

Results from all methods used in this thesis have illustrated a distinctive pattern of gap junction distribution within cell types of the inner ear. Generally in the sensory supporting cells smaller gap junction plaques are seen at the apices of cells with larger plaques present more basally between the cell body regions. That gap

junctions are numerous and often very large within the inner ear indicates that these are highly important structures; their possible role in K⁺ recycling to maintain ion homeostasis that is vital to cochlea function (Kikuchi *et al.* 1995) is an appealing hypothesis. It is also possible that these large gap junction plaques between supporting cell bodies, in particular inner pillar cells, may have a role in preserving the complex structural integrity of the organ of Corti.

The cochlear lateral wall gap junctions connect fibrocyte cells of the spiral ligament and the basal and intermediate cells of the stria vascularis with the conspicuous exception of the strial marginal cells. The basal and intermediate cells of the stria are a coupled unit separated from the marginal cells by the absence of gap junctions. This separation may be important for maintenance of the endocochlear potential essential for auditory function.

Connexins 26 and 30 have been found to be the major isoforms in inner ear gap junctions (Lautermann *et al.*, 1998; Forge *et al.* 2003). It was necessary to acknowledge recent queries that have arisen regarding the specificity of some anti-connexin antibodies. The Cx26 and Cx30 antibodies used in this thesis were tested with transfected cells to confirm that they are specific for the isoform that they were designed to identify. Connexin 43 is also present at lower levels in a specific area of the cochlear lateral wall and between vestibular supporting cells in the mature ear. Despite having been reported to cause deafness in humans Cx31 has not been observed in the mature mouse inner ear. Cx32 also causes a deafness phenotype in humans as part of Charcot-Marie-Tooth syndrome; this isoform is not present in the mouse inner ear, which may be due to expression differences between species or

may be an effect of Cx32 absence in the nervous system beyond the inner ear affecting signal transmission to the brain.

During development of the mouse cochlea, both embryonically and postnatally, there is a more complex array of connexin proteins expressed. Cx26 and Cx30 were present through all developmental stages studied (from E13.5 to P10), Cx31, Cx43 and Cx50 were also observed at specific stages of development. Cx31 was seen until postnatal day 2; Cx43 is widely expressed in embryonic stages and was downregulated after birth to a much lower level of expression in the mature tissue; Cx50 was seen to be involved during embryonic development but was not expressed after E19.5. Cx45 is also present in the inner ear during development but a full study of its spatio-temporal expression pattern has yet to be completed. A recent publication (Cohen-Salmon *et al.*, 2002) reported the generation of a mouse with a targeted deletion of Cx26. The cochlea of this mouse was seen to develop normally but degenerated after postnatal day 15. It is feasible that this observed phenomenon means that Cx26 is not vital during development due to the presence of other isoforms that can compensate. This hypothesis fits well with the findings in this thesis that reports an intricate interaction of connexin isoforms within the cochlea during development whereby particular isoforms are observed in distinct regions at specific times.

Why do Cx26 mutations cause deafness?

Isoforms Cx26 and Cx30 are expressed in other areas of the body, yet Cx26 mutations in humans often cause non-syndromic deafness. This may be due to the extreme importance of ion homeostasis in the inner ear, which may not be necessary for functioning of the other organs. The absence of a vestibular disturbance in patients with Cx26 mutations may be due to compensation for the dysfunction by other sensory inputs. The significant difference between the auditory system and vestibular system may be the endocochlear potential which is exclusive to the cochlea. There may be alternative connexin isoforms that are able to compensate for the Cx26 absence in other body tissues. Dominant Cx26 mutations cause syndromes that exhibit skin disease with hearing loss; there may be a special need for the Cx26 isoform in the inner ear and skin.

The abundance of co-localisation of Cx26 and Cx30 throughout the ear introduces the possibility of heteromeric or heterotypic junctions comprising these two isoforms. Both the immunohistochemistry results and the immunogold labelling suggested that Cx26 and Cx30 form heteromeric junctions within the inner ear. Studies of heteromeric channels has shown them to exhibit unique properties different from those channels which contain only one isoform; the formation of heteromeric channels can affect a variety of channel properties including differences in permeability, plaque size and gating. It may be that Cx26 and Cx30 are required to operate together within gap junction channels and plaques to achieve normal auditory function, the physiological properties of the gap junction channels may be exclusively adapted to suit their purpose within the cochlea.

Studies of deafness-causing mutations of Cx26 protein transfected into HeLa cells provide evidence that these mutations can have dominant negative effects on both Cx26 and Cx30 (Marziano *et al.*, 2003). The *in vitro* expression studies demonstrated that Cx26 and Cx30 can oligomerise to form heteromeric connexons, supporting the results shown with immunogold labelling of these connexins.

The hypothesis leading to the investigations performed for this thesis was that Cx26 was the only isoform present in the cochlea so deafness was caused by its absence simply due to the lack of any other connexins that could compensate. This explained why some other tissues that express Cx26 were not affected by the non-functional Cx26 protein and that the phenotype in patients with these mutations was non-syndromic deafness. In the light of work presented here and the aforementioned *in vitro* studies with Cx26 mutations it is possible that a defective Cx26 prevents the formation of heteromeric channels that are essential for auditory function.

Although it was the initial reports of human connexin mutations causing deafness that prompted this study of connexins and gap junctions in the mammalian inner ear it is important to realise that results from a mouse model cannot be literally translated to the situation in humans. The precise nature of connexin isoform expression is demonstrated by a study of the lenses of connexin knockout mice; it became apparent that two different strains of mice had disparate phenotypes in response to the removal of Cx46 whereby one strain developed a cataract but the other strain didn't (Gong *et al.*, 1999). That there can be such a discrepancy between

strains of mice highlights the possibility of variations in connexin expression between mammalian species.

Future studies

That there are distinct differences in connexin expression in the developing and mature mouse cochlea is fascinating. It would be interesting to look at other isoforms through all developmental stages, especially newly discovered connexins. As some isoforms appear to have very discreet expression patterns it would be intriguing to look at earlier stages and follow every isoform through all developmental stages to maturity.

A further study to monitor and quantitate cell coupling is needed to corroborate the protein expression patterns and to ascertain the functionality of the gap junctions observed. A preliminary *in vitro* dye transfer study was performed as part of this thesis; unfortunately this did not provide conclusive results due to rapid deterioration of the epithelia. Future work using this dye transfer technique with improved methodology would be worthwhile to assess functional coupling in the inner ear.

The response of the cochlea and vestibular organs to damage, with respect to the involvement of gap junctions, would be significant. It would be interesting to compare the isoforms involved during development with any isoforms expressed subsequent to injury. This study may help answer questions relating to repair and regeneration in the inner ear.

Advances in knockout mice technology have presented new opportunities for the study of the effects of removing specific connexins. Studies of a conditional Cx26 knockout may provide further clues to the mechanisms by which Cx26 mutations cause deafness in humans. The inner ears of Cx30 knockout mice would also be interesting to study; as would a double Cx26 and Cx30 knockout mouse.

References

- (1998). Genome sequence of the nematode *C. elegans*: a platform for investigating biology. The *C. elegans* Sequencing Consortium. *Science* **282**, 2012-8.
- Adams, M. D., Celniker, S. E., Holt, R. A., Evans, C. A., Gocayne, J. D., Amanatides, P. G., Scherer, S. E., Li, P. W., Hoskins, R. A., Galle, R. F., George, R. A., Lewis, S. E., Richards, S., Ashburner, M., Henderson, S. N., Sutton, G. G., Wortman, J. R., Yandell, M. D., Zhang, Q., Chen, L. X., Brandon, R. C., Rogers, Y. H., Blazej, R. G., Champe, M., Pfeiffer, B. D., Wan, K. H., Doyle, C., Baxter, E. G., Helt, G., Nelson, C. R., Gabor, G. L., Abril, J. F., Agbayani, A., An, H. J., Andrews-Pfannkoch, C., Baldwin, D., Ballew, R. M., Basu, A., Baxendale, J., Bayraktaroglu, L., Beasley, E. M., Beeson, K. Y., Benos, P. V., Berman, B. P., Bhandari, D., Bolshakov, S., Borkova, D., Botchan, M. R., Bouck, J., Brokstein, P., Brottier, P., Burtis, K. C., Busam, D. A., Butler, H., Cadieu, E., Center, A., Chandra, I., Cherry, J. M., Cawley, S., Dahlke, C., Davenport, L. B., Davies, P., de Pablos, B., Delcher, A., Deng, Z., Mays, A. D., Dew, I., Dietz, S. M., Dodson, K., Doup, L. E., Downes, M., Dugan-Rocha, S., Dunkov, B. C., Dunn, P., Durbin, K. J., Evangelista, C. C., Ferraz, C., Ferriera, S., Fleischmann, W., Fosler, C., Gabrielian, A. E., Garg, N. S., Gelbart, W. M., Glasser, K., Glodek, A., Gong, F., Gorrell, J. H., Gu, Z., Guan, P., Harris, M., Harris, N. L., Harvey, D., Heiman, T. J., Hernandez, J. R., Houck, J., Hostin, D., Houston, K. A., Howland, T. J., Wei, M. H., Ibegwam, C., et al. (2000). The genome sequence of *Drosophila melanogaster*. *Science* **287**, 2185-95.
- Allen, F., and Warner, A. (1991). Gap junctional communication during neuromuscular junction formation. *Neuron* **6**, 101-11.
- Bagger-Sjoberg, D., and Flock, A. (1977). Freeze-fracturing of the auditory basilar papilla in the lizard *Calotes versicolor*. *Cell Tissue Res* **177**, 431-43.
- Becker, D. L., Evans, W. H., Green, C. R., and Warner, A. (1995). Functional analysis of amino acid sequences in connexin43 involved in intercellular communication through gap junctions. *J Cell Sci* **108** (Pt 4), 1455-67.
- Becker, D. L., Leclerc-David, C., and Warner, A. (1992). The relationship of gap junctions and compaction in the preimplantation mouse embryo. *Dev Suppl*, 113-8.
- Benedetti, E. L., Dunia, I., Recouvreur, M., Nicolas, P., Kumar, N. M., and Bloemendal, H. (2000). Structural organization of gap junctions as revealed by freeze-fracture and SDS fracture-labeling. *Eur J Cell Biol* **79**, 575-82.
- Benedetti, E. L., and Emmelot, P. (1968). Hexagonal array of subunits in tight junctions separated from isolated rat liver plasma membranes. *J Cell Biol* **38**, 15-24.

- Bennett, M. V., Barrio, L. C., Bargiello, T. A., Spray, D. C., Hertzberg, E., and Saez, J. C. (1991). Gap junctions: new tools, new answers, new questions. *Neuron* **6**, 305-20.
- Bennett, M. V., and Verselis, V. K. (1992). Biophysics of gap junctions. *Semin Cell Biol* **3**, 29-47.
- Bergoffen, J., Scherer, S. S., Wang, S., Scott, M. O., Bone, L. J., Paul, D. L., Chen, K., Lensch, M. W., Chance, P. F., and Fischbeck, K. H. (1993). Connexin mutations in X-linked Charcot-Marie-Tooth disease. *Science* **262**, 2039-42.
- Beyer, E. C., Paul, D. L., and Goodenough, D. A. (1987). Connexin43: a protein from rat heart homologous to a gap junction protein from liver. *J Cell Biol* **105**, 2621-9.
- Boettger, T., Hubner, C.A., Maier, H., Rust, M.B., Beck, F.X., Jentsch, T.J. (2002). Deafness and renal tubular acidosis in mice lacking the K-Cl cotransporter Kcc4. *Nature* **416**, 874-878.
- Bonnerot, C., Rocancourt, D., Briand, P., Grimber, G., and Nicolas, J. F. (1987). A beta-galactosidase hybrid protein targeted to nuclei as a marker for developmental studies. *Proc Natl Acad Sci U S A* **84**, 6795-9.
- Carlisle, L., Steel, K., and Forge, A. (1990). Endocochlear potential generation is associated with intercellular communication in the stria vascularis: structural analysis in the viable dominant spotting mouse mutant. *Cell Tissue Res* **262**, 329-37.
- Chen, L., and Meng, M. Q. (1995). Compact and scattered gap junctions in diffusion mediated cell-cell communication. *J Theor Biol* **176**, 39-45.
- Coats, A. C. (1965). Temperature effects on the peripheral auditory apparatus. *Science* **150**, 1481-3.
- Cohen-Salmon, M., Ott, T., Michel, V., Hardelin, J.P., Perfettini, I., Eybalin M., Wu T., Marcus D.C., Wangemann P., Willecke K., Petit C. (2002). Targeted ablation of connexin26 in the inner ear epithelial gap junction network causes hearing impairment and cell death. *Curr Biol* **12**, 1106-1111
- Common, J.E., Becker, D., Di, W.L., Leigh, I.M., O'Toole, E.A., Kelsell, D.P. (2002). Functional studies of human skin disease- and deafness-associated connexin 30 mutations. *Biochem Biophys Res Commun.* **298(5)**:651-6.
- Coppen, S. R., Dupont, E., Rothery, S., and Severs, N. J. (1998). Connexin45 expression is preferentially associated with the ventricular conduction system in mouse and rat heart. *Circ Res* **82**, 232-43.
- Corwin, J. (1997). Introduction: Inner ear development - initial indications of the molecular mechanisms. *Semin Cell Dev Biol* **8**, 215-216.

- Corwin, J. T., Jones, J. E., Katayama, A., Kelley, M. W., and Warchol, M. E. (1991). Hair cell regeneration: the identities of progenitor cells, potential triggers and instructive cues. *Ciba Found Symp* **160**, 103-20; discussion 120-30.
- Dahl, G. (1996). Where are the gates in gap junction channels? *Clin Exp Pharmacol Physiol* **23**, 1047-52.
- Dahl, G., Werner, R., Levine, E., and Rabadan-Diehl, C. (1992). Mutational analysis of gap junction formation. *Biophys J* **62**, 172-80; discussion 180-2.
- Davies, T. C., Barr, K. J., Jones, D. H., Zhu, D., and Kidder, G. M. (1996). Multiple members of the connexin gene family participate in preimplantation development of the mouse. *Dev Genet* **18**, 234-43.
- Denoyelle, F., Lina-Granade, G., Plauchu, H., Bruzzone, R., Chaib, H., Levi-Acobas, F., Weil, D., and Petit, C. (1998). Connexin 26 gene linked to a dominant deafness. *Nature* **393**, 319-20.
- Denoyelle, F., Weil, D., Maw, M. A., Wilcox, S. A., Lench, N. J., Allen-Powell, D. R., Osborn, A. H., Dahl, H. H., Middleton, A., Houseman, M. J., Dode, C., Marlin, S., Boulila-ElGaied, A., Grati, M., Ayadi, H., BenArab, S., Bitoun, P., Lina-Granade, G., Godet, J., Mustapha, M., Loiselet, J., El-Zir, E., Audois, A., Joannard, A., Petit, C., and et al. (1997). Prelingual deafness: high prevalence of a 30delG mutation in the connexin 26 gene. *Hum Mol Genet* **6**, 2173-7.
- Dermietzel, R., Traub, O., Hwang, T. K., Beyer, E., Bennett, M. V., Spray, D. C., and Willecke, K. (1989). Differential expression of three gap junction proteins in developing and mature brain tissues. *Proc Natl Acad Sci U S A* **86**, 10148-52.
- Dewey, M. M., and Barr, L. (1962). Intercellular Connection between Smooth Muscle Cells: The Nexus. *Science* **137**, 670-672.
- Eddison, M., Le Roux, I., and Lewis, J. (2000). Notch signaling in the development of the inner ear: lessons from *Drosophila*. *Proc Natl Acad Sci U S A* **97**, 11692-9.
- Elfgang, C., Eckert, R., Lichtenberg-Frate, H., Butterweck, A., Traub, O., Klein, R. A., Hulser, D. F., and Willecke, K. (1995). Specific permeability and selective formation of gap junction channels in connexin-transfected HeLa cells. *J Cell Biol* **129**, 805-17.
- Estivill, X., Fortina, P., Surrey, S., Rabionet, R., Melchionda, S., D'Agruma, L., Mansfield, E., Rappaport, E., Govea, N., Mila, M., Zelante, L., and Gasparini, P. (1998). Connexin-26 mutations in sporadic and inherited sensorineural deafness. *Lancet* **351**, 394-8.

- Evans, W. H., Ahmad, S., Diez, J., George, C. H., Kendall, J. M., and Martin, P. E. (1999). Trafficking pathways leading to the formation of gap junctions. *Novartis Found Symp* **219**, 44-54; discussion 54-9.
- Evans, W.H. and Martin, P.E. (2002). Gap junctions: structure and function [review]. *Mol Membr Biol* **19**, 121-136.
- Falk, M. M. (2000). Connexin-specific distribution within gap junctions revealed in living cells. *J Cell Sci* **113** (Pt 22), 4109-20.
- Falk, M. M. (2001). Connexins/connexons. Cell-free expression. *Methods Mol Biol* **154**, 91-116.
- Forge, A. (1984). Gap junctions in the stria vascularis and effects of ethacrynic acid. *Hear Res* **13**, 189-200.
- Forge, A., Souter, M., and Denman-Johnson, K. (1997). Structural development of sensory cells in the ear. *Semin Cell Dev Biol* **8**, 225-237.
- Frenz, C. M., and Van De Water, T. R. (2000). Immunolocalization of connexin 26 in the developing mouse cochlea. *Brain Res Brain Res Rev* **32**, 172-80.
- Fujimoto, K., Nagafuchi, A., Tsukita, S., Kuraoka, A., Ohokuma, A., and Shibata, Y. (1997). Dynamics of connexins, E-cadherin and alpha-catenin on cell membranes during gap junction formation. *J Cell Sci* **110** (Pt 3), 311-22.
- Furuse, M., Hirase, T., Itoh, M., Nagafuchi, A., Yonemura, S., and Tsukita, S. (1993). Occludin: a novel integral membrane protein localizing at tight junctions. *J Cell Biol* **123**, 1777-88.
- Fuse, Y., Doi, K., Hasegawa, T., Sugii, A., Hibino, H., Kubo, T. (1999) Three novel connexin26 gene mutations in autosomal recessive non-syndromic deafness. *Neuroreport*. **10**(9), 1853-7.
- Gabriel, H. D., Jung, D., Butzler, C., Temme, A., Traub, O., Winterhager, E., and Willecke, K. (1998). Transplacental uptake of glucose is decreased in embryonic lethal connexin26-deficient mice. *J Cell Biol* **140**, 1453-61.
- Gasparini, P., Estivill, X., Volpini, V., Totaro, A., Castellvi-Bel, S., Govea, N., Mila, M., Della Monica, M., Ventruto, V., De Benedetto, M., Stanziale, P., Zelante, L., Mansfield, E. S., Sandkuijl, L., Surrey, S., and Fortina, P. (1997). Linkage of DFNB1 to non-syndromic neurosensory autosomal-recessive deafness in Mediterranean families. *Eur J Hum Genet* **5**, 83-8.
- George, C. H., Kendall, J. M., and Evans, W. H. (1999). Intracellular trafficking pathways in the assembly of connexins into gap junctions. *J Biol Chem* **274**, 8678-85.

- Ginzberg, R. D., and Gilula, N. B. (1979). Modulation of cell junctions during differentiation of the chicken otocyst sensory epithelium. *Dev Biol* **68**, 110-29.
- Gong, X., Agopian, K., Kumar, N. M., and Gilula, N. B. (1999). Genetic factors influence cataract formation in alpha 3 connexin knockout mice. *Dev Genet* **24**, 27-32.
- Gong, X., Li, E., Klier, G., Huang, Q., Wu, Y., Lei, H., Kumar, N. M., Horwitz, J., and Gilula, N. B. (1997). Disruption of alpha3 connexin gene leads to proteolysis and cataractogenesis in mice. *Cell* **91**, 833-43.
- Goodenough, D. A. (1975). The structure of cell membranes involved in intercellular communication. *Am J Clin Pathol* **63**, 636-45.
- Green, C. R., Bowles, L., Crawley, A., and Tickle, C. (1994). Expression of the connexin43 gap junctional protein in tissues at the tip of the chick limb bud is related to the epithelial-mesenchymal interactions that mediate morphogenesis. *Dev Biol* **161**, 12-21.
- Green, C. R., Peters, N. S., Gourdie, R. G., Rothery, S., and Severs, N. J. (1993). Validation of immunohistochemical quantification in confocal scanning laser microscopy: a comparative assessment of gap junction size with confocal and ultrastructural techniques. *J Histochem Cytochem* **41**, 1339-49.
- Green, C. R., and Severs, N. J. (1993). Robert Feulgen Prize Lecture. Distribution and role of gap junctions in normal myocardium and human ischaemic heart disease. *Histochemistry* **99**, 105-20.
- Grifa, A., Wagner, C. A., D'Ambrosio, L., Melchionda, S., Bernardi, F., Lopez-Bigas, N., Rabionet, R., Arbones, M., Monica, M. D., Estivill, X., Zelante, L., Lang, F., and Gasparini, P. (1999). Mutations in GJB6 cause nonsyndromic autosomal dominant deafness at DFNA3 locus. *Nat Genet* **23**, 16-8.
- Gulley, R. L., and Reese, T. S. (1976). Intercellular junctions in the reticular lamina of the organ of Corti. *J Neurocytol* **5**, 479-507.
- Guthrie, S. C., and Gilula, N. B. (1989). Gap junctional communication and development. *Trends Neurosci* **12**, 12-6.
- Hama, K. (1980a). Fine structure of the afferent synapse and gap junctions on the sensory hair cell in the saccular macula of goldfish: a freeze-fracture study. *J Neurocytol* **9**, 845-60.
- Hama, K. (1980b). Gap junctions between hair cells and supporting cells in the goldfish saccular macula. A freeze fracture study. *Nagoya J Med Sci* **42**, 71-4.

- Heathcote, K., Syrris, P., Carter, N. D., and Patton, M. A. (2000). A connexin 26 mutation causes a syndrome of sensorineural hearing loss and palmoplantar hyperkeratosis (MIM 148350). *J Med Genet* **37**, 50-1.
- Heynkes, R., Kozjek, G., Traub, O., and Willecke, K. (1986). Identification of a rat liver cDNA and mRNA coding for the 28 kDa gap junction protein. *FEBS Lett* **205**, 56-60.
- Huang, G. Y., Cooper, E. S., Waldo, K., Kirby, M. L., Gilula, N. B., and Lo, C. W. (1998). Gap junction-mediated cell-cell communication modulates mouse neural crest migration. *J Cell Biol* **143**, 1725-34.
- Iurato, S., Franke, K., Luciano, L., Wermbter, G., Pannese, E., and Reale, E. (1976). Intercellular junctions in the organ of Corti as revealed by freeze fracturing. *Acta Otolaryngol* **82**, 57-69.
- Jacob, A., and Beyer, E. C. (2001). Mouse connexin 45: genomic cloning and exon usage. *DNA Cell Biol* **20**, 11-9.
- Jahnke, K. (1975). The fine structure of freeze-fractured intercellular junctions in the guinea pig inner ear. *Acta Otolaryngol Suppl* **336**, 1-40.
- Jordan, K., Chodock, R., Hand, A. R., and Laird, D. W. (2001). The origin of annular junctions: a mechanism of gap junction internalization. *J Cell Sci* **114**, 763-73.
- Kadle, R., Zhang, J. T., and Nicholson, B. J. (1991). Tissue-specific distribution of differentially phosphorylated forms of Cx43. *Mol Cell Biol* **11**, 363-9.
- Kanno, Y. (1984). Cell coupling junctions. *Cell Struct Funct* **9 Suppl**, s51-3.
- Kaufmann, M. H. (1998). "The Atlas of Mouse Development." Academic Press, London; San Diego.
- Kelsell, D. P., Dunlop, J., Stevens, H. P., Lench, N. J., Liang, J. N., Parry, G., Mueller, R. F., and Leigh, I. M. (1997). Connexin 26 mutations in hereditary non-syndromic sensorineural deafness. *Nature* **387**, 80-3.
- Kikuchi, T., Adams, J. C., Paul, D. L., and Kimura, R. S. (1994). Gap junction systems in the rat vestibular labyrinth: immunohistochemical and ultrastructural analysis. *Acta Otolaryngol* **114**, 520-8.
- Kikuchi, T., Kimura, R. S., Paul, D. L., and Adams, J. C. (1995). Gap junctions in the rat cochlea: immunohistochemical and ultrastructural analysis. *Anat Embryol (Berl)* **191**, 101-18.
- Kikuchi, T., Kimura, R. S., Paul, D. L., Takasaka, T., and Adams, J. C. (2000). Gap junction systems in the mammalian cochlea. *Brain Res Brain Res Rev* **32**, 163-6.

- Kirchhoff, S., Nelles, E., Hagendorff, A., Kruger, O., Traub, O., and Willecke, K. (1998). Reduced cardiac conduction velocity and predisposition to arrhythmias in connexin40-deficient mice. *Curr Biol* **8**, 299-302.
- Kumai, M., Nishii, K., Nakamura, K., Takeda, N., Suzuki, M., and Shibata, Y. (2000). Loss of connexin45 causes a cushion defect in early cardiogenesis. *Development* **127**, 3501-12.
- Kumar, N. M., and Gilula, N. B. (1986). Cloning and characterization of human and rat liver cDNAs coding for a gap junction protein. *J Cell Biol* **103**, 767-76.
- Kumar, N. M., and Gilula, N. B. (1996). The gap junction communication channel. *Cell* **84**, 381-8.
- Kunzelmann, P., Schroder, W., Traub, O., Steinhauser, C., Dermietzel, R., and Willecke, K. (1999). Late onset and increasing expression of the gap junction protein connexin30 in adult murine brain and long-term cultured astrocytes. *Glia* **25**, 111-9.
- Laing, J. G., and Beyer, E. C. (1995). The gap junction protein connexin43 is degraded via the ubiquitin proteasome pathway. *J Biol Chem* **270**, 26399-403.
- Laird, D. W. (1996). The life cycle of a connexin: gap junction formation, removal, and degradation. *J Bioenerg Biomembr* **28**, 311-8.
- Lal, R., John, S. A., Laird, D. W., and Arnsdorf, M. F. (1995). Heart gap junction preparations reveal hemiplaques by atomic force microscopy. *Am J Physiol* **268**, C968-77.
- Lampe, P. D., and Lau, A. F. (2000). Regulation of gap junctions by phosphorylation of connexins. *Arch Biochem Biophys* **384**, 205-15.
- Lautermann, J., ten Cate, W.J., Altenhoff, P., Grummer, R., Traub, O., Frank, H., Jahnke, K., Winterhager, E. (1998). Expression of the gap-junction connexins 26 and 30 in the rat cochlea. *Cell Tiss Res* **294**, 415-420.
- Lautermann, J., Frank, H., Jahnke, K., Traub, O., Winterhager, E. (1999). Developmental expression patterns of connexin26 and -30 in the rat cochlea. *Dev Genet* **25**, 306-311.
- Lazrak, A., and Peracchia, C. (1993). Gap junction gating sensitivity to physiological internal calcium regardless of pH in Novikoff hepatoma cells. *Biophys J* **65**, 2002-12.
- Lewis, J. (1991). Rules for the production of sensory cells. *Ciba Found Symp* **160**, 25-39; discussion 40-53.
- Liu, X.Z, Xia, X.J, Adams, J., Chen, Z.Y., Welch, K.O., Tekin, M., Ouyang, X.M., Kristiansen, A., Pandya, A., Balkany, T., Arnos, K.S., Nance, W.E. (2001).

Mutations in GJA1 (connexin 43) are associated with non-syndromic autosomal recessive deafness. *Hum Mol Genet* **10**, 2945-2951.

Lo, C. W. (1996). The role of gap junction membrane channels in development. *J Bioenerg Biomembr* **28**, 379-85.

Lo, C. W. (2000). Role of gap junctions in cardiac conduction and development: insights from the connexin knockout mice. *Circ Res* **87**, 346-8.

Lo, C. W., Cohen, M. F., Huang, G. Y., Lazatin, B. O., Patel, N., Sullivan, R., Pauken, C., and Park, S. M. (1997). Cx43 gap junction gene expression and gap junctional communication in mouse neural crest cells. *Dev Genet* **20**, 119-32.

Lo, C. W., and Gilula, N. B. (1979a). Gap junctional communication in the post-implantation mouse embryo. *Cell* **18**, 411-22.

Lo, C. W., and Gilula, N. B. (1979b). Gap junctional communication in the preimplantation mouse embryo. *Cell* **18**, 399-409.

Loewenstein, W. R. (1981). Junctional intercellular communication: the cell-to-cell membrane channel. *Physiol Rev* **61**, 829-913.

Maestrini, E., Korge, B. P., Ocana-Sierra, J., Calzolari, E., Cambiaghi, S., Scudder, P. M., Hovnanian, A., Monaco, A. P., and Munro, C. S. (1999). A missense mutation in connexin26, D66H, causes mutilating keratoderma with sensorineural deafness (Vohwinkel's syndrome) in three unrelated families. *Hum Mol Genet* **8**, 1237-43.

Makowski, L., Caspar, D. L., Phillips, W. C., and Goodenough, D. A. (1977). Gap junction structures. II. Analysis of the x-ray diffraction data. *J Cell Biol* **74**, 629-45.

Manthey, D., Banach, K., Desplantez, T., Lee, C. G., Kozak, C. A., Traub, O., Weingart, R., and Willecke, K. (2001). Intracellular domains of mouse connexin26 and -30 affect diffusional and electrical properties of gap junction channels. *J Membr Biol* **181**, 137-48.

Manthey, D., and Willecke, K. (2001). Transfection and expression of exogenous connexins in mammalian cells. *Methods Mol Biol* **154**, 187-99.

Marcus, D.C., Wu, T., Wangemann, P., Kofuji, P. (2002). KCNJ10 (Kir4.1) potassium channel knockout abolishes endocochlear potential. *Am J Physiol Cell Physiol*. **282**(2), C403-7.

Martin, P. (1990). Tissue patterning in the developing mouse limb. *Int J Dev Biol* **34**, 323-36.

- Martin, P., and Swanson, G. J. (1993). Descriptive and experimental analysis of the epithelial remodellings that control semicircular canal formation in the developing mouse inner ear. *Dev Biol* **159**, 549-58.
- Martin, P. E., Coleman, S. L., Casalotti, S. O., Forge, A., and Evans, W. H. (1999). Properties of connexin26 gap junctional proteins derived from mutations associated with non-syndromal hereditary deafness. *Hum Mol Genet* **8**, 2369-76.
- McDowell, B., Davies, S., and Forge, A. (1989). The effect of gentamicin-induced hair cell loss on the tight junctions of the reticular lamina. *Hear Res* **40**, 221-32.
- Merchan-Perez, A., Gil-Loyzaga, P., Bartolome, M. V., Remezal, M., Fernandez, P., and Rodriguez, T. (1999). Decalcification by ascorbic acid for immuno- and affinochemical techniques on the inner ear. *Histochem Cell Biol* **112**, 125-30.
- Meyer, R. A., Laird, D. W., Revel, J. P., and Johnson, R. G. (1992). Inhibition of gap junction and adherens junction assembly by connexin and A-CAM antibodies. *J Cell Biol* **119**, 179-89.
- Morsli, H., Choo, D., Ryan, A., Johnson, R., and Wu, D. K. (1998). Development of the mouse inner ear and origin of its sensory organs. *J Neurosci* **18**, 3327-35.
- Murgia, A., Orzan, E., Polli, R., Martella, M., Vinanzi, C., Leonardi, E., Arslan, E., and Zacchello, F. (1999). Cx26 deafness: mutation analysis and clinical variability. *J Med Genet* **36**, 829-32.
- Nadol, J. B., Jr. (1978). Intercellular junctions in the organ of Corti. *Ann Otol Rhinol Laryngol* **87**, 70-80.
- Nicholson, S. M., Ressot, C., Gomes, D., D'Andrea, P., Perea, J., Duval, N., and Bruzzone, R. (1999). Connexin32 in the peripheral nervous system. Functional analysis of mutations associated with X-linked Charcot-Marie-Tooth syndrome and implications for the pathophysiology of the disease. *Ann N Y Acad Sci* **883**, 168-85.
- Nishi, M., Kumar, N. M., and Gilula, N. B. (1991). Developmental regulation of gap junction gene expression during mouse embryonic development. *Dev Biol* **146**, 117-30.
- Paul, D. L. (1986). Molecular cloning of cDNA for rat liver gap junction protein. *J Cell Biol* **103**, 123-34.
- Paul, D. L., Ebihara, L., Takemoto, L. J., Swenson, K. I., and Goodenough, D. A. (1991). Connexin46, a novel lens gap junction protein, induces voltage-gated currents in nonjunctional plasma membrane of *Xenopus* oocytes. *J Cell Biol* **115**, 1077-89.

- Payton, B. W., Bennett, M. V., and Pappas, G. D. (1969a). Permeability and structure of junctional membranes at an electrotonic synapse. *Science* **166**, 1641-3.
- Payton, B. W., Bennett, M. V., and Pappas, G. D. (1969b). Temperature-dependence of resistance at an electrotonic synapse. *Science* **165**, 594-7.
- Perkins, G., Renken, C., Martone, M. E., Young, S. J., Ellisman, M., and Frey, T. (1997). Electron tomography of neuronal mitochondria: three-dimensional structure and organization of cristae and membrane contacts. *J Struct Biol* **119**, 260-72.
- Pfeffer, S. R., and Rothman, J. E. (1987). Biosynthetic protein transport and sorting by the endoplasmic reticulum and Golgi. *Annu Rev Biochem* **56**, 829-52.
- Phelan, P., Bacon, J. P., Davies, J. A., Stebbings, L. A., Todman, M. G., Avery, L., Baines, R. A., Barnes, T. M., Ford, C., Hekimi, S., Lee, R., Shaw, J. E., Starich, T. A., Curtin, K. D., Sun, Y. A., and Wyman, R. J. (1998a). Innexins: a family of invertebrate gap-junction proteins. *Trends Genet* **14**, 348-9.
- Phelan, P., Nakagawa, M., Wilkin, M. B., Moffat, K. G., O'Kane, C. J., Davies, J. A., and Bacon, J. P. (1996). Mutations in shaking-B prevent electrical synapse formation in the *Drosophila* giant fiber system. *J Neurosci* **16**, 1101-13.
- Phelan, P., Stebbings, L. A., Baines, R. A., Bacon, J. P., Davies, J. A., and Ford, C. (1998b). *Drosophila* Shaking-B protein forms gap junctions in paired *Xenopus* oocytes. *Nature* **391**, 181-4.
- Pinto da Silva, P., and Branton, D. (1970). Membrane splitting in freeze-etching. Covalently bound ferritin as a membrane marker. *J Cell Biol* **45**, 598-605.
- Plum, A., Winterhager, E., Pesch, J., Lautermann, J., Hallas, G., Rosentreter, B., Traub, O., Herberhold, C., and Willecke, K. (2001). Connexin31-deficiency in mice causes transient placental dysmorphogenesis but does not impair hearing and skin differentiation. *Dev Biol* **231**, 334-47.
- Potter, D. D., Furshpan, E. J., and Lennox, E. S. (1966). Connections between cells of the developing squid as revealed by electrophysiological methods. *Proc Natl Acad Sci U S A* **55**, 328-36.
- Rabionet, R., Gasparini, P., and Estivill, X. (2000a). Molecular genetics of hearing impairment due to mutations in gap junction genes encoding beta connexins. *Hum Mutat* **16**, 190-202.
- Rabionet, R., Zelante, L., Lopez-Bigas, N., D'Agruma, L., Melchionda, S., Restagno, G., Arbones, M. L., Gasparini, P., and Estivill, X. (2000b). Molecular basis of childhood deafness resulting from mutations in the GJB2 (connexin 26) gene. *Hum Genet* **106**, 40-4.

- Reaume, A. G., de Sousa, P. A., Kulkarni, S., Langille, B. L., Zhu, D., Davies, T. C., Juneja, S. C., Kidder, G. M., and Rossant, J. (1995). Cardiac malformation in neonatal mice lacking connexin43. *Science* **267**, 1831-4.
- Reuss, B., Hellmann, P., Traub, O., Butterweck, A., and Winterhager, E. (1997). Expression of connexin31 and connexin43 genes in early rat embryos. *Dev Genet* **21**, 82-90.
- Revel, J. P. (1986). Gap junctions in development. *Dev Biol (N Y 1985)* **3**, 191-204.
- Revel, J. P., and Karnovsky, M. J. (1967). Hexagonal array of subunits in intercellular junctions of the mouse heart and liver. *J Cell Biol* **33**, C7-C12.
- Richard, G., Smith, L. E., Bailey, R. A., Itin, P., Hohl, D., Epstein, E. H., Jr., DiGiovanna, J. J., Compton, J. G., and Bale, S. J. (1998). Mutations in the human connexin gene GJB3 cause erythrokeratoderma variabilis. *Nat Genet* **20**, 366-9.
- Risek, B., Guthrie, S., Kumar, N., and Gilula, N. B. (1990). Modulation of gap junction transcript and protein expression during pregnancy in the rat. *J Cell Biol* **110**, 269-82.
- Risek, B., Klier, F. G., and Gilula, N. B. (1992). Multiple gap junction genes are utilized during rat skin and hair development. *Development* **116**, 639-51.
- Rong, P., Wang, X., Niesman, I., Wu, Y., Benedetti, L. E., Dunia, I., Levy, E., and Gong, X. (2002). Disruption of Gja8 (alpha8 connexin) in mice leads to microphthalmia associated with retardation of lens growth and lens fiber maturation. *Development* **129**, 167-74.
- Rose, B., and Loewenstein, W. R. (1975a). Calcium ion distribution in cytoplasm visualised by aequorin: diffusion in cytosol restricted by energized sequestering. *Science* **190**, 1204-6.
- Rose, B., and Loewenstein, W. R. (1975b). Permeability of cell junction depends on local cytoplasmic calcium activity. *Nature* **254**, 250-2.
- Rose, B., and Loewenstein, W. R. (1976). Permeability of a cell junction and the local cytoplasmic free ionized calcium concentration: a study with aequorin. *J Membr Biol* **28**, 87-119.
- Rozental, R., Morales, M., Mehler, M. F., Urban, M., Kremer, M., Dermietzel, R., Kessler, J. A., and Spray, D. C. (1998). Changes in the properties of gap junctions during neuronal differentiation of hippocampal progenitor cells. *J Neurosci* **18**, 1753-62.
- Ruben, R. J., and Sidman, R. L. (1967). Serial section radioautography of the inner ear. Histological technique. *Arch Otolaryngol* **86**, 32-7.

- Saez, J. C., Nairn, A. C., Czernik, A. J., Spray, D. C., Hertzberg, E. L., Greengard, P., and Bennett, M. V. (1990). Phosphorylation of connexin 32, a hepatocyte gap-junction protein, by cAMP-dependent protein kinase, protein kinase C and Ca²⁺/calmodulin-dependent protein kinase II. *Eur J Biochem* **192**, 263-73.
- Salomon, D., Chanson, M., Vischer, S., Masgrau, E., Vozzi, C., Saurat, J. H., Spray, D. C., and Meda, P. (1992). Gap junctional communication of primary human keratinocytes: characterization by dual voltage clamp and dye transfer. *Exp Cell Res* **201**, 452-61.
- Santos-Sacchi, J. (1984). A re-evaluation of cell coupling in the organ of Corti. *Hear Res* **14**, 203-4.
- Santos-Sacchi, J. (1985). The effects of cytoplasmic acidification upon electrical coupling in the organ of Corti. *Hear Res* **19**, 207-15.
- Santos-Sacchi, J. (1986a). Dye coupling in the organ of Corti. *Cell Tissue Res* **245**, 525-9.
- Santos-Sacchi, J. (1986b). The temperature dependence of electrical coupling in the organ of Corti. *Hear Res* **21**, 205-11.
- Santos-Sacchi, J. (1987). Electrical coupling differs in the in vitro and in vivo organ of Corti. *Hear Res* **25**, 227-32.
- Santos-Sacchi, J., and Dallos, P. (1983). Intercellular communication in the supporting cells of the organ of Corti. *Hear Res* **9**, 317-26.
- Santos-Sacchi, J., and Marovitz, W. F. (1985). A ferritin-containing cell type in the stria vascularis of the mouse inner ear. *Acta Otolaryngol* **100**, 26-32.
- Scherer, S. S., Xu, Y. T., Nelles, E., Fischbeck, K., Willecke, K., and Bone, L. J. (1998). Connexin32-null mice develop demyelinating peripheral neuropathy. *Glia* **24**, 8-20.
- Schulte, B. A., and Adams, J. C. (1989). Distribution of immunoreactive Na⁺,K⁺-ATPase in gerbil cochlea. *J Histochem Cytochem* **37**, 127-34.
- Schulte, B. A., and Steel, K. P. (1994). Expression of alpha and beta subunit isoforms of Na,K-ATPase in the mouse inner ear and changes with mutations at the Wv or Sld loci. *Hear Res* **78**, 65-76.
- Scott, D. A., Kraft, M. L., Stone, E. M., Sheffield, V. C., and Smith, R. J. (1998). Connexin mutations and hearing loss. *Nature* **391**, 32.
- Severs, N. J. (1999). Cardiovascular disease. *Novartis Found Symp* **219**, 188-206; discussion 206-11.

- Severs, N. J., Rothery, S., Dupont, E., Coppen, S. R., Yeh, H. I., Ko, Y. S., Matsushita, T., Kaba, R., and Halliday, D. (2001). Immunocytochemical analysis of connexin expression in the healthy and diseased cardiovascular system. *Microsc Res Tech* **52**, 301-22.
- Sher, A. E. (1971). The embryonic and postnatal development of the inner ear of the mouse. *Acta Otolaryngol Suppl* **285**, 1-77.
- Sia, M. A., Woodward, T. L., Turner, J. D., and Laird, D. W. (1999). Quiescent mammary epithelial cells have reduced connexin43 but maintain a high level of gap junction intercellular communication. *Dev Genet* **24**, 111-22.
- Simon, A. M., Goodenough, D. A., Li, E., and Paul, D. L. (1997). Female infertility in mice lacking connexin 37. *Nature* **385**, 525-9.
- Simpson, I., Rose, B., and Loewenstein, W. R. (1977). Size limit of molecules permeating the junctional membrane channels. *Science* **195**, 294-6.
- Souter, M., and Forge, A. (1998). Intercellular junctional maturation in the stria vascularis: possible association with onset and rise of endocochlear potential. *Hear Res* **119**, 81-95.
- Spray, D. C., and Bennett, M. V. (1985). Physiology and pharmacology of gap junctions. *Annu Rev Physiol* **47**, 281-303.
- Spray, D. C., and Burt, J. M. (1990). Structure-activity relations of the cardiac gap junction channel. *Am J Physiol* **258**, C195-205.
- Spray, D. C., Moreno, A. P., Kessler, J. A., and Dermietzel, R. (1991). Characterization of gap junctions between cultured leptomeningeal cells. *Brain Res* **568**, 1-14.
- Starich, T. A., Lee, R. Y., Panzarella, C., Avery, L., and Shaw, J. E. (1996). eat-5 and unc-7 represent a multigene family in *Caenorhabditis elegans* involved in cell-cell coupling. *J Cell Biol* **134**, 537-48.
- Steel, K. P., Barkway, C., and Bock, G. R. (1987). Strial dysfunction in mice with cochleo-saccular abnormalities. *Hear Res* **27**, 11-26.
- Traub, O., Look, J., Paul, D., and Willecke, K. (1987). Cyclic adenosine monophosphate stimulates biosynthesis and phosphorylation of the 26 kDa gap junction protein in cultured mouse hepatocytes. *Eur J Cell Biol* **43**, 48-54.
- Turin, L., and Warner, A. (1977). Carbon dioxide reversibly abolishes ionic communication between cells of early amphibian embryo. *Nature* **270**, 56-7.
- Unger, V. M., Kumar, N. M., Gilula, N. B., and Yeager, M. (1999a). Electron cryo-crystallography of a recombinant cardiac gap junction channel. *Novartis Found Symp* **219**, 22-30; discussion 31-43.

- Unger, V. M., Kumar, N. M., Gilula, N. B., and Yeager, M. (1999b). Expression, two-dimensional crystallization, and electron cryo-crystallography of recombinant gap junction membrane channels. *J Struct Biol* **128**, 98-105.
- Unger, V. M., Kumar, N. M., Gilula, N. B., and Yeager, M. (1999c). Three-dimensional structure of a recombinant gap junction membrane channel. *Science* **283**, 1176-80.
- Valiunas, V. (2002). Biophysical properties of connexin-45 gap junction hemichannels studied in vertebrate cells. *J Gen Physiol* **119**, 147-64.
- Vaney, D. I., Nelson, J. C., and Pow, D. V. (1998). Neurotransmitter coupling through gap junctions in the retina. *J Neurosci* **18**, 10594-602.
- Van Steensel, M.A., van Geel, M., Nahuys, M., Smitt, J.H., Steijlen, P.M. (2002). A novel connexin 26 mutation in a patient diagnosed with keratitis-ichthyosis-deafness syndrome. *J Invest Dermatol.* **118**(4), 724-7.
- Veenstra, R. D., Wang, H. Z., Westphale, E. M., and Beyer, E. C. (1992). Multiple connexins confer distinct regulatory and conductance properties of gap junctions in developing heart. *Circ Res* **71**, 1277-83.
- Verselis, V. K., Bennett, M. V., and Bargiello, T. A. (1991). A voltage-dependent gap junction in *Drosophila melanogaster*. *Biophys J* **59**, 114-26.
- Wangemann, P., and Schacht, J. (1996). In "The Cochlea: Handbook of Auditory Research" (P. Dallos, R. Fay, and A. Popper, Eds.). Springer.
- Wangemann, P. (2002). K⁺ cycling and the endocochlear potential. *Hear Res* **165**, 1-9.
- Warner, A. (1992). Gap junctions in development--a perspective. *Semin Cell Biol* **3**, 81-91.
- Warner, A. E., Guthrie, S. C., and Gilula, N. B. (1984). Antibodies to gap-junctional protein selectively disrupt junctional communication in the early amphibian embryo. *Nature* **311**, 127-31.
- White, T. W., and Bruzzone, R. (1996). Multiple connexin proteins in single intercellular channels: connexin compatibility and functional consequences. *J Bioenerg Biomembr* **28**, 339-50.
- White, T. W., Bruzzone, R., Goodenough, D. A., and Paul, D. L. (1992). Mouse Cx50, a functional member of the connexin family of gap junction proteins, is the lens fiber protein MP70. *Mol Biol Cell* **3**, 711-20.
- White, T. W., and Paul, D. L. (1999). Genetic diseases and gene knockouts reveal diverse connexin functions. *Annu Rev Physiol* **61**, 283-310.

- Winterhager, E., Grummer, R., Jahn, E., Willecke, K., and Traub, O. (1993). Spatial and temporal expression of connexin26 and connexin43 in rat endometrium during trophoblast invasion. *Dev Biol* **157**, 399-409.
- Xia, J. H., Liu, C. Y., Tang, B. S., Pan, Q., Huang, L., Dai, H. P., Zhang, B. R., Xie, W., Hu, D. X., Zheng, D., Shi, X. L., Wang, D. A., Xia, K., Yu, K. P., Liao, X. D., Feng, Y., Yang, Y. F., Xiao, J. Y., Xie, D. H., and Huang, J. Z. (1998). Mutations in the gene encoding gap junction protein beta-3 associated with autosomal dominant hearing impairment. *Nat Genet* **20**, 370-3.
- Yeager, M., Unger, V. M., and Falk, M. M. (1998). Synthesis, assembly and structure of gap junction intercellular channels. *Curr Opin Struct Biol* **8**, 517-24.
- Zelante, L., Gasparini, P., Estivill, X., Melchionda, S., D'Agruma, L., Govea, N., Mila, M., Monica, M. D., Lutfi, J., Shohat, M., Mansfield, E., Delgrosso, K., Rappaport, E., Surrey, S., and Fortina, P. (1997). Connexin26 mutations associated with the most common form of non-syndromic neurosensory autosomal recessive deafness (DFNB1) in Mediterraneans. *Hum Mol Genet* **6**, 1605-9.
- Zhu, H. (1999). Summary of connexon pairings. In "Gap Junction Mediated Signalling in Health and Disease: Novartis Symposia" (Wiley, Ed.). Wiley, Chichester, New York.

Appendix 1

| <u>Connexin isoforms studied</u> | <u>Positive control tissue</u> |
|----------------------------------|--------------------------------|
| Cx26 | LIVER |
| Cx30 | BRAIN |
| Cx30.3 | SKIN |
| Cx31 | SKIN |
| Cx31.1 | SKIN |
| Cx32 | LIVER |
| Cx37 | HEART |
| Cx40 | HEART |
| Cx43 | HEART |
| Cx45 | HEART |
| Cx46 | LENS |
| Cx46.6 | EMBRYO |
| Cx50 | LENS |

Appendix 2

A 10% acrylamide separating gel contained 5mL 30% acrylamide/0.8% bisacrylamide, 3.75mL 1.5M Tris buffer at pH8.8, 6mL water, 150 μ L 10% sodium dodecyl sulphate, 7.5 μ L TEMED, 100 μ L 10% ammonium persulphate.

Appendix 3

Antibodies used throughout the thesis

| Isoform | Name | Sequence | Source |
|---------|------------------------|-----------------------------------|--------|
| Cx26 | Gap 28h polyclonal | Residues 113-124 Cytoplasmic loop | 1 |
| Cx26 | Anti-cx26 polyclonal | C-terminal tail | 6 |
| Cx26 | β 2J monoclonal | Residues 112-125 Cytoplasmic loop | 2 |
| Cx26 | Des3 polyclonal | Residues 106-119 Cytoplasmic loop | 4 |
| Cx30 | Anti-cx30 polyclonal | C-terminal tail | 6 |
| Cx31 | Anti- cx31 polyclonal | Cytoplasmic loop | 7 |
| Cx31 | β 3S polyclonal | Residues 250-261 C-terminal tail | 2 |
| Cx32 | β 1J | | 2 |
| Cx32 | Gap2A monoclonal | | 4 |
| Cx32 | Des1 polyclonal | 102-112, 116-124 Cytoplasmic loop | 4 |
| Cx32 | Des5 polyclonal | Residues 108-119 Cytoplasmic loop | 4 |
| Cx32 | Gap 31h polyclonal | Residues 2-18 Amino-terminal | 1 |
| Cx32 | Gap 34r polyclonal | Residues 260-279 C-terminal tail | 1 |
| Cx37 | Y16Y polyclonal | YLPMGEGPSSPPCPTY C-terminal tail | 3 |
| Cx37 | | | 4 |
| Cx40 | | | 4 |
| Cx40 | S15C polyclonal | SLVQGLTPPPDFNQC C-terminal tail | 3 |
| Cx43 | Gap1a monoclonal | | 4 |
| Cx43 | Gap 15 polyclonal | Residues 131-142 Cytoplasmic loop | 4 |
| Cx43 | Gap 33r polyclonal | Residues 314-325 C-terminal tail | 1 |
| Cx43 | α 1J polyclonal | | 2 |

| | | | |
|-------------|------------------------|----------------------------------|---|
| Cx43 | α 1S polyclonal | Residues 370-381 C-terminal tail | 2 |
| Cx43 | Anti-cx43 monoclonal | Residues 252-270 | 5 |
| Cx45 | Q14E polyclonal | QAYSHQNNPHGPRE C-terminal tail | 3 |
| Cx45 | α 6J polyclonal | Cytoplasmic loop | 2 |
| Cx46 | α 3S polyclonal | C-terminal tail | 2 |
| Cx46 | α 3J polyclonal | Cytoplasmic loop | 2 |
| Cx50 | α 8 monoclonal | | 2 |

¹W.H. Evans, University of Wales, Cardiff

²Gilula lab, The Scripps Research Institute (TSRI)

³Severs lab, Imperial College School of Science, Technology and Medicine

⁴Becker lab, University College London

⁵Chemicon

⁶Zymed

⁷Alpha diagnostic and Willecke lab, Bonn

Thanks to all who kindly donated aliquots of their antibodies.

Appendix 4

As an alternative blocking solution

Blocking solution made up as 1% Bovine serum albumin in phosphate-buffered saline.